NAVAL POSTGRADUATE SCHOOL
Monterey, California

THESIS

ANALYSIS OF MARITIME MOBILE SATELLITE COMMUNICATION SYSTEMS

by

Augusto J. Zapata

December 1988

Thesis Advisor Tri T. Ha

REPORT DOCUMENTATION PAGE

1a Report Security Classification: Unclassified	1b Restrictive Markings
2a Security Classification Authority	3 Distribution Availability of Report: Approved for public release; distribution is unlimited.
2b Declassification Downgrading Schedule	
4 Performing Organization Report Number(s)	5 Monitoring Organization Report Number(s)
6a Name of Performing Organization: Naval Postgraduate School; 6b Office Symbol (*if applicable*): 32	7a Name of Monitoring Organization: Naval Postgraduate School
6c Address (*city, state, and ZIP code*): Monterey, CA 93943-5000	7b Address (*city, state, and ZIP code*): Monterey, CA 93943-5000
8a Name of Funding Sponsoring Organization; 8b Office Symbol (*if applicable*)	9 Procurement Instrument Identification Number
8c Address (*city, state, and ZIP code*)	10 Source of Funding Numbers: Program Element No; Project No; Task No; Work Unit Accession No

11 Title (*include security classification*): ANALYSIS OF MARITIME MOBILE SATELLITE COMMUNICATION SYSTEMS

12 Personal Author(s): Augusto J. Zapata

13a Type of Report	13b Time Covered	14 Date of Report (*year, month, day*)	15 Page Count
Master's Thesis	From To	December 1988	83

16 Supplementary Notation: The views expressed in this thesis are those of the author and do not reflect the official policy or position of the Department of Defense or the U.S. Government.

17 Cosati Codes			18 Subject Terms (*continue on reverse if necessary and identify by block number*)
Field	Group	Subgroup	Mobile Satellite Communications, Rician Fading, Unslotted Aloha Throughput

19 Abstract (*continue on reverse if necessary and identify by block number*)

The communication channel between a satellite and a ship earth station (SES) is described by a model which includes multipath fading, doppler shift and noise. Multipath fading is caused by reflections from the sea surface. These reflections can affect the system performance, especially at low elevation angles or when SES is using low gain antennas. Doppler shift is a very important effect when using low altitude satellites, because of the high velocities involved.

This thesis describes and presents a software simulator for multipath fading in the maritime communications environment. Analysis of throughput of an unslotted Aloha maritime mobile satellite communication channel is also presented.

20 Distribution Availability of Abstract	21 Abstract Security Classification	
☒ unclassified unlimited ☐ same as report ☐ DTIC users	Unclassified	
22a Name of Responsible Individual: Tri T. Ha	22b Telephone (*include Area code*): (408) 384-2991	22c Office Symbol: 62Ha

DD FORM 1473,84 MAR 83 APR edition may be used until exhausted
All other editions are obsolete

Approved for public release; distribution is unlimited.

Analysis of Maritime Mobile Satellite Communication Systems

by

Augusto J. Zapata
Lieutenant , Colombian Navy
B.S., Escuela Naval Almirante Padilla, 1985

Submitted in partial fulfillment of the
requirements for the degree of

MASTER OF SCIENCE IN ELECTRICAL ENGINEERING

from the

NAVAL POSTGRADUATE SCHOOL
December 1988

Author: 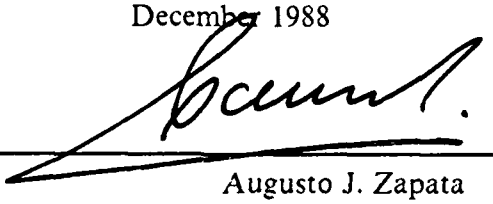

Augusto J. Zapata

Approved by: 

Tri T. Ha, Thesis Advisor

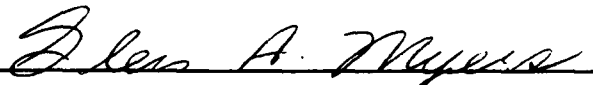

Glen A. Myers, Second Reader

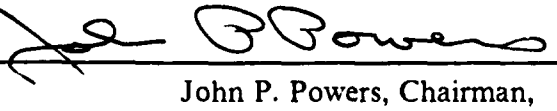

John P. Powers, Chairman,
Department of Electrical Engineering

Gordon E. Schacher,
Dean of Science and Engineering

ABSTRACT

The communication channel between a satellite and a ship earth station (SES) is described by a model which includes multipath fading, doppler shift and noise. Multipath fading is caused by reflections from the sea surface. These reflections can affect the system performance, especially at low elevation angles or when SES is using low gain antennas. Doppler shift is a very important effect when using low altitude satellites, because of the high velocities involved.

This thesis describes and presents a software simulator for multipath fading in the maritime communications environment. Analysis of throughput of an unslotted Aloha maritime mobile satellite communication channel is also presented.

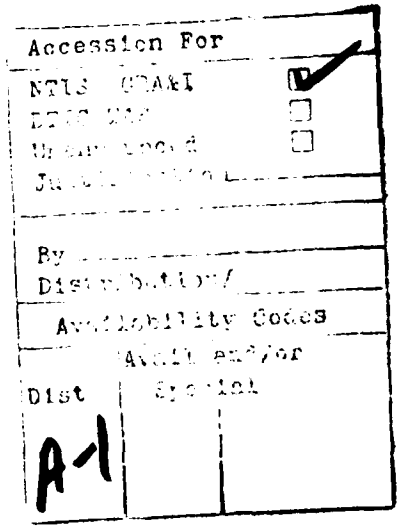

TABLE OF CONTENTS

LIST OF TABLES

LIST OF FIGURES

I. INTRODUCTION

Future satellite systems for maritime, aeronautical and land mobile applications (with mobile terminals for low data rate and digital voice transmission) will have small antennas having gains between 2 and 12 dB and a broad beamwidth. These antennas pick up multipath reflections of satellite signals causing severe fading of the received signals.

Several fading simulators, using hardware, software, or both, have been designed. Among them are: JPL, CRC and Virginia Tech. All of them deal with land mobile communications and with geostationary satellites.

In the future, low altitude satellites will become important alternatives for mobile communications because of the crowded geostationary orbit. Studies have demonstrated that five satellites in circular orbit will provide continuous single coverage of the earth; seven satellites will provide double coverage at some minimum elevation angle. By the same criterion it was found that eleven satellites can provide continuous triple coverage and fourteen satellites, quadruple coverage. Continuous single coverage means that any two stations on earth can communicate using this constellation of five satellites at any moment. Double coverage, on the other hand, will provide an additional communication path; triple coverage will provide three different paths and so on.

Besides the economical achievement of maximum coverage, many other factors have to be taken into account in system design. These results may prove of some interest to planners of satellite systems for mobile communications and surveillance [Ref. 1]

Low earth orbits (LEO) are generally circular or slightly eccentric. In order to simplify the analysis and equations described in this thesis, the focus will be on circular orbits.

This thesis presents a fading simulation program for mobile maritime satellite communications involving low altitude satellites.

Chapter II describes the different signals involved in the maritime communications channel, the atmospheric effects that affect them, and also demonstrates the application of the theory of Rician fading statistics.

Chapter III describes the simulation program, explains the purpose of each of its components and illustrates some results obtained by running several simulations for different values of frequency and satellite's velocity.

Chapter IV describes the throughput of unslotted Aloha with power capture probability in a Rician fading environment.

Finally, Appendix A contains a listing of the computer program of the simulator, and Appendix B shows the derivation of the formulas used in chapter IV.

II. PHYSICS OF MARITIME MOBILE SATELLITE PROPAGATION

A. INTRODUCTION

Any signal in maritime mobile communications is typically dominated by a multipath fading process caused by reflections coming from the surface of the sea. These multipath signals are expected to be stronger at low satellite elevation angles, where the main lobe of the antenna of the ship earth station (SES) picks them up. No specular component is expected, except for the very calm, mirror-like sea; therefore, a model with Rician statistics is suggested in this chapter.

B. MULTIPATH FADING AMPLITUDE

It is well known that multipath reflections from the sea surface consist of specular and diffuse components. The relative strength of these components is due to wave height and to elevation angle, with the former the dominant factor [Ref.2]. For a smooth sea state the specular component dominates. As wave height increases, the diffuse component also increases, and over a wave height of 0.5 m, the diffuse component becomes constant. Sea state probability studies have been done in the past and it was concluded that wave heights are usually in a 0.5 to 5 m. range [Ref. 3]. Based on these observations, it is assumed that sea conditions will be rough most of the time and thus amplitude fading can be expressed in statistical terms.

C. STATISTICAL MODEL FOR MULTIPATH FADING AMPLITUDE

For a satellite maritime link, the dominant multipath component is the diffuse component. The signal can therefore be represented by two components: **direct and diffuse** (see Figure 1).

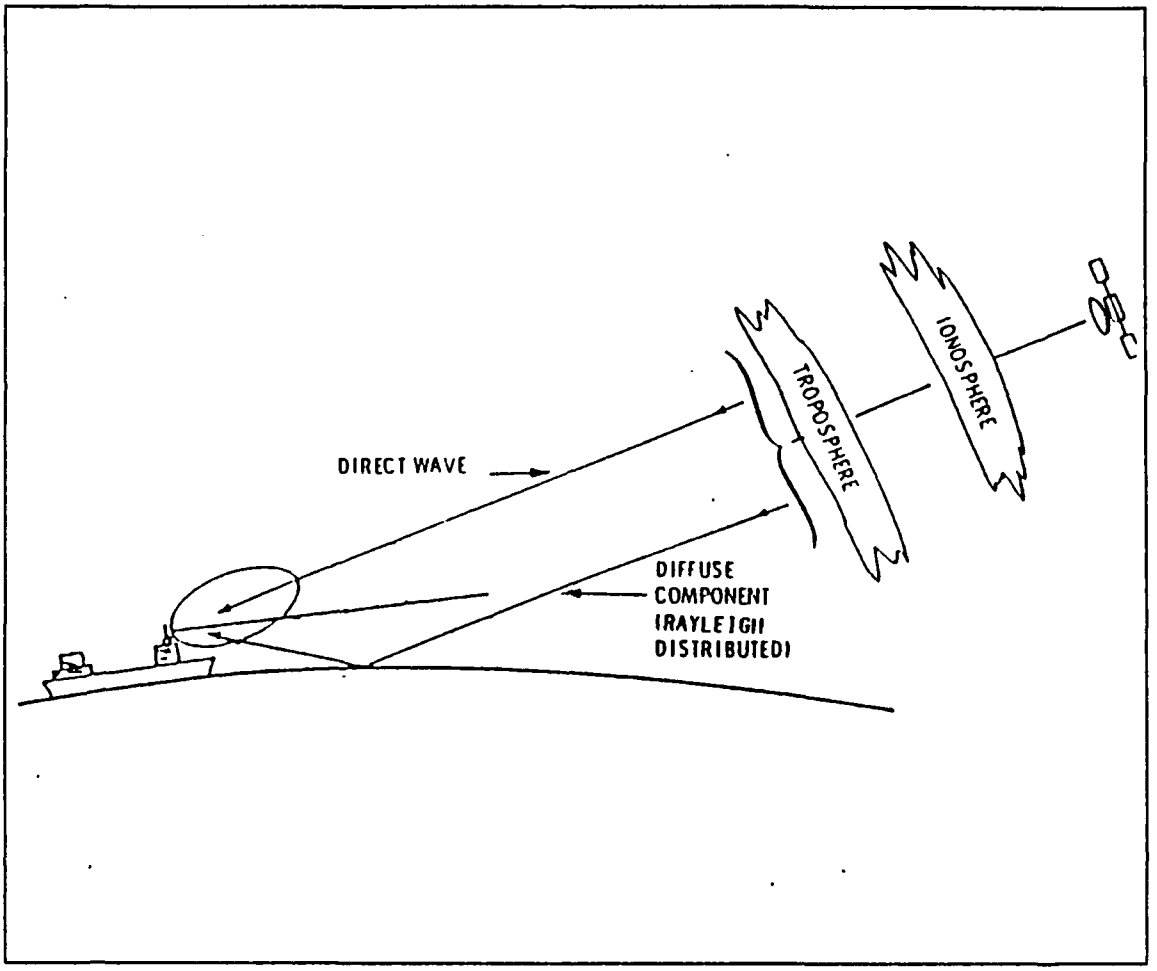

Figure 1. Propagation model for maritime mobile satellite communications

The direct component is the line of sight (LOS) signal from the satellite. The diffuse component is the resultant of many random scattered waves arriving in a uniform angular distribution [Ref. 4]. If each of the waves is represented by a random phasor, the total diffuse component at the output of the antenna is

$$R_{dif} = r \exp[j\theta] = \sum_{i=1}^{\infty} A_i \exp[j\phi_i] \tag{2.1}$$

where

- r is the amplitude of the diffuse component
- ϕ is the phase of the diffuse component with respect to the direct component

- A_i is the amplitude of the i^{th} scattered wave with respect to the direct component.

If the scattered waves are sufficiently random and their phase is uniformly distributed over 2π, Beckmann shows that the diffuse component will be Rayleigh distributed with a density function given by [Ref. 5]

$$p(r) = \frac{2r}{\alpha} \exp\left[-\frac{r^2}{\alpha} \right] \qquad r \geq 0 \tag{2.2}$$

$$p(r) = 0 \qquad r < 0$$

where

- r is the received diffuse signal level (voltage)
- $\alpha = E\{r^2\}$

The Rayleigh distribution requires the scattered waves to have a uniform phase distribution over an interval of 2π. If the terrain does not provide for this requirement, the Rayleigh distribution will not be valid [Ref. 6].

The vector sum of a direct signal, with a Rayleigh fading component, results in a composite signal with Rician envelope statistics [Ref. 7], and the probability density function is:

$$p(r) = \frac{2r}{\alpha} \exp\left(-\frac{r^2 + A_0^2}{\alpha} \right) I_0\left(\frac{2A_0 r}{\alpha} \right) \qquad r \geq 0 \tag{2.3}$$

$$p(r) = 0 \qquad r < 0$$

where

- r represents the envelope of the Rayleigh fading signal
- $\alpha = E\{r^2\}$
- A_0 is the amplitude of the direct signal
- I_0 is the modified Bessel function of zero order

By normalizing the direct component to unity, this reduces to:

$$p(R) = \frac{2R}{k} \exp\left(-\frac{R^2 + 1}{k} \right) I_0\left(\frac{2R}{k} \right) \qquad R \geq 0 \tag{2.4}$$

$$p(R) = 0 \qquad R < 0$$

where

- k is equal to the power in the multipath component over the power in the direct component, that is:

$$k = \frac{\alpha}{A_0^2}$$

- R is the ratio of the amplitude of the fading signal to the amplitude of the direct component

$$R = \frac{r}{A_0}$$

The parameter k is called the **Rice factor**. It is considered a key parameter in the Rician distribution, and its decibel equivalent is $K = 10 \log_{10} k$. Figure 2 illustrates several Rician distributions for different values of A_0.

The phase of the received signal is not uniformly distributed [Ref. 5] and its density function is given by:

$$p(\theta) = \frac{1}{2\pi} \exp\left(- \frac{A_0^2}{\alpha} \right) \{1 + G\sqrt{\pi} \exp(G^2)(1 + erf(G))\} \qquad 0 \le \theta \le 2\pi \qquad (2.5)$$

where

- G is defined as:

$$G = \frac{A_0 \cos\theta}{\sqrt{\alpha}}$$

- erf (G) is the error function defined as:

$$erf(G) = \frac{1}{\sqrt{2\pi}} \int_0^G \exp\left[- \frac{y^2}{2} \right] dy$$

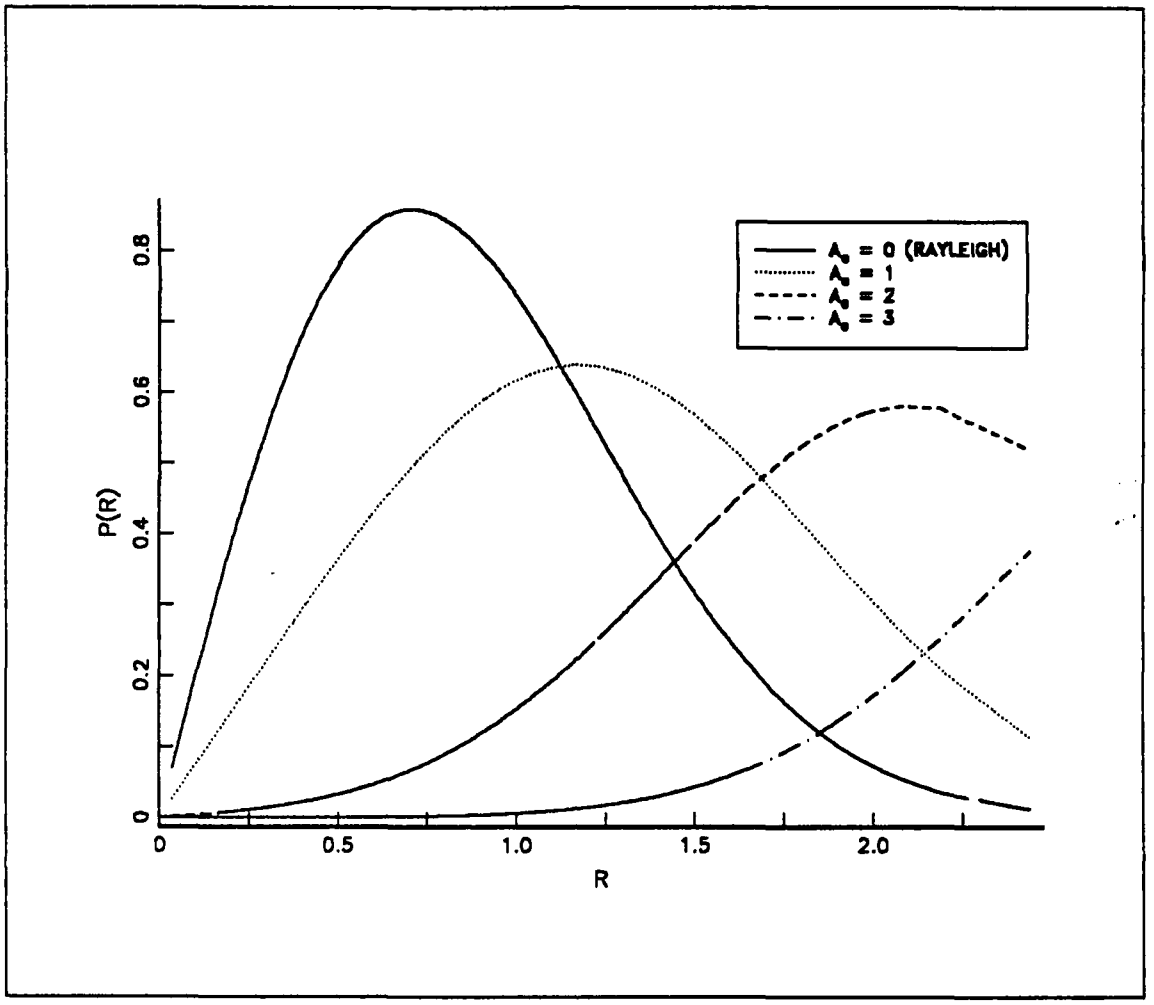

Figure 2. Rician density function for α = 1, f = 869 MHz, V = 0 Kts.

1. Cumulative Distribution Function (CDF)

The cumulative distribution function (CDF) refers either to the function G(A) for which the signal exceeds a level A, or to the function F(A) for which the signal is below a level A. The former is the one used in this thesis.

The theoretical expression for the Rician CDF is obtained by integrating equation (2.3):

$$G(A) = P(r \geq A) = \int_A^{\infty} p(r)dr \tag{2.6}$$

Figure 3 illustrates a Rician CDF.

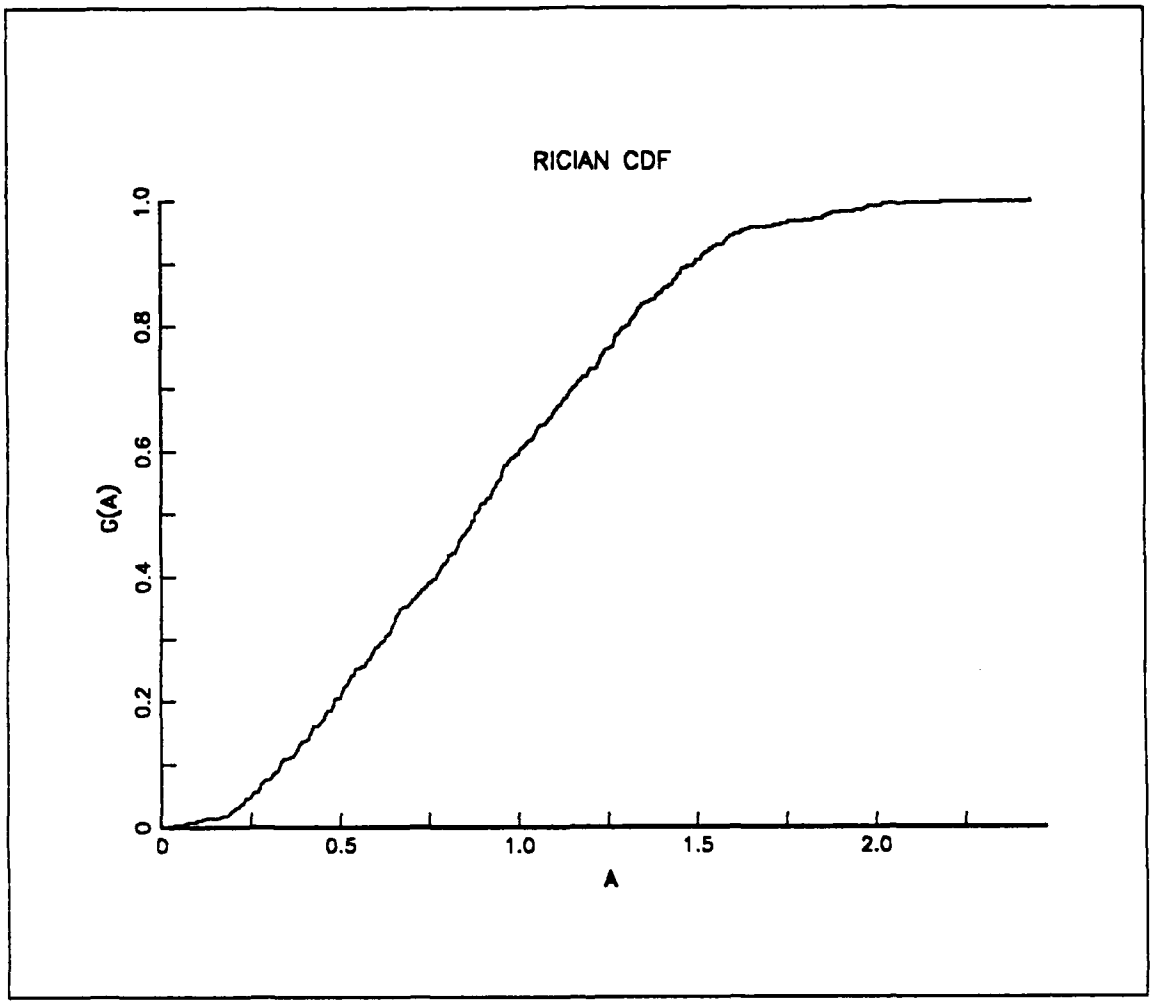

Figure 3. Cumulative Distribution Function (CDF)

Usually the CDF is plotted in Rayleigh paper which has the especial characteristic that a Rayleigh curve drawn in it is a straight line. This is useful for evaluating any outcome by visually comparing it with the Rayleigh line. Figure 4 illustrates the same Rician CDF seen in Figure 3 but on probability paper.

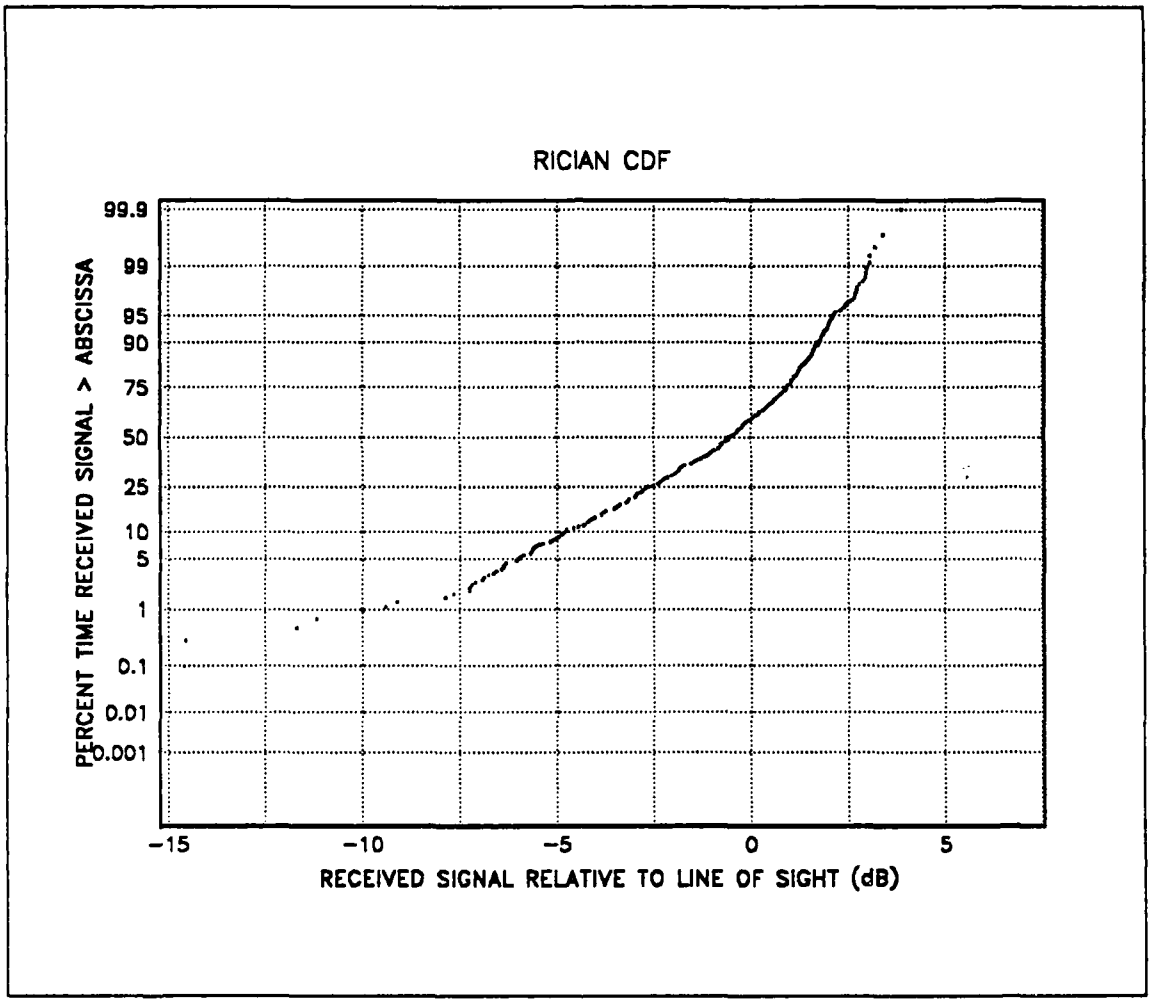

Figure 4. Cumulative Distribution Function (CDF) on probability paper.

D. ATMOSPHERIC EFFECTS ON THE FADING SIGNAL COMPONENTS

The direct and the diffuse components are both affected by Ionospheric and Tropospheric effects. These effects include Faraday rotation, group delay, absorption, dispersion, refraction and scintillation, all of which result from interaction with the earth's magnetic field and the ambient electron content as the signal passes through the Ionosphere. Table 1 [Ref. 8] summarizes some typical maximun values obtained for an elevation angle of 30 °, one way propagation, at two different frequencies. Faraday rotation can be minimized using circular polarization. Scintillation can be important at low

latitudes (9° N to 21 ° S) and auroral latitudes (above 59 ° N), but they are insignificant for elevation angles greather than 10 ° and frequencies below 10 Ghz [Ref. 9].

Table 1. ESTIMATED MAXIMUM IONOSPHERIC EFFECTS [REF. 8]: For an elevation angle of 30 ° , one way propagation, and a zenith electron column of 10^{18} electrons/m^3

Effect	Frequency dependence	Magnitude	
		850 MHz	1600 MHz
Faraday Rotation	$1/f^2$	150 °	42 °
Group delay	$1/f^2$	0.35 s	0.1 s
Variation in direction of arrival	$1/f^2$	16 sec of arc	4.7 sec of arc
Refraction	$1/f^2$	> 50″	> 14″
Absorption (mid-lats)	$1/f^2$	> 0.014 dB	> 0.004 dB
Dispersion	$1/f^3$	0.65 nsec/MHz.	0.1 nsec MHz

Tropospheric effects result from moisture in the atmosphere and tend to become more severe as frequency increases. Table 2 [Ref. 10] summarizes some estimated values for an elevation angle of 30 °, one way propagation, at two different frequencies.

The antenna pattern will influence the magnitude of the diffuse component. The antenna gain rolls off below the horizon; therefore, the contribution of the diffuse component is due to scattered waves arriving from angles above the horizon.

The current treatment assumes that the diffuse component is 8 to 14 dB (rms) below the direct component [Ref. 9].

Table 2. ESTIMATED TROPOSPHERIC ATTENUATION [REF. 10]: For an elevation angle of 30 °, and one way propagation

Effect	Magnitude (dB)	
	850 MHz	1600 MHz
Clear air absorption		
3 g m^3 (dry)	0.06	0.07
7.5 g m^3 (average)	0.06	0.07
17 g m^3 (moist)	0.06	0.07
Cloud attenuation		
0.5 g m^3, 1 Km thick	< 0.01	< 0.01
1 g m^3, 2 Km thick	< 0.01	< 0.01
Fog attenuation		
0.05 g m^3 (average), 0 to 75 Kmt ht.	-----	-----
0.05 g m^3 (heavy), 0 to 150 mt ht.	-----	-----
Rain attenuation		
5 mm h	< 0.01	< 0.01
25 mm h	< 0.1	< 0.1

III. SOFTWARE FADE SIMULATOR FOR A MARITIME MOBILE COMMUNICATION CHANNEL

A. INTRODUCTION

Arredondo et al. [Ref. 11] describe a hardware simulator to simulate multipath fading for mobile radio, and Karim [Ref. 12] describes a different solution to implement this simulator using software. This thesis follows both reference models, adding a constant signal (direct component) to obtain Rician statistics. It emphasises the doppler effect caused by the high velocity of low altitude satellites and the vehicle's velocity. Figure 5 is a block diagram of the suggested model.

B. SIMULATOR DESCRIPTION

1. Rayleigh Multipath Fading Generator.

The most important part of the simulator is the **Rayleigh multipath fading** component. Its implementation follows the model of Arredondo et al. [Ref. 11] and Karim [Ref. 12]. Two independent Gaussian sources with zero mean and equal variance are generated. They are passed through a shaping filter and finally added in quadrature to obtain a signal with an envelope that is Rayleigh distributed in amplitude and uniformly distributed in phase.

The generator is illustrated in Figure 6. A key aspect in the design of this generator is the **shaping filter.**

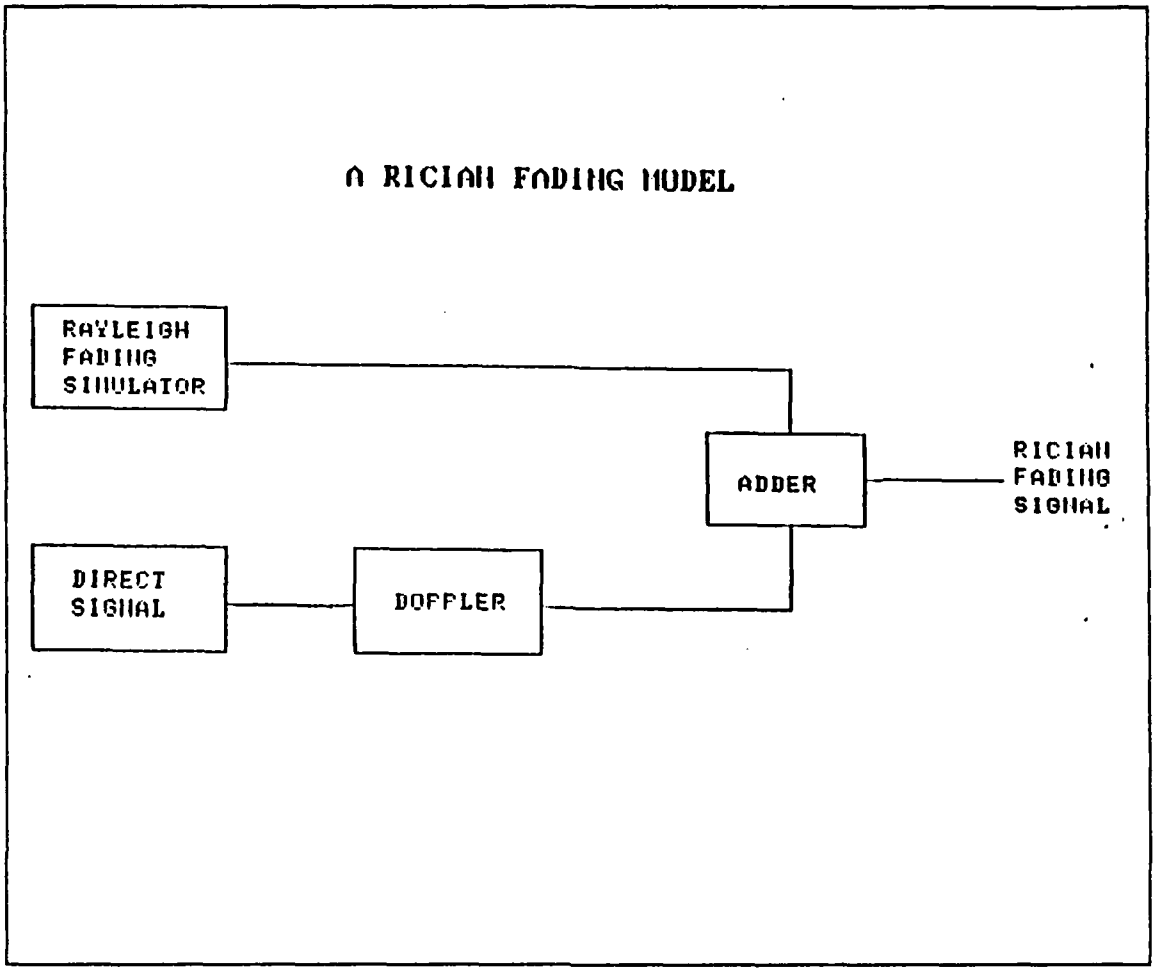

Figure 5. Rician fading simulator block diagram

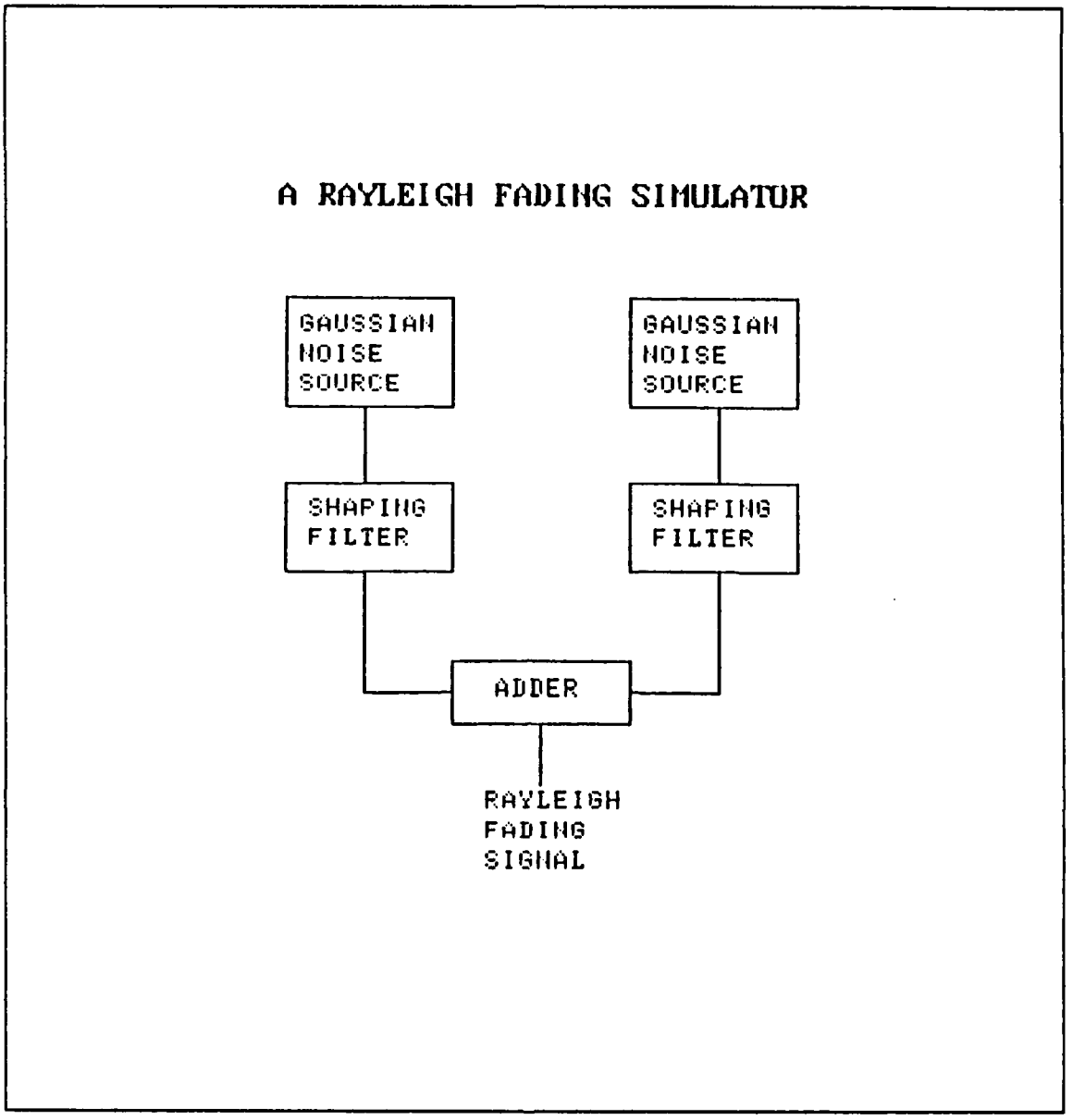

Figure 6. Rayleigh fading generator block diagram

Shaping Filter: The spectral density $S(\omega)$ of the envelope of the Rayleigh fading signal received by an *omnidirectional* antenna is given by [Ref. 12] :

$$S(\omega) = \frac{\sigma^2}{\omega_d}\left[1 - \left(\frac{\omega - \omega_o}{\omega_d}\right)^2\right]^{-0.5} \qquad |\omega - \omega_{o|} \leq \omega_d \qquad (3.1)$$

where

- ω_o is the carrier frequency.
- ω_d is the doppler shift due to the velocity of the vehicle and the velocity of the satellite.
- σ^2 is the variance of the two independent Gaussian sequences.

Refering to equation (3.1), taking ω relative to ω_o and noting that we are only interested in relative values of the signal, the transfer function $H(\omega)$ that has to be obtained to shape the input is given by:

$$H(\omega) = [1 - (\frac{\omega}{\omega_d})^2]^{-0.25} \tag{3.2}$$

This function is unbounded for $\omega = \omega_d$, but following the model of Arredondo et al. [Ref. 11], the actual transfer function has a maximum at $0.95\omega_d$ and falls to 0 with a slope of -18 dB octave. It is done this way so that the output envelope of the simulator closely fits a Rayleigh distribution.

This transfer function will be implemented as the transfer function H(z) of a non-recursive digital filter with sampling frequency $\omega_s = 2\omega_d$, and the procedure is discussed in Karim model [Ref.12].

$$H(z) = \sum_{i=0}^{20} W_i a_{i-10} z^{-i} \tag{3.3}$$

where

- W_i is the Hamming window.
- a_i is the Fourier coefficient of the Fourier series expansion of equation (3.2).
- z is $\exp(j\omega T)$ where $T = \frac{2\pi}{\omega_s}$.

Figure 7 illustrates both the theoretical and actual transfer functions.

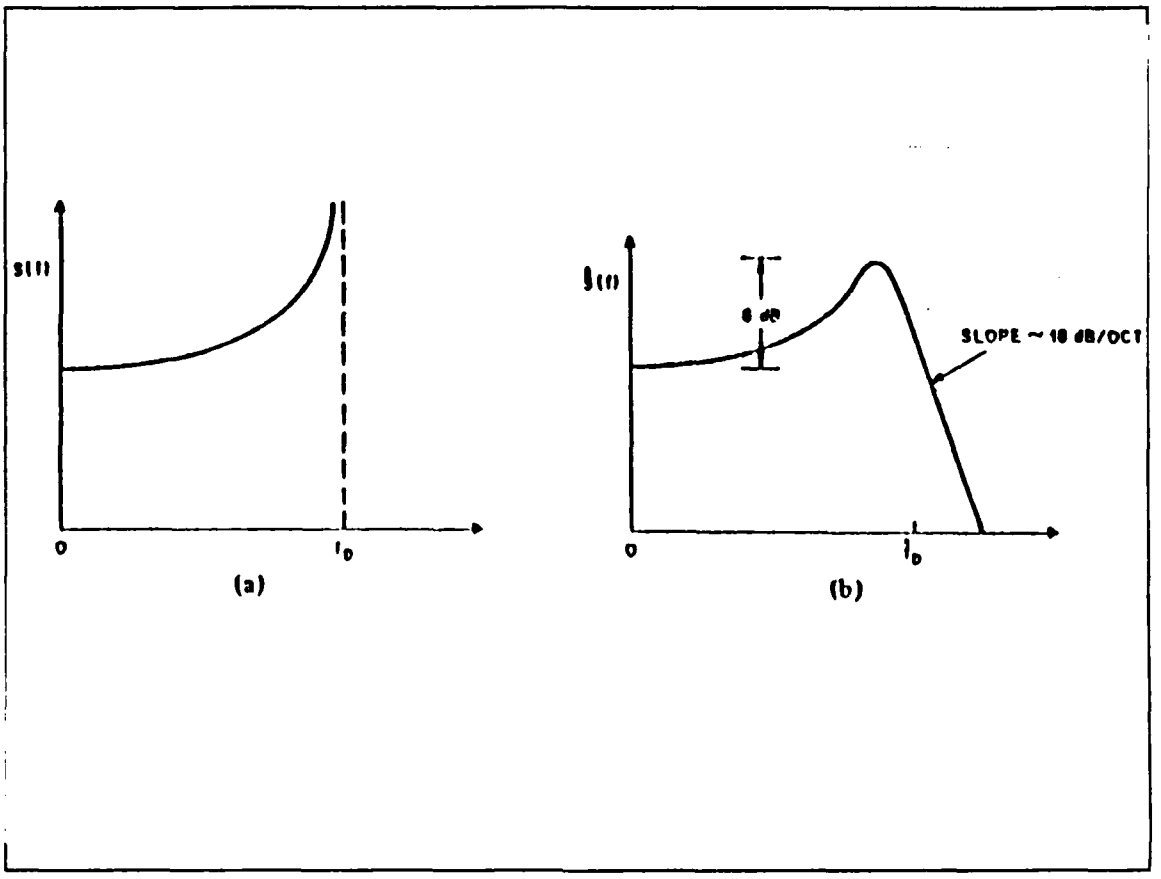

Figure 7. a) Spectral density of complex envelope, b) Shaping filter freq. response.: [Ref. 11]

Doppler Shift [Ref. 13]

Doppler shift is caused by a length change with time in the propagation path. Let the signal from the satellite be $A_0 \cos(2\pi f_0 t)$. This signal arrives to the receiver after a time delay $g(t)$, where g is a function describing the time variation in path length. Therefore the received signal is given by $A_0 cos[2\pi f_0(t \pm g(t))]$. Differentiating the phase we can obtain the frequency of the received wave, that is:

$$\frac{1}{2\pi}\frac{d}{dt}[2\pi f_0(t \pm g(t))] = f_0\left(1 \pm \frac{dg(t)}{dt}\right) \tag{3.4}$$

Thus the shift frequency is:

$$\Delta f = \pm f_0 \frac{dg(t)}{dt} \tag{3.5}$$

Since $g(t) = \frac{D(t)}{C}$ where

- $D(t)$ is the slant range, and
- C is the speed of light,

we have $\frac{dg(t)}{dt} = \frac{d[D(t)/C]}{dt} = \frac{v}{C}$

where v is the relative velocity of the receiver with respect to the source. Due to the higher velocity of the satellite compared with the velocity of the receiver on earth, the latter becomes negligible. For the purpose of this thesis, only the radial component of the velocity of the satellite v_r will be considered.

Therefore equation (3.5) becomes:

$$\Delta f = \pm f_0 \frac{v_r}{C} \tag{3.5a}$$

For satellites

$$d(t) = [(H + R_e)^2 + R_e^2 - 2R_e(H + R_e)\cos\theta] \tag{3.6}$$

where

- H is the altitude of the satellite orbit
- R_e is the radius of earth = 6378.155 Km
- θ is a linear function of time for circular orbits.

Due to the fact that earth terminals are not located at the center of the earth, there is a maximum Doppler shift at maximum slant range (satellite "rise" and "set"), as shown in Figure 8. From the same figure the following are obtained:

$$R_s = R_e + H \tag{3.7}$$

$$\gamma = \sin^{-1}\left(\frac{R_e}{R_s}\right) \tag{3.8}$$

$$v_r = v \sin\gamma \tag{3.9}$$

where

- R_s is the total radius of the satellite orbit.
- γ is the angle described in Figure 8
- v_r is the radial velocity of the satellite, from which the maximum value of Doppler shift is obtained.

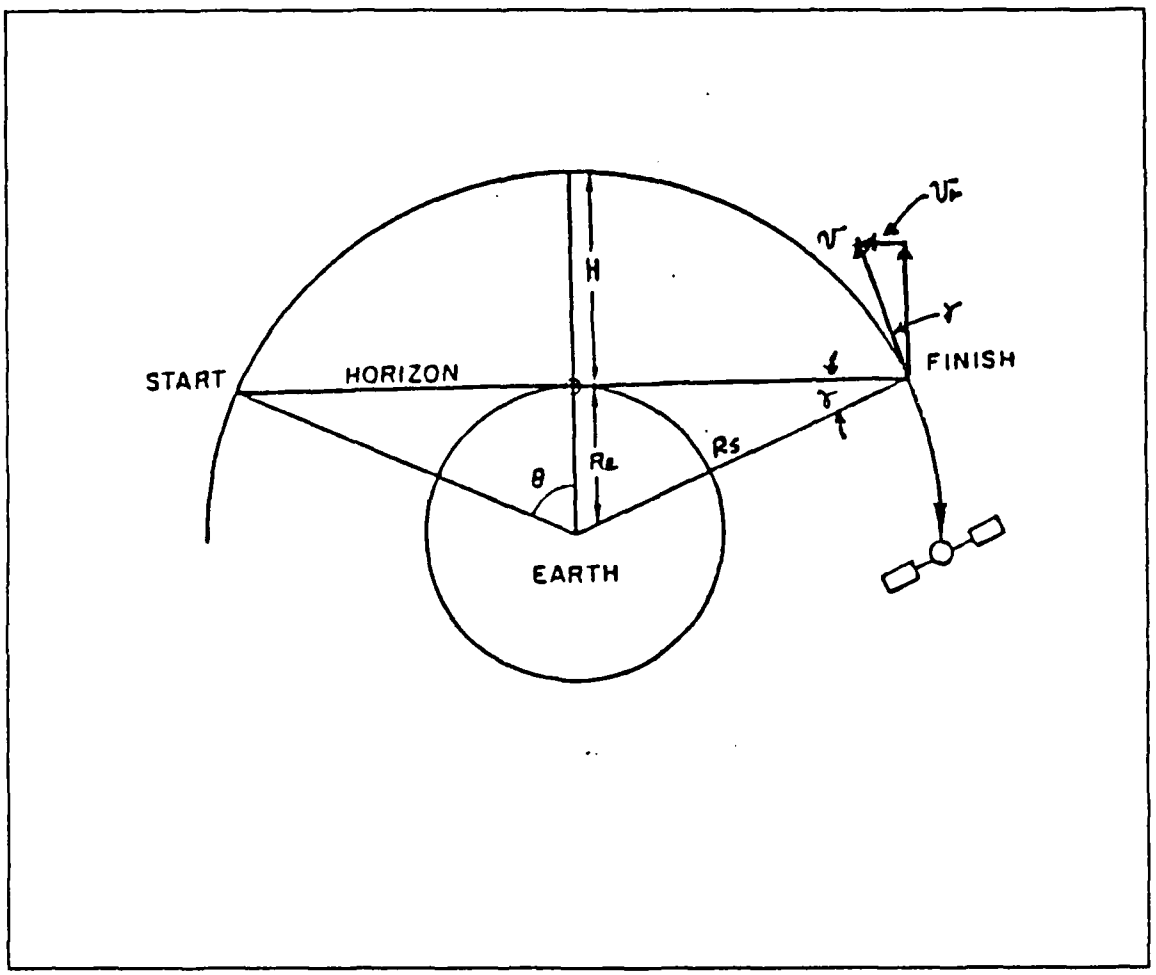

Figure 8. Doppler shift from a low altitude satellite

Therefore, the maximum value of Doppler shift is:

$$f_{d,max} = \pm f_0\left(\frac{v_{r,max}}{C}\right) = \pm \frac{v_{r,max}}{\lambda} \tag{3.10}$$

where

- f_d is the doppler frequency

- λ is the wavelength of the carrier frequency
- f_0 is the transmitted carrier frequency.

For a circular orbit satellite, the velocity is given by:

$$v = \sqrt{\frac{\mu_e}{R_s}} \tag{3.11}$$

where

- $\mu_e \simeq g(m_{earth} + m_{sat}) \simeq g(m_{earth}) \simeq 3.986013x10^5 \frac{Km^3}{sec^2}$

From equations (3.9), (3.10) and (3.11) we obtain:

$$f_{d,max} = \pm f_0\left(\frac{vR_e}{CR_s}\right) = \pm f_0\left(\frac{\sqrt{\frac{\mu_e}{R_s}}\,R_e}{CR_s}\right) \simeq \pm \frac{13.42 f_0}{R_s^{\frac{3}{2}}} \tag{3.12}$$

2. Direct Component part.

Let the direct component of the signal transmitted by the satellite be $A_0 \cos(\omega_0 t)$. The signal at the receiver will be affected by the velocity of the satellite, the velocity of the vehicle, or both, causing a Doppler shift. Davarian [Ref. 14] suggests a hardware solution to take care of the Doppler shift in the direct component; this is shown in Figure 10. As a result, the signal at the receiver will be $A_0 cos[(\omega_0 + \omega_d)t]$ at satellite rise and $A_0 cos[(\omega_0 - \omega_d)t]$ at satellite set. One of these signals is added to the Rayleigh fading signal to obtain the Rician fading Signal.

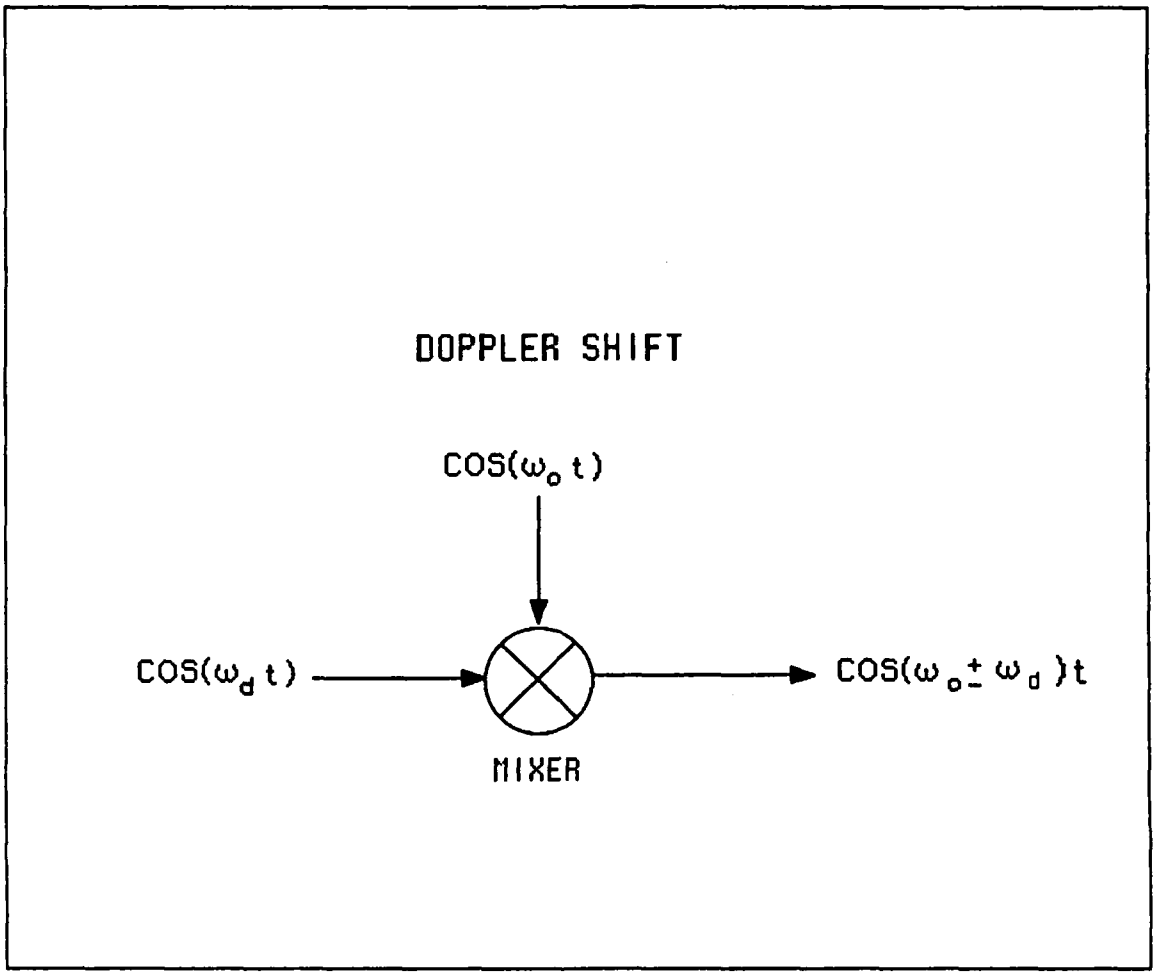

Figure 9. Block diagram for frequency shifting of the direct path [Ref. 14]: ω_0 is the angular frequency of the carrier and ω_d denotes the Doppler shift.

C. COMPUTER PROGRAM

A computer program was developed to simulate Rician fading statistics for a maritime mobile satellite communications channel. The computer program is written in Fortran and is included as Appendix A.

D. ANALYSIS OF RESULTS

The simulation of several sequences of multipath Rician fading was done assuming a communication mobile maritime link with a satellite in circular orbit at an altitude of 500 nautical miles. As was stated earlier in this chapter, the speed of the maritime vehicle is considered negligible in comparison to the speed of the satellite. As a result, the vehicle's speed is not taken into account. Figures 10 through 12 show the generated Rician sequences for values of K (Rician factor) equal to 0, 5 and 10 dB, a frequency of 869 MHz and a velocity of 30 knots. Figures 13 through 15 illustrate the histogram of the preceeding sequences. Figures 16 through 31 show the cumulative distribution function (CDF), using probability paper, of several multipath sequences for the different combinations of the following parameters K = -26, -10, 0, 10 dB, frequency = 869, 1501 MHz, and velocity = 0, 14357 Kts.

In order to analize the generated Rician sequences we look at two different CDF graphs. Comparing Figures 16 and 28 using the same frequency and velocity for values of K = -26 dB and K = 10 dB, it can be noticed that for the former value of K the received signal is greater than the abscissa for a longer period of time. This means that for a larger Rice factor (K) we have more fading and therefore less strength in the received signal at the antenna.

Additionally, the difference in the CDF can be noticed between the curves with 0 velocity (0 doppler) and the curves with a velocity of 14357 Kts (max. doppler); as was expected, the difference is larger at higher frequencies.

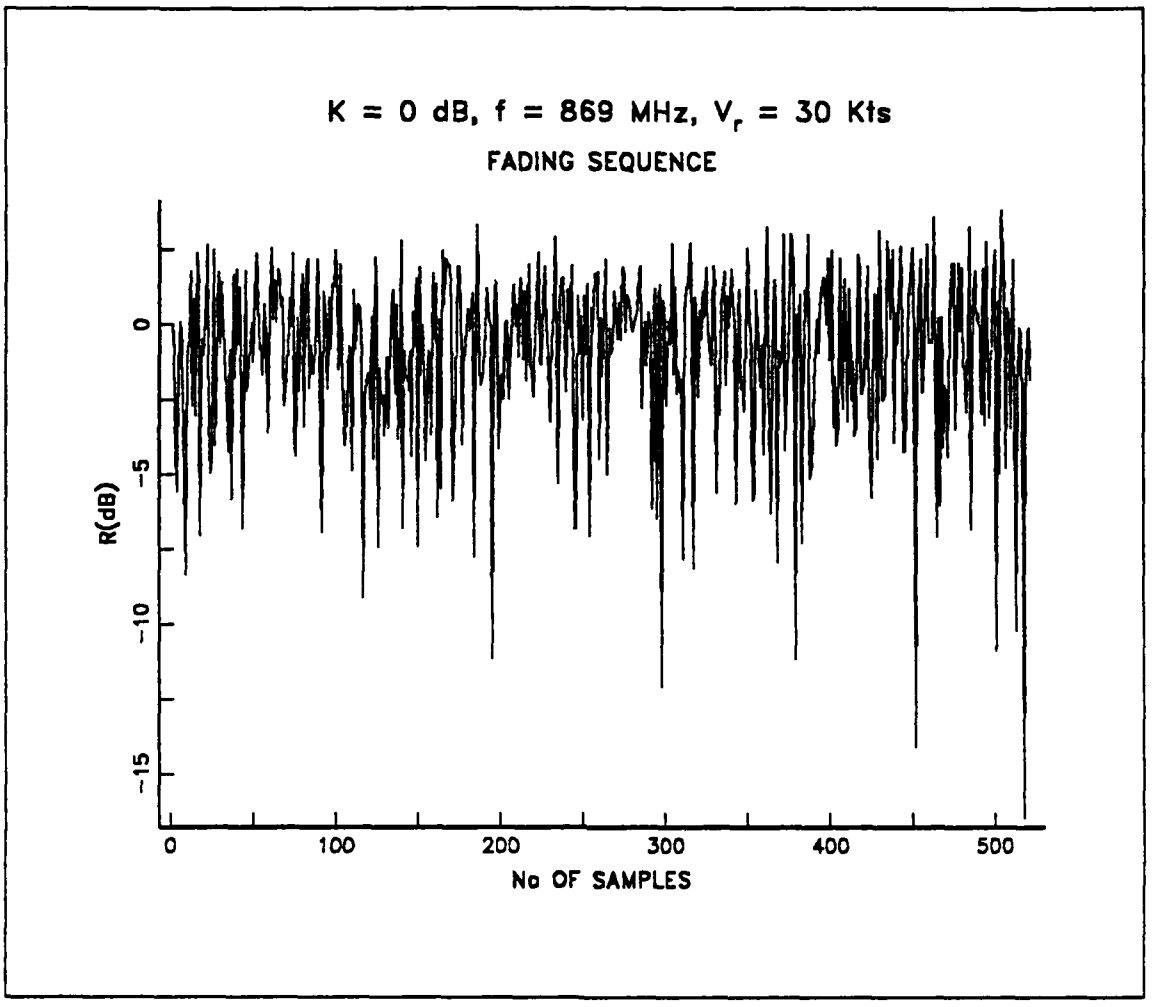

Figure 10. Rician fading sequence for K = 0 dB, f = 869 MHz, V = 30 Kts.

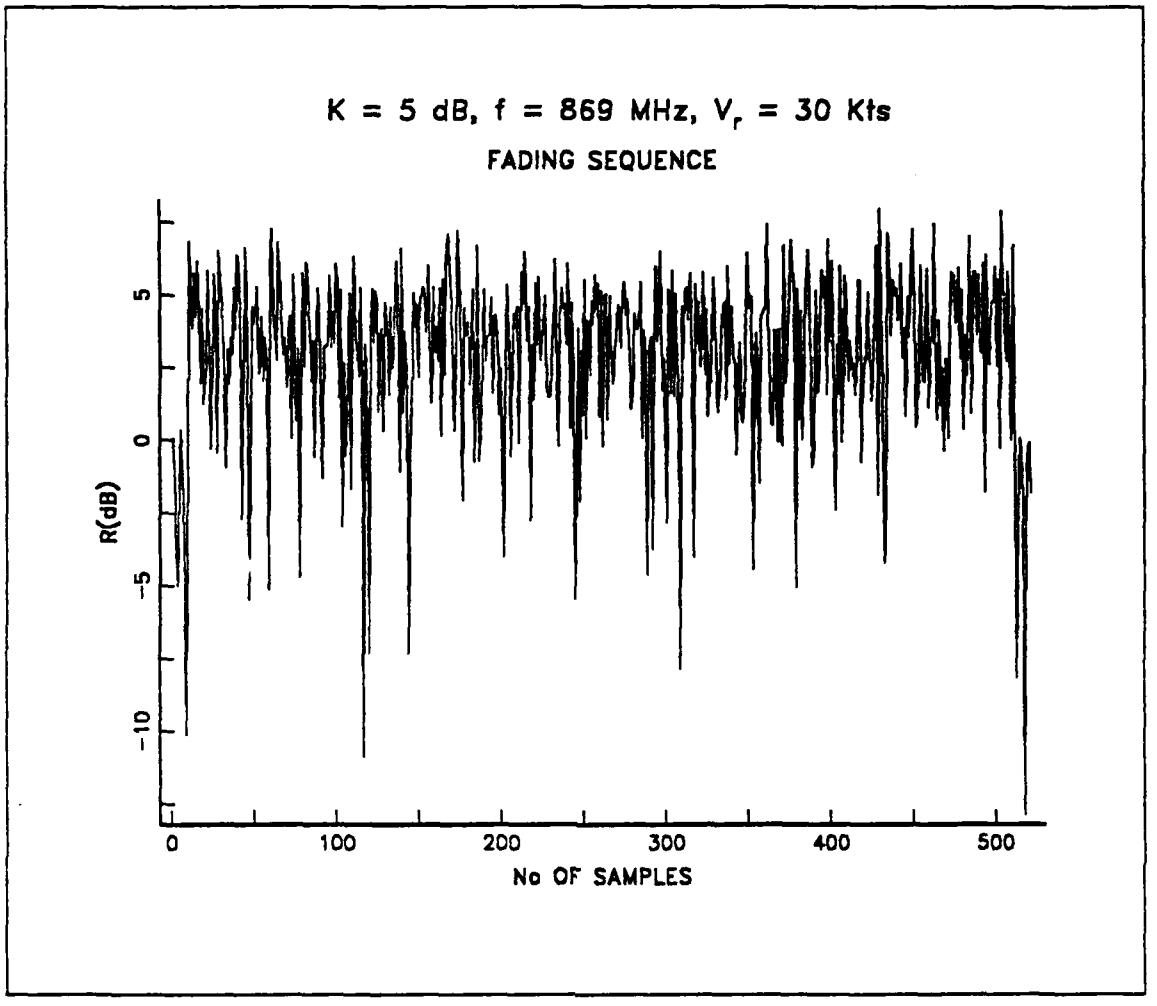

Figure 11. Rician fading sequence for K = 5 dB, f = 869 MHz, V = 30 Kts.

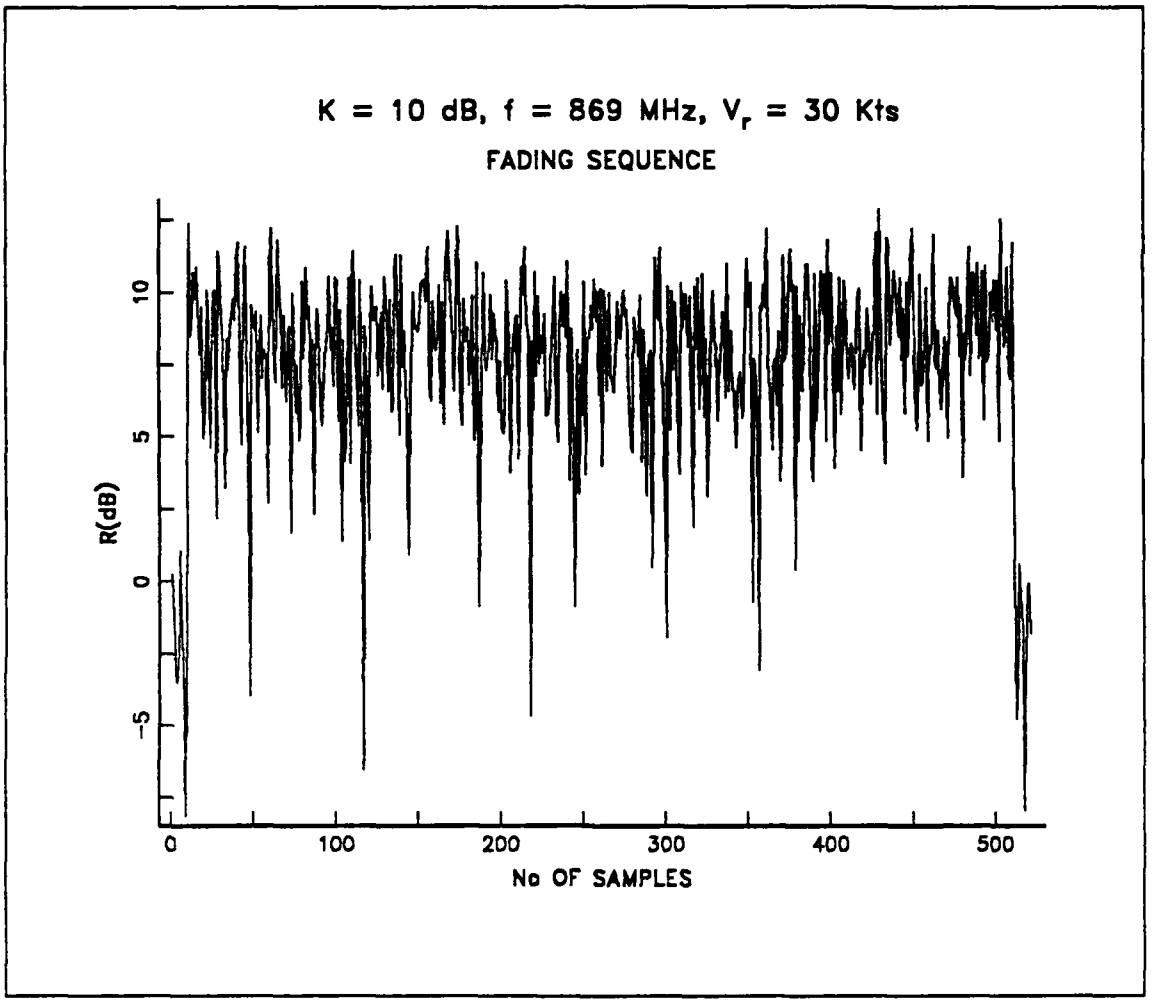

Figure 12. Rician fading sequence for K = 10 dB, f = 869 MHz, V = 30 Kts.

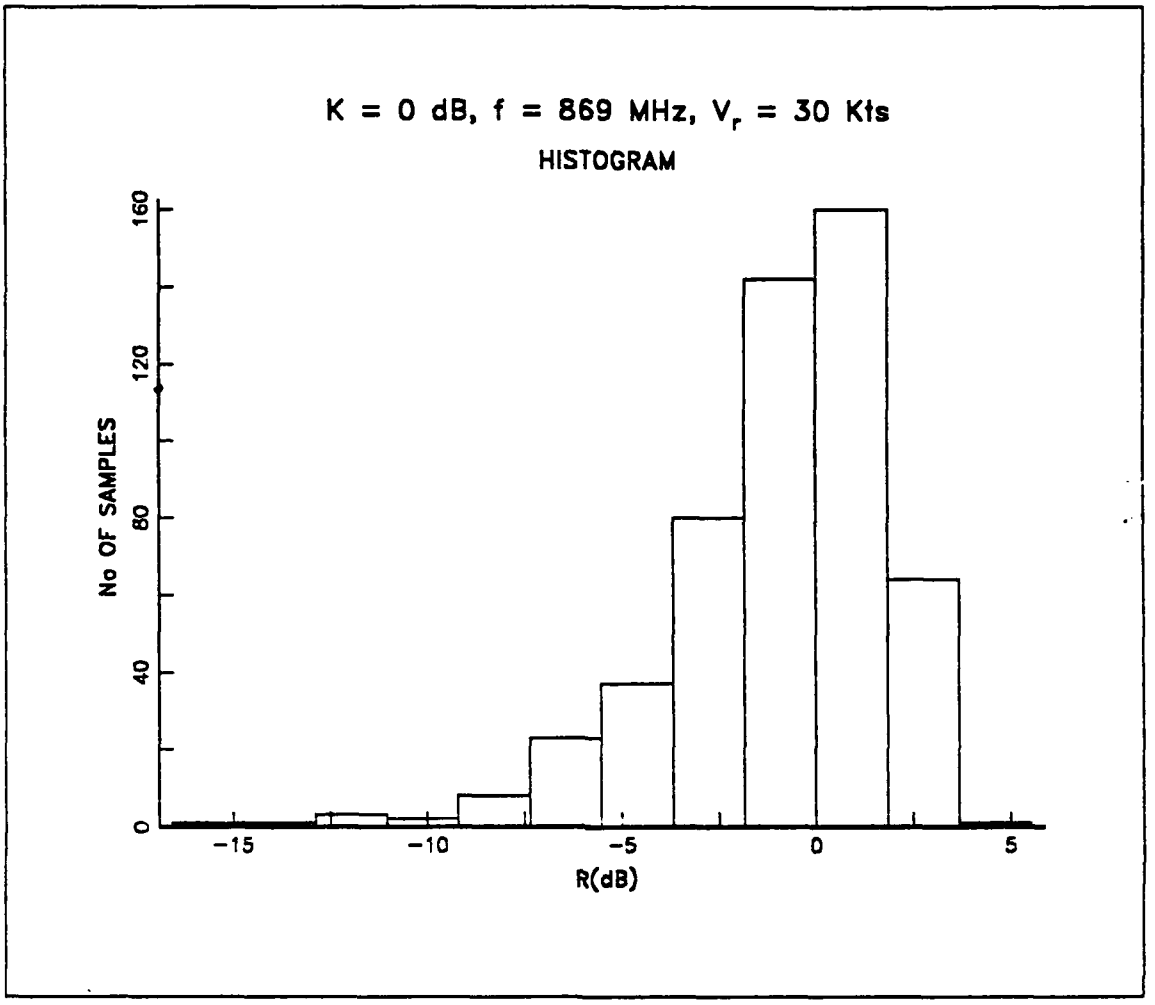

Figure 13. Histogram of a Rician fading sequence for K = 0 dB, f = 869 MHz, V = 30 Kts.

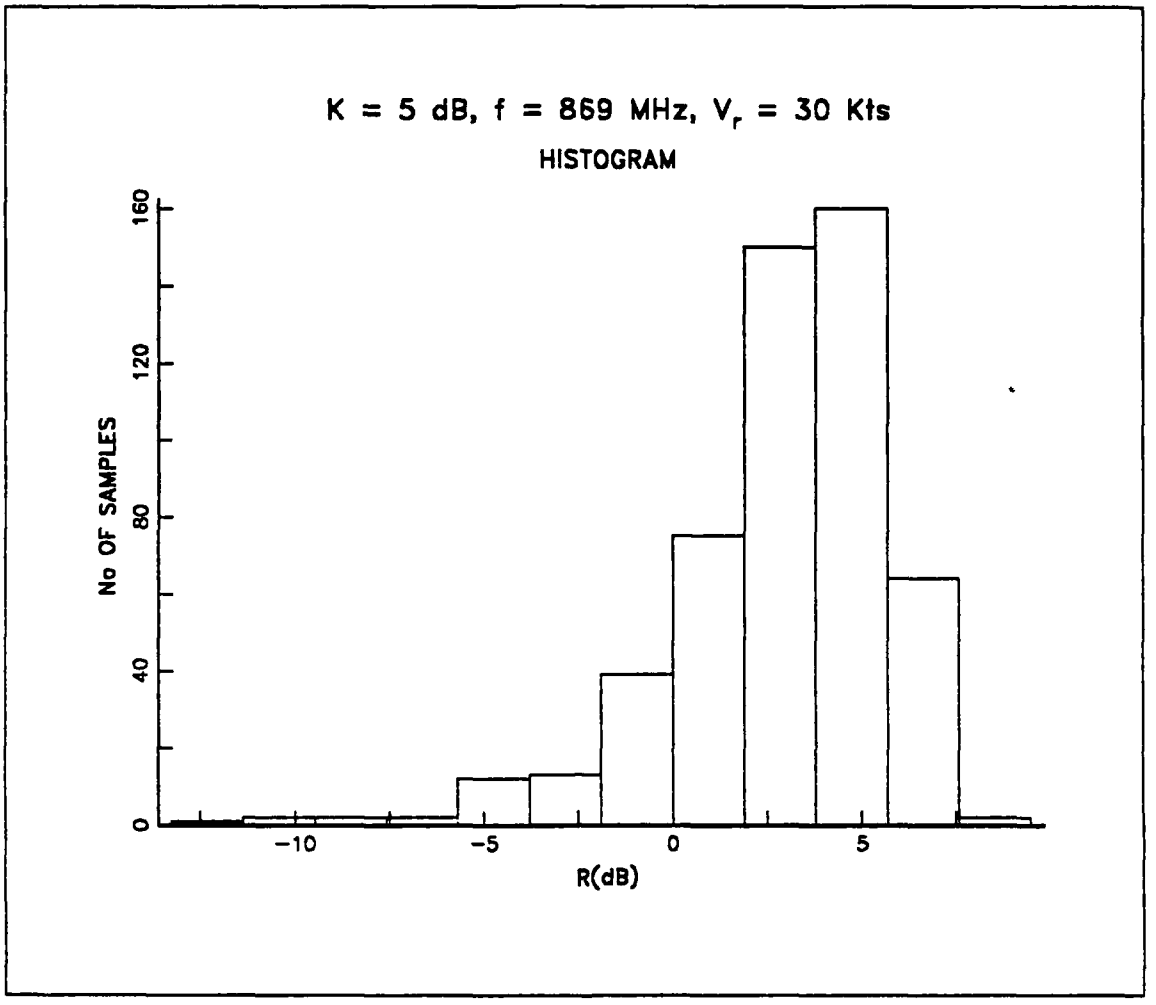

Figure 14. Histogram of a Rician fading sequence for K = 5 dB, f = 869 MHz, V = 30 Kts.

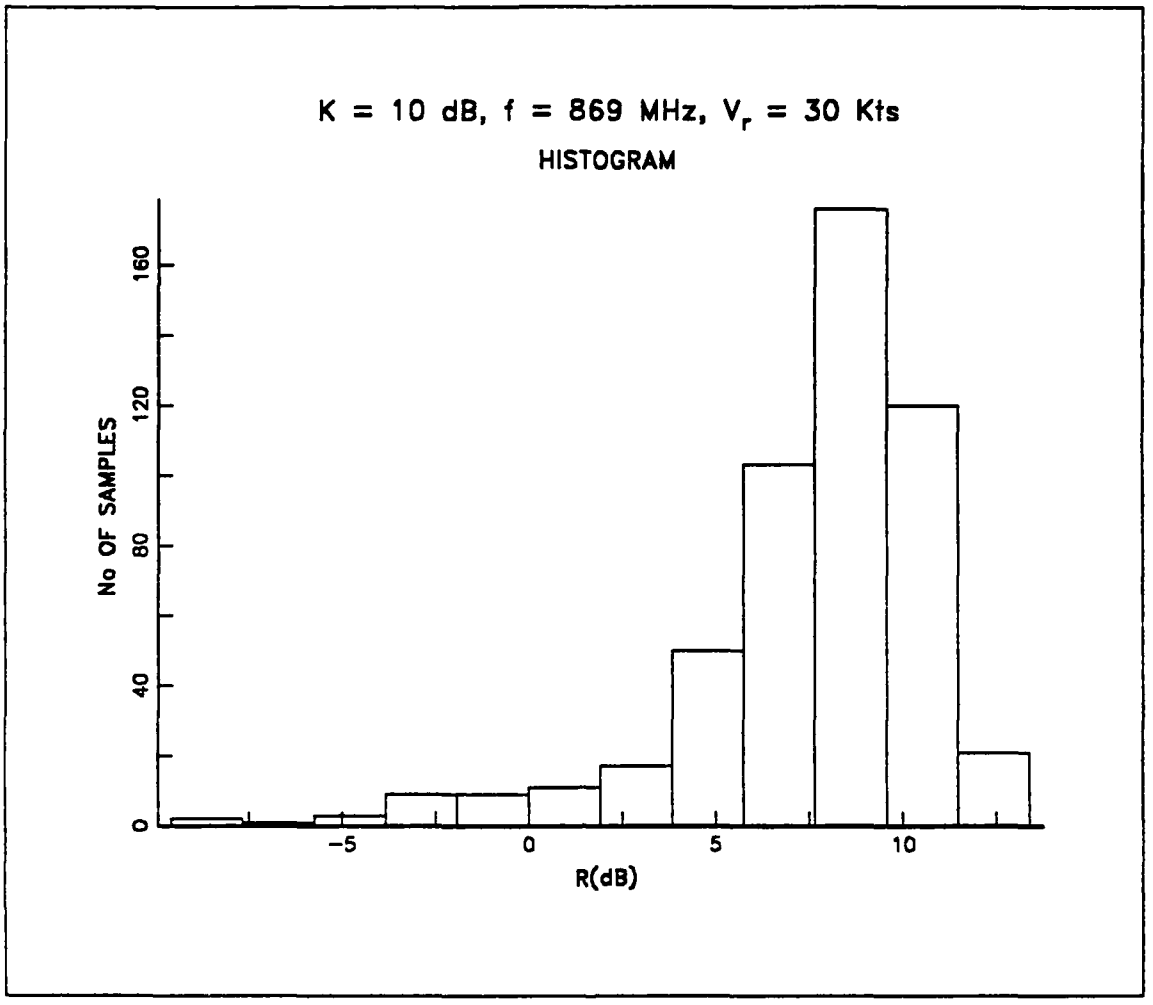

Figure 15. Histogram of a Rician fading sequence for K = 10 dB, f = 869 MHz, V = 30 Kts.

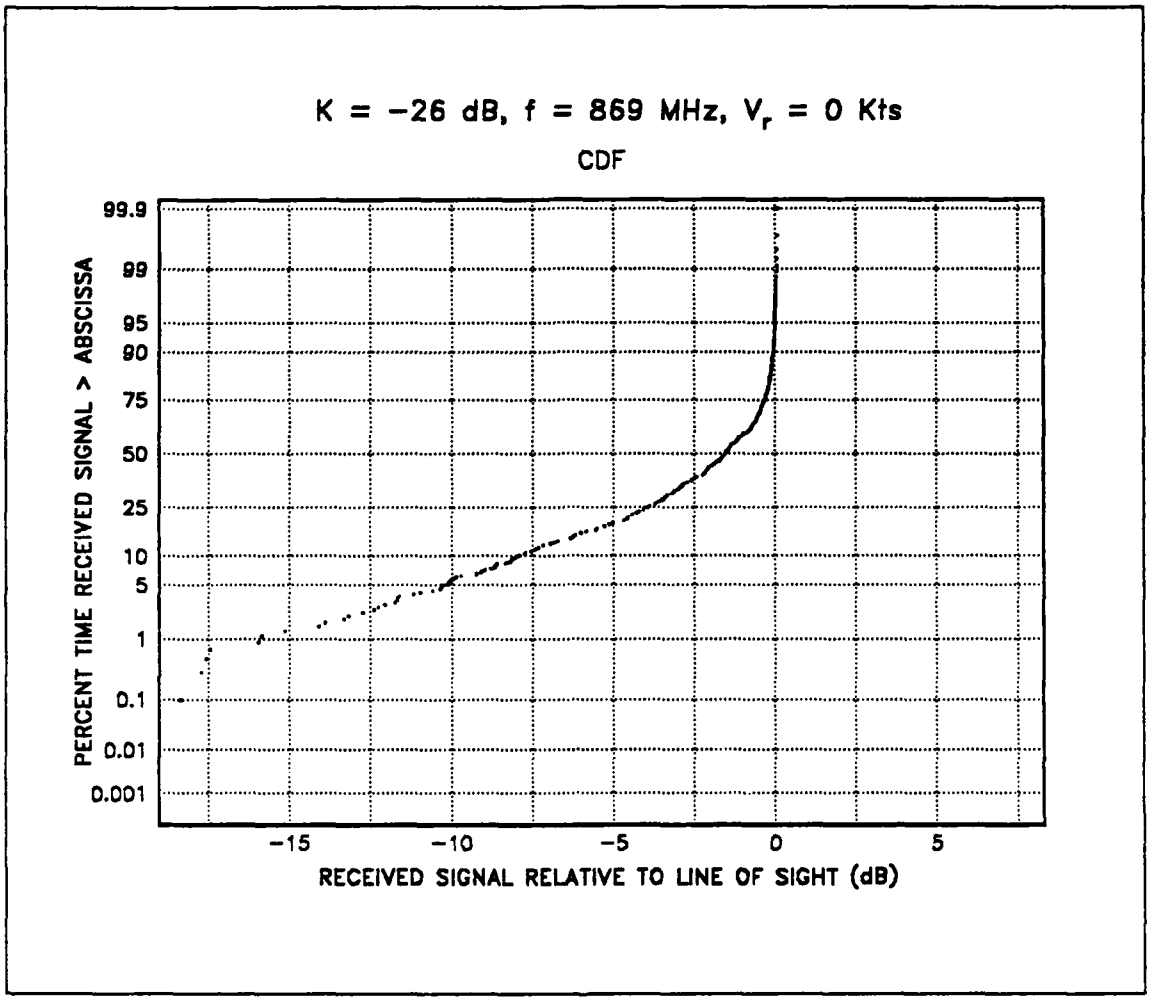

Figure 16. CDF of a Rician fading sequence for K = -26 dB, f = 869 MHz, V = 0 Kts.

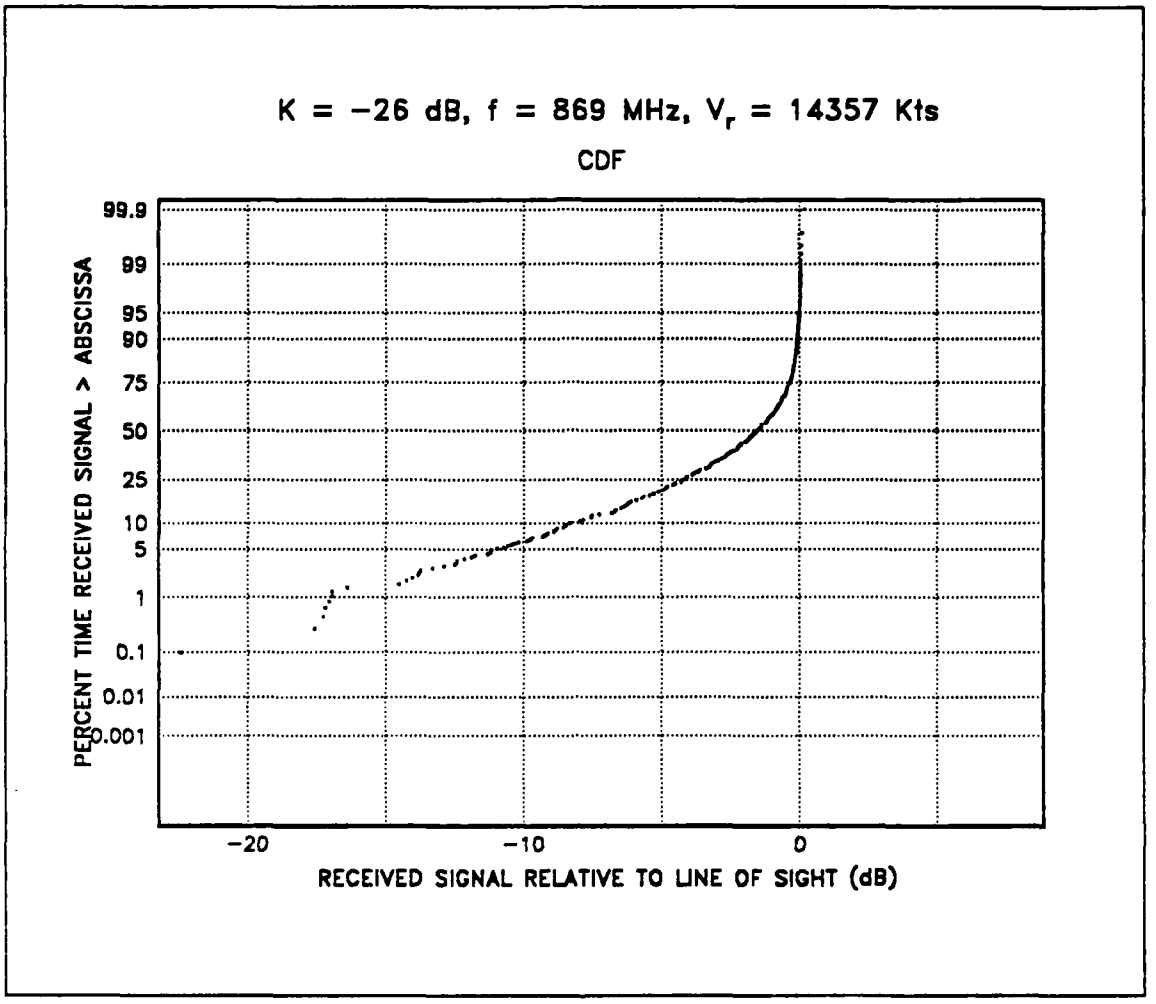

Figure 17. CDF of a Rician fading sequence for K = -26 dB, f = 869 MHz, V = 14357 Kts.

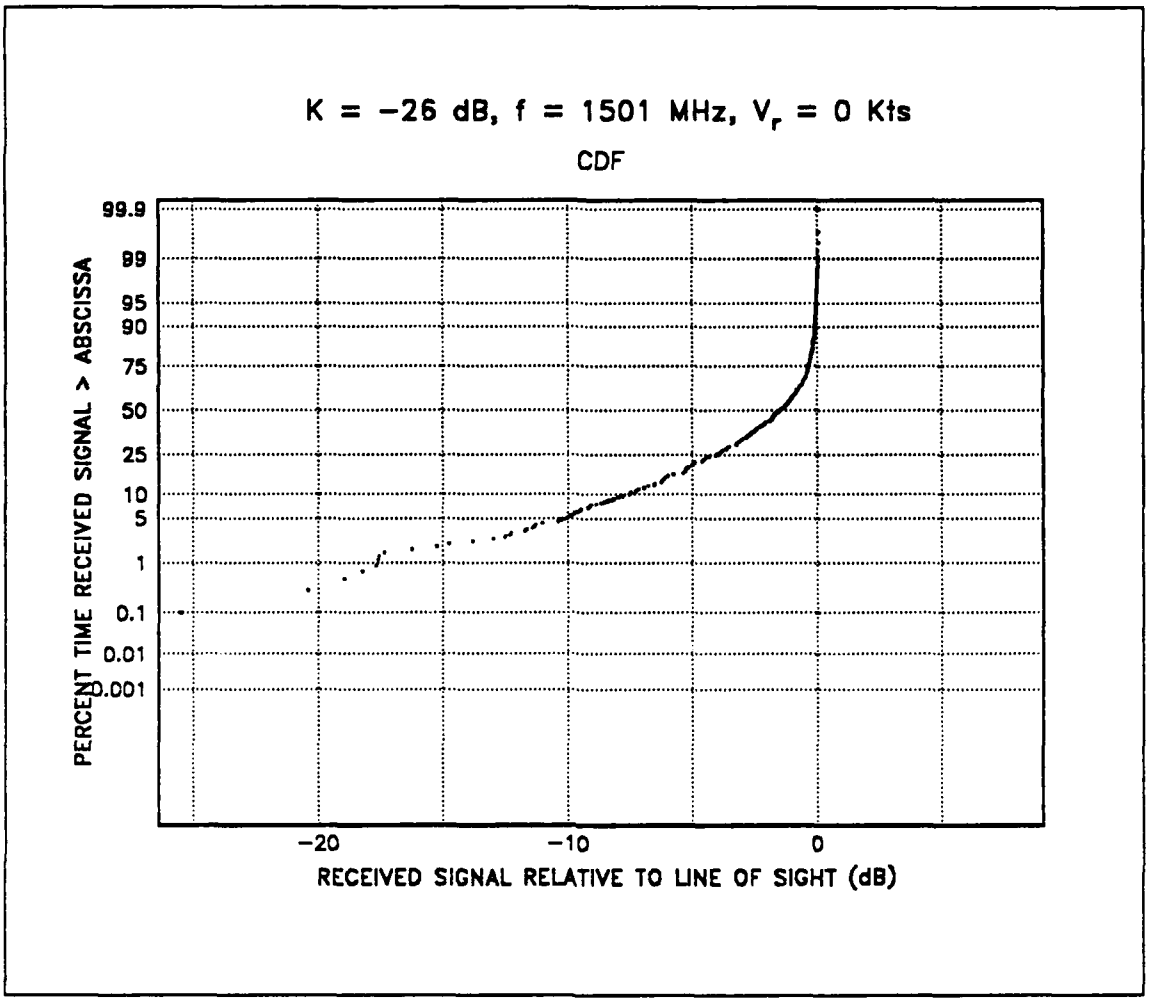

Figure 18. CDF of a Rician fading sequence for K = -26 dB, f = 1501 MHz, V = 0 Kts.

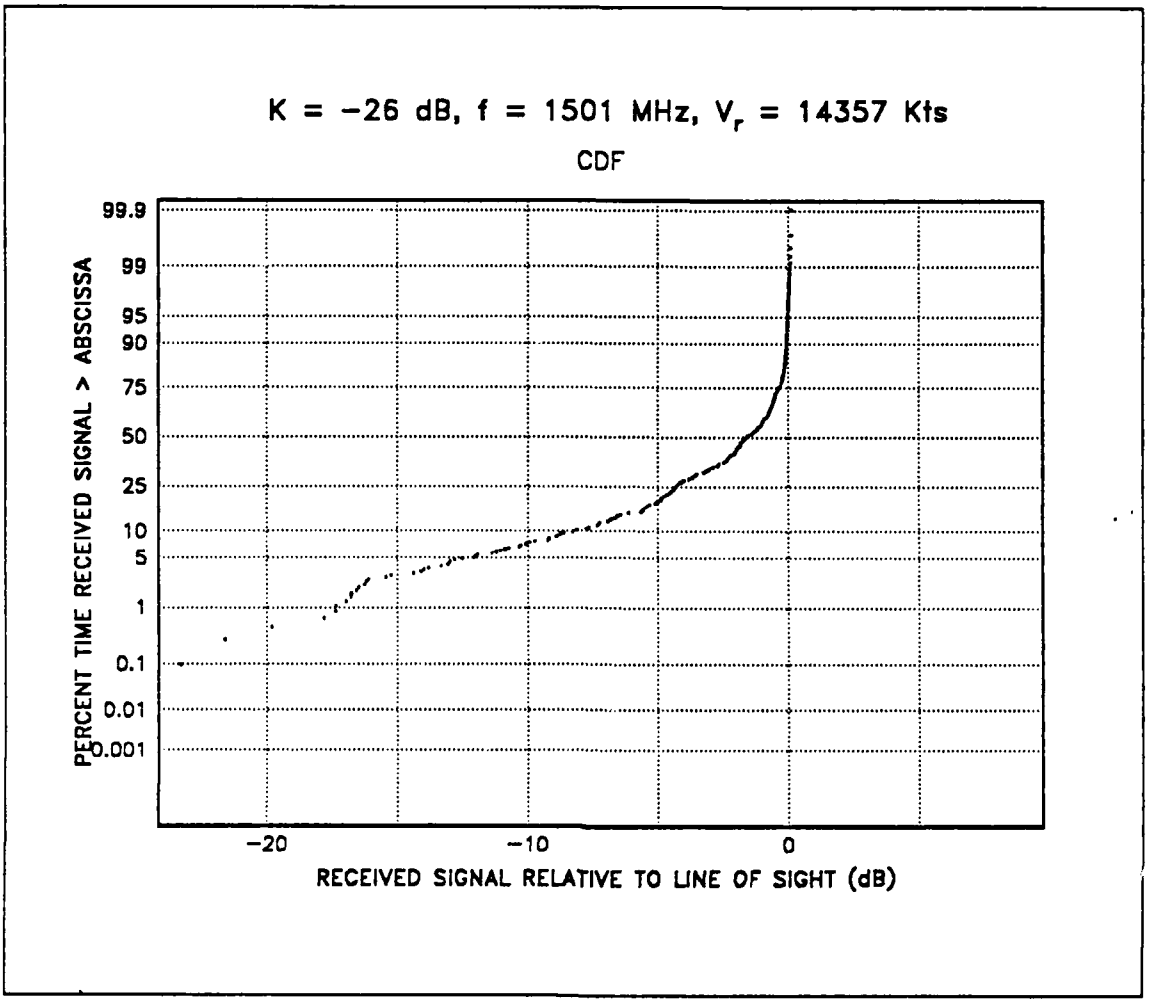

Figure 19. CDF of a Rician fading sequence for K = -26 dB, f = 1501 MHz, V = 14357 Kts.

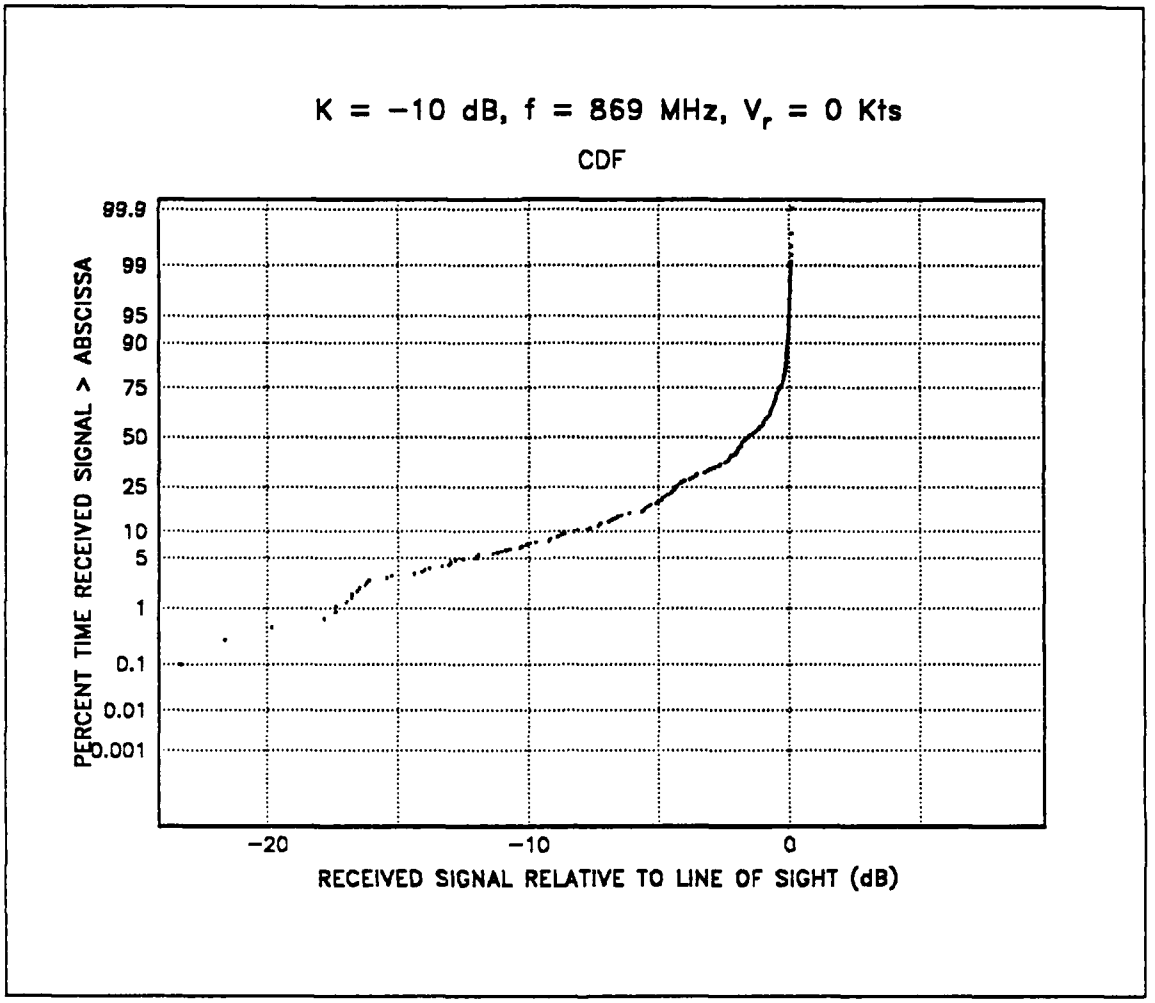

Figure 20. CDF of a Rician fading sequence for K = -10 dB, f = 869 MHz, V = 0 Kts.

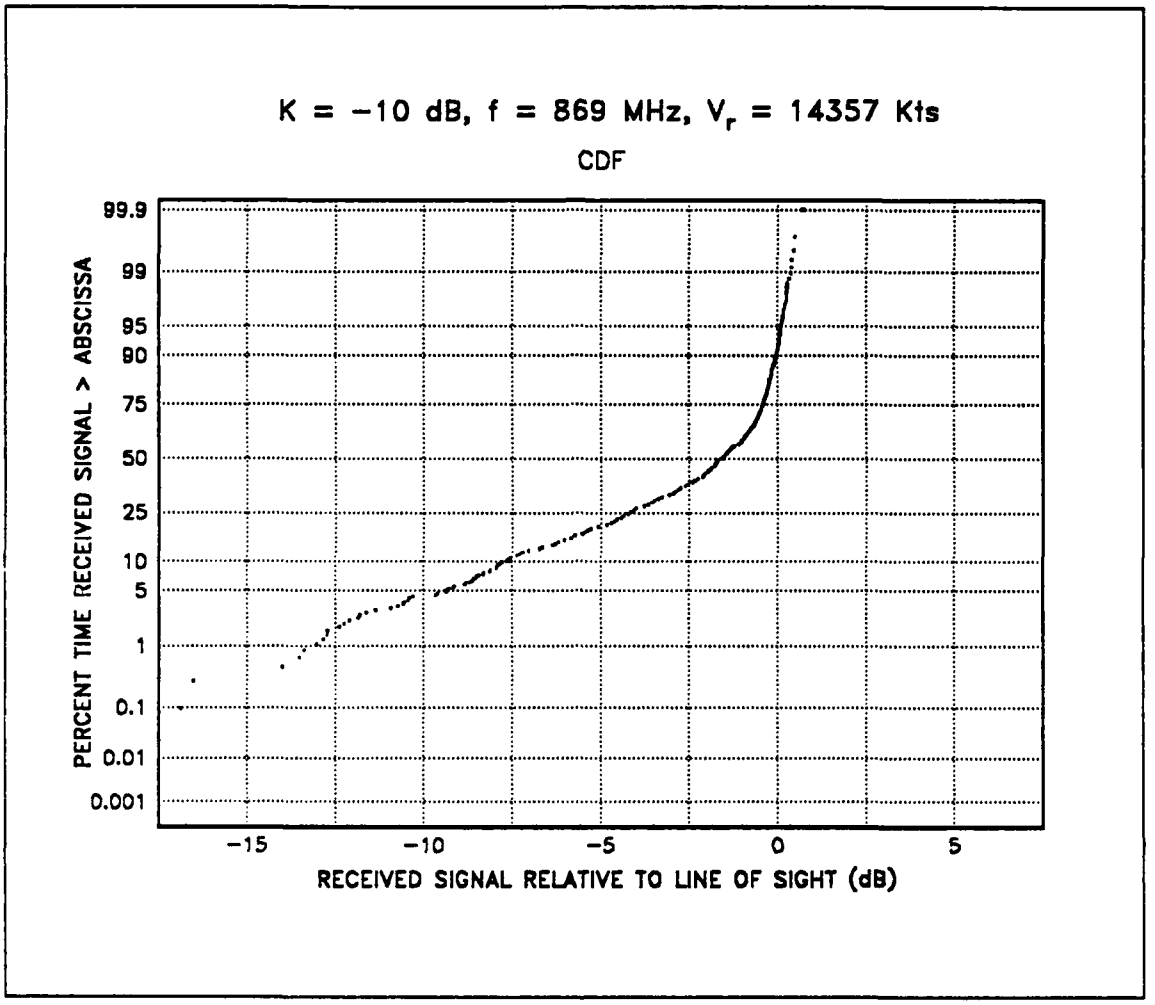

Figure 21. CDF of a Rician fading sequence for K = -10 dB, f = 869 MHz, V = 14357 Kts.

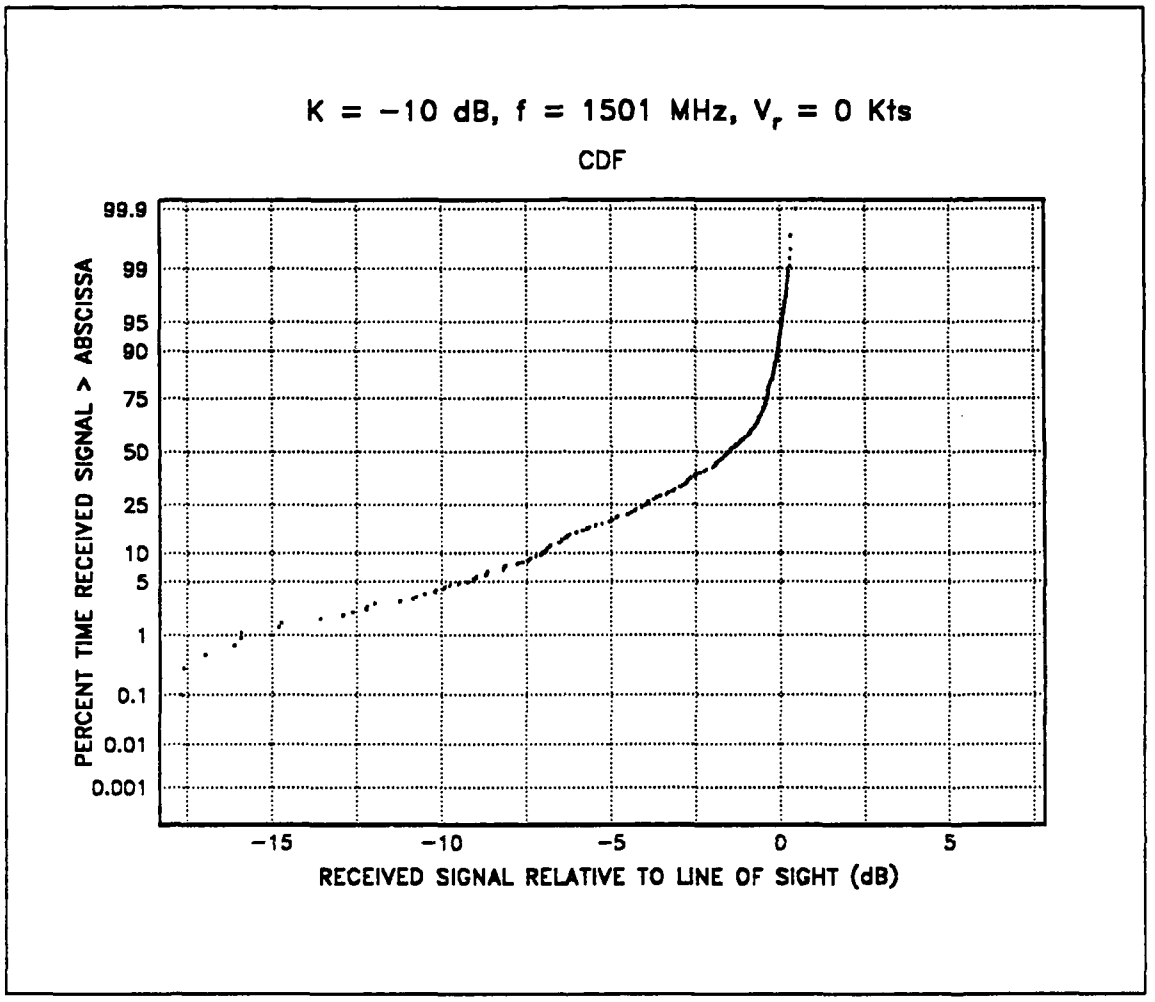

Figure 22. CDF of a Rician fading sequence for K = -10 dB, f = 1501 MHz, V = 0 Kts.

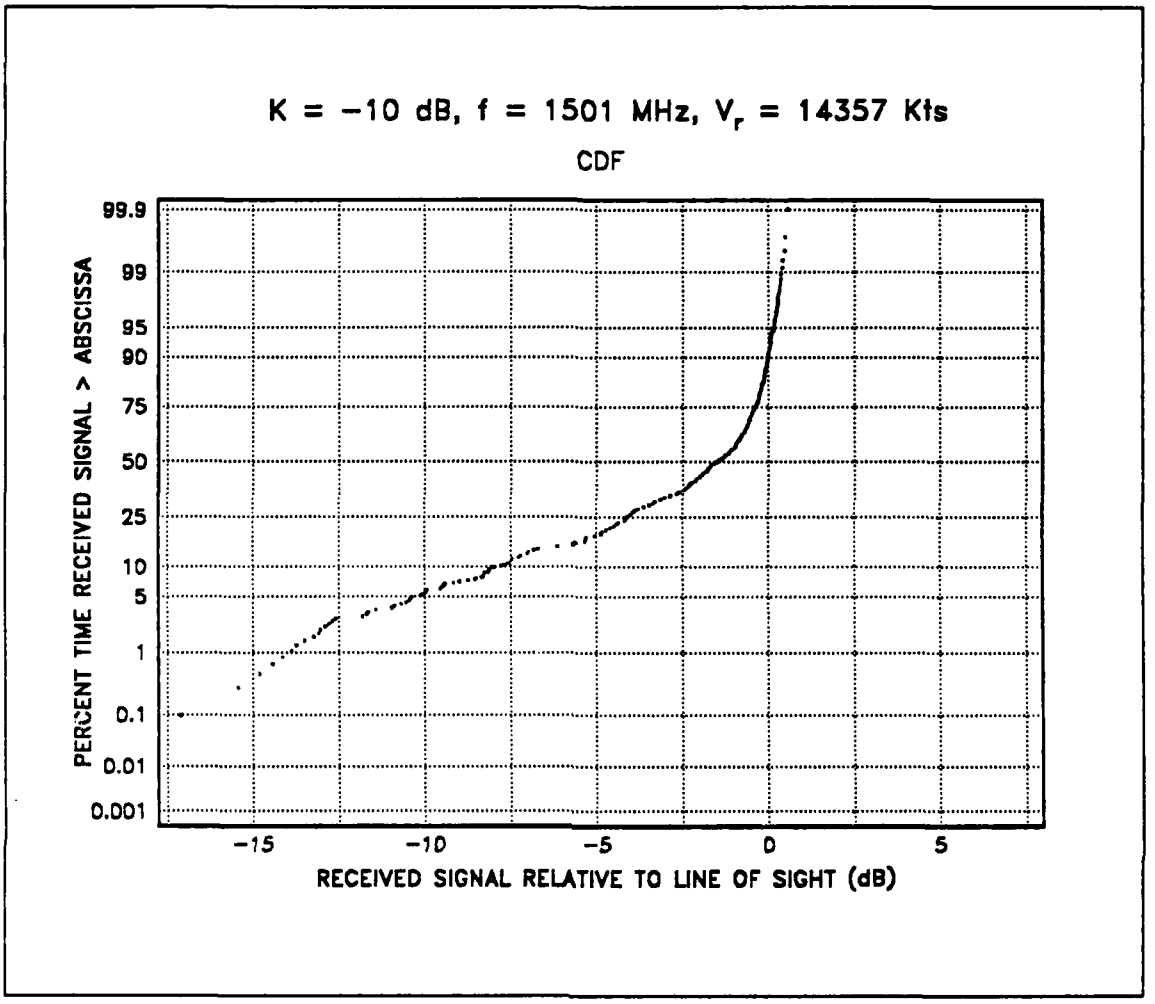

Figure 23. CDF of a Rician fading sequence for K = -10 dB, f = 1501 MHz, V = 14357 Kts.

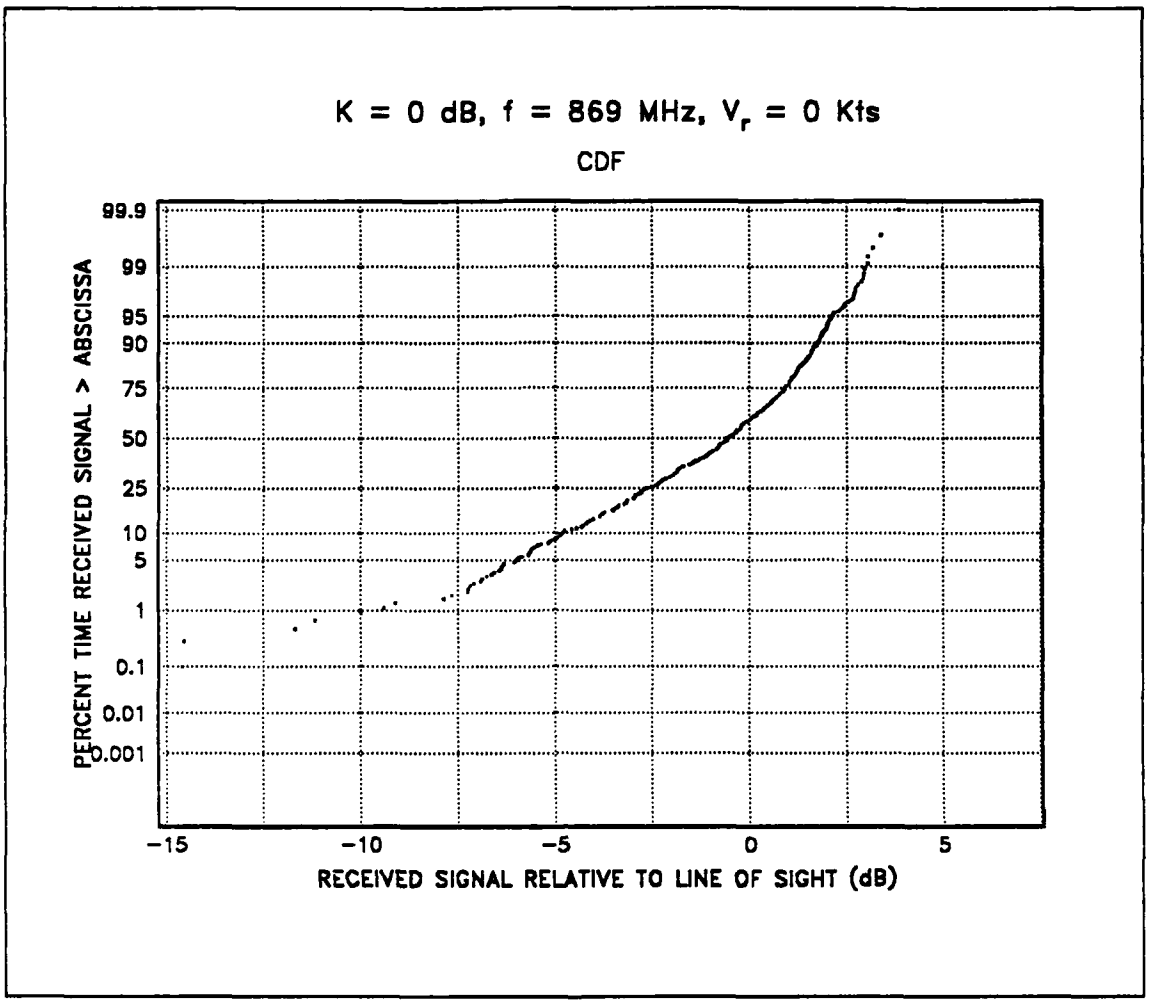

Figure 24. CDF of a Rician fading sequence for K = 0 dB, f = 869 MHz, V = 0 Kts.

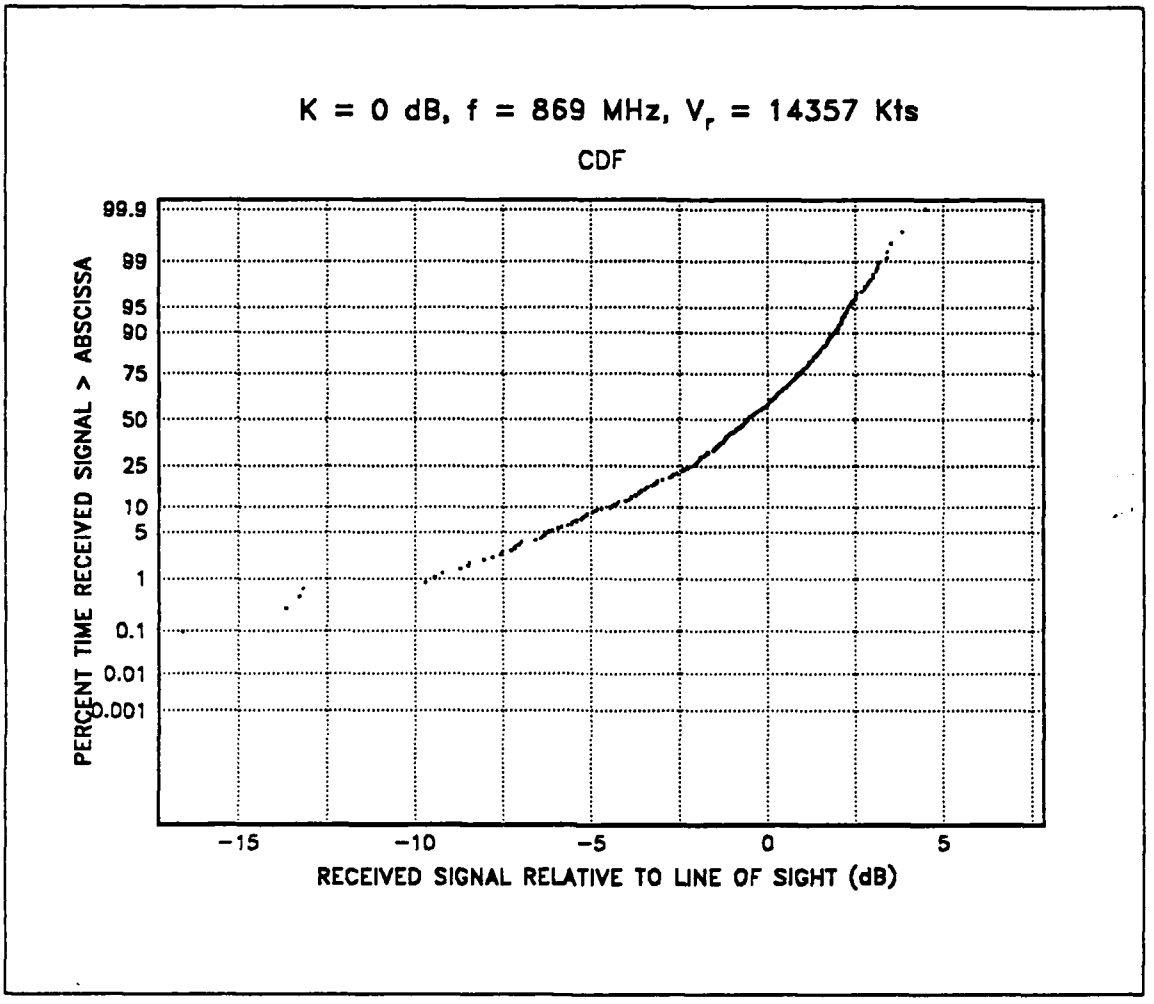

Figure 25. CDF of a Rician fading sequence for K = 0 dB, f = 869 MHz, V = 14357 Kts.

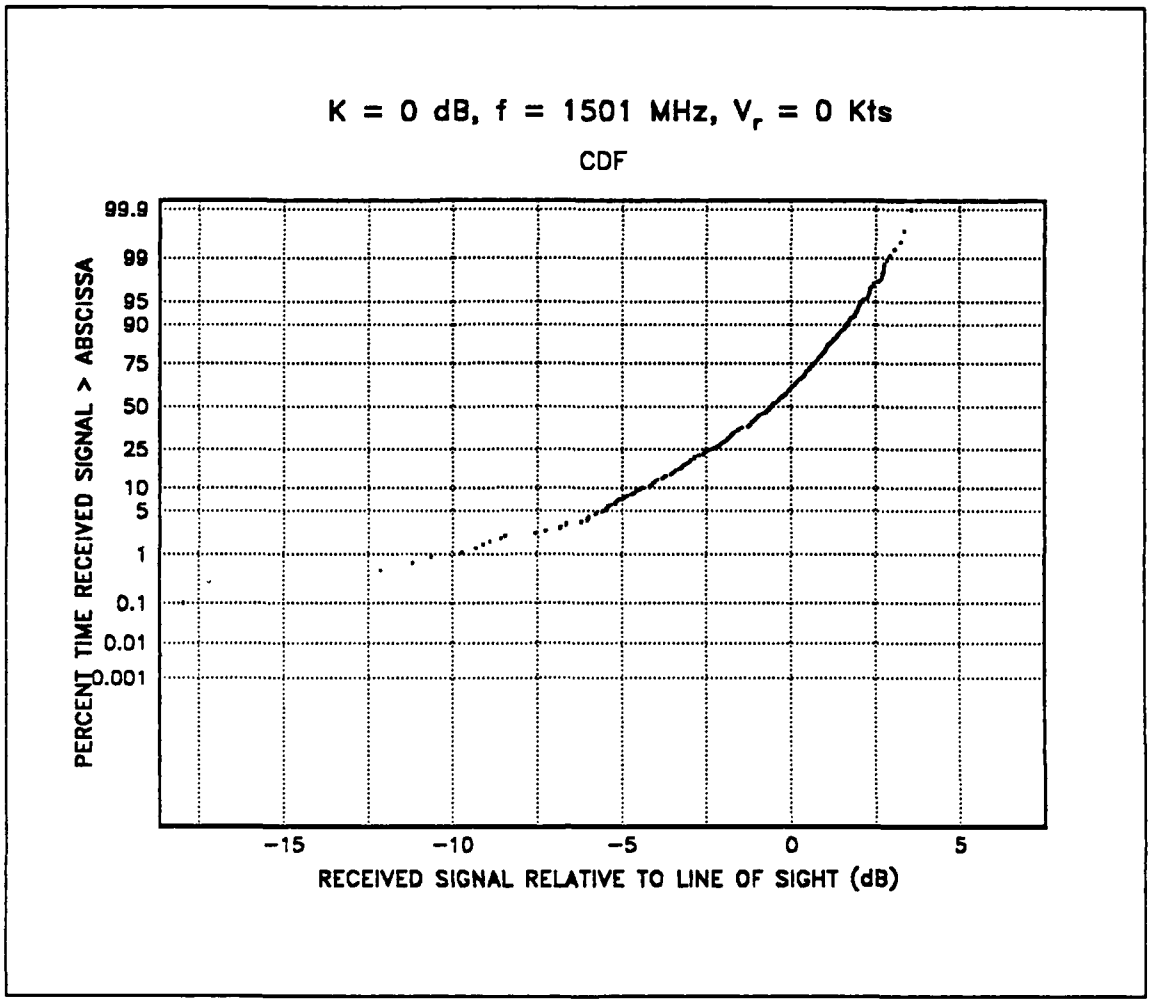

Figure 26. CDF of a Rician fading sequence for K = 0 dB, f = 1501 MHz, V = 0 Kts.

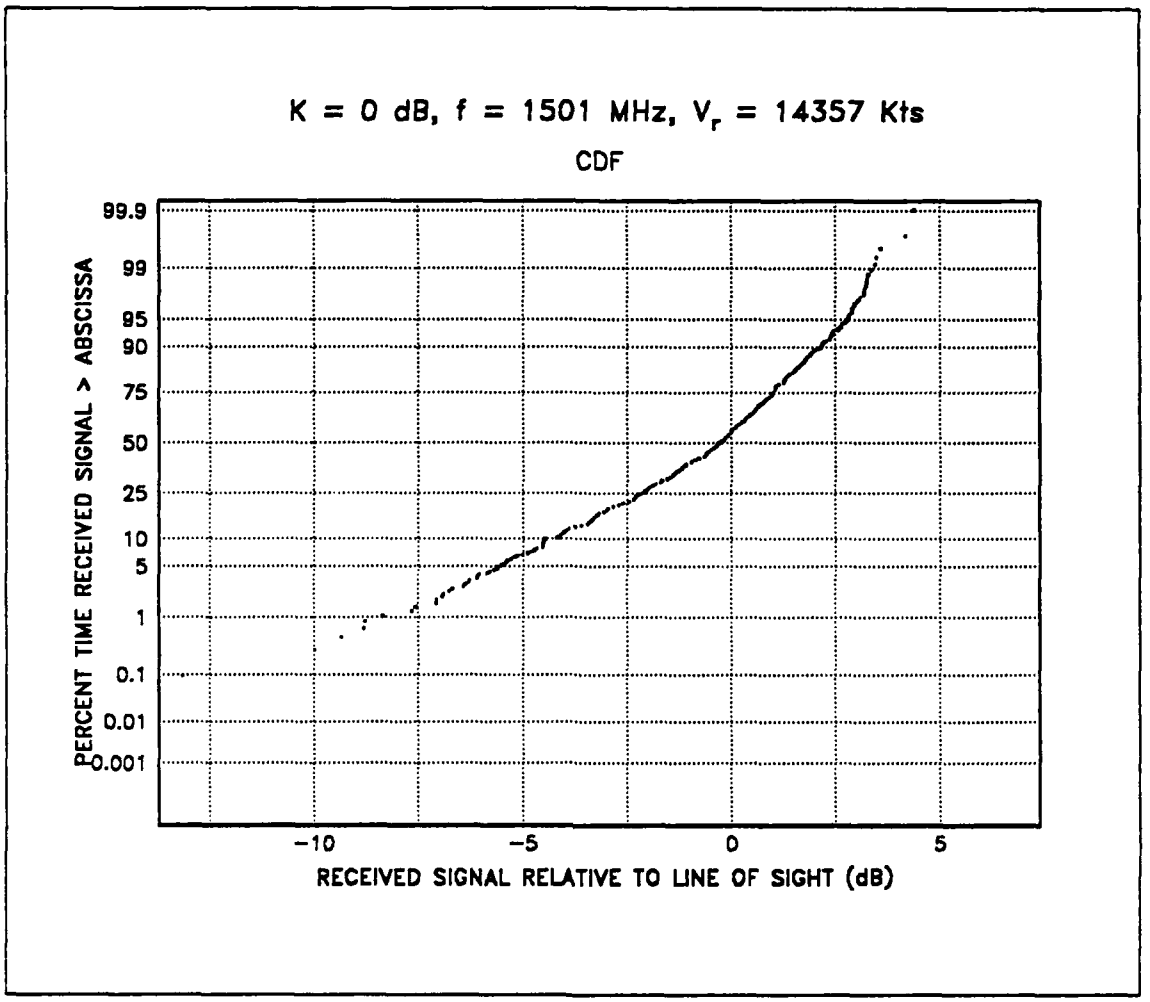

Figure 27. CDF of a Rician fading sequence for K = 0 dB, f = 1501 MHz, V = 14357 Kts.

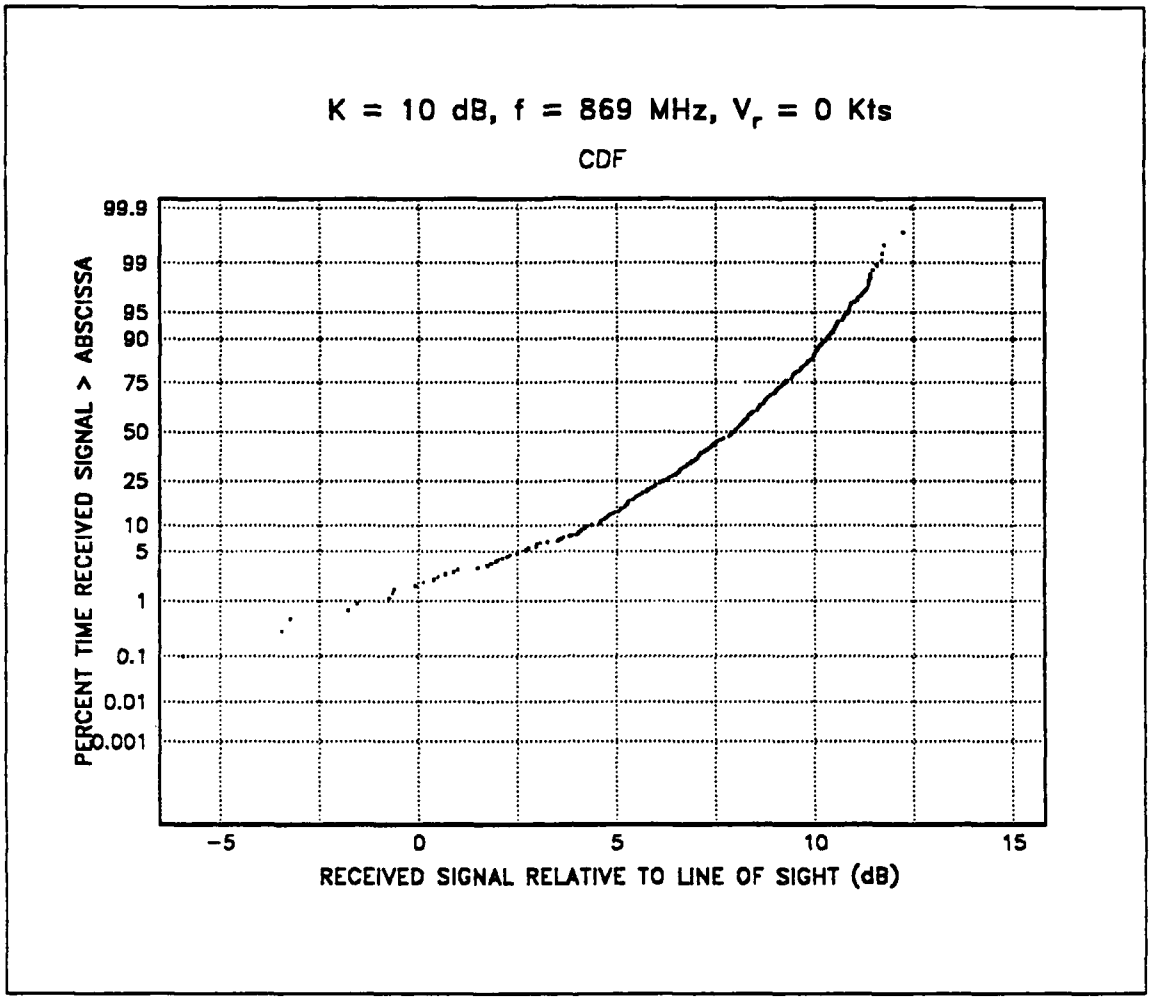

Figure 28. CDF of a Rician fading sequence for K = 10 dB, f = 869 MHz, V = 0 Kts.

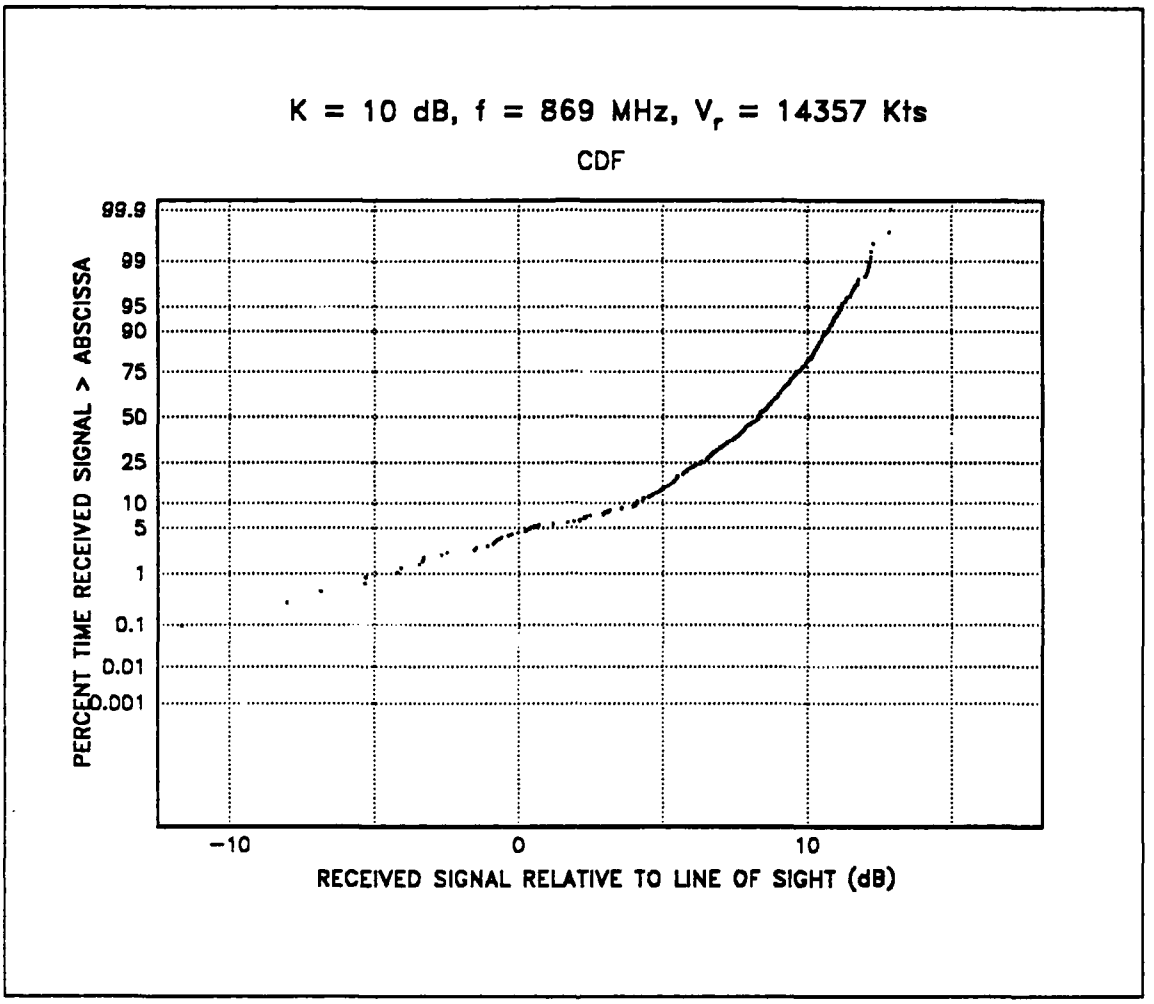

Figure 29. CDF of a Rician fading sequence for K = 10 dB, f = 869 MHz, V = 14357 Kts.

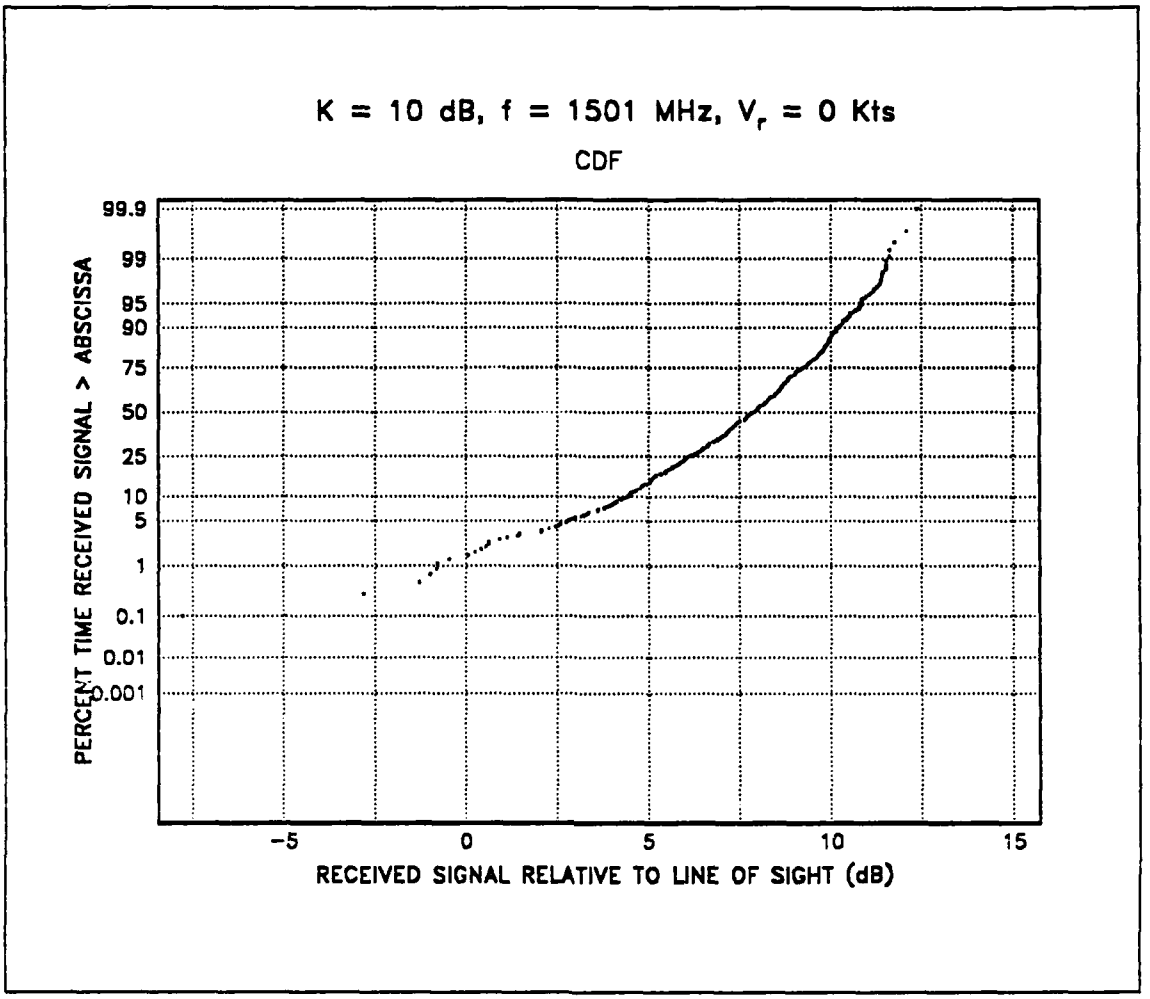

Figure 30. CDF of a Rician fading sequence for K = 10 dB, f = 1501 MHz, V = 0 Kts.

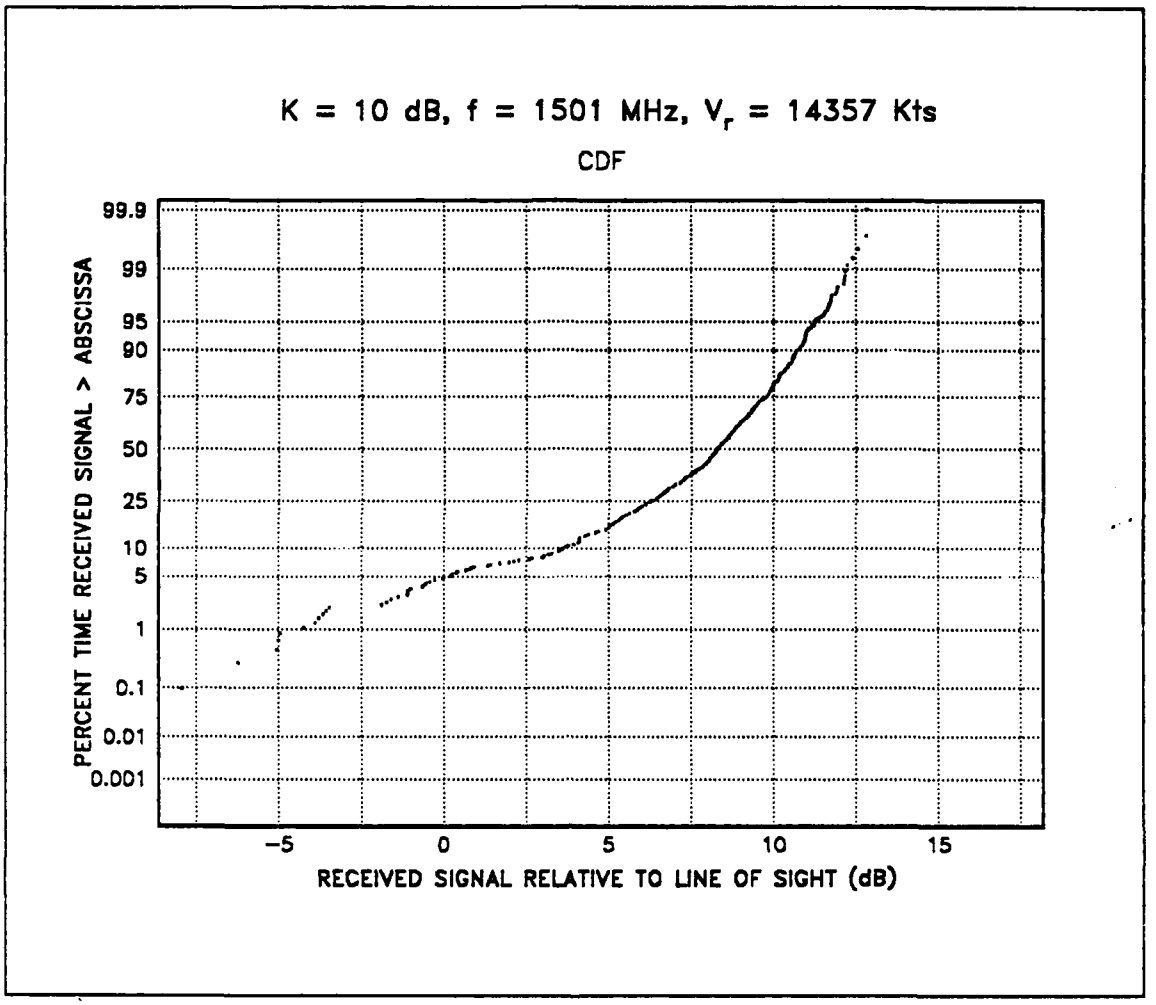

Figure 31. CDF of a Rician fading sequence for K = 10 dB, f = 1501 MHz, V = 14357 Kts.

IV. CAPACITY OF UNSLOTTED ALOHA MARITIME MOBILE SATELLITE SYSTEMS

A. INTRODUCTION

Aloha is a multiple access method commonly used in data communications. This chapter analyzes the throughput of unslotted Aloha with power capture in a Rician fading environment.

B. UNSLOTTED ALOHA THROUGHPUT

In the Aloha system, a satellite channel with a capacity of R bits per second is shared by a large population of users. Each user's station randomly transmits packets at the channel bit rate R whenever its buffer contains one packet. When packets from different stations overlap (packet collision), the transmission error can be detected at the transmitting stations on the downlink. The stations then retransmit the packets until they are free from overlap. To avoid repeated collisions, the interval of packet transmission is randomized for each station [Ref. 15].

In unslotted Aloha there are two types of capture effect: created and natural. Created capture effects occur when random power levels are used. In this case, the packet with the higher power level may capture the receiver when its signal-to-interference ratio exceeds a preset threshold. Natural capture effects occur in mobile radio communications when varying distances between mobile nodes and base stations, as well as channel fading, cause varying signal powers at the base station's receiver [Ref. 16].

As stated in the paper by Borchardt et al. [Ref. 17] about unslotted Aloha, let us assume an infinite number of uncoordinated users communicating to a base station using fixed length packets. The channel traffic is approximated by a Poisson proccess with parameter G packets per packet length. Thus the probability that a tagged packet is overlapped by n other packets during its transmission is the arrival probability of n packets during the interval $(t_0 - T, t_0 + T)$, where t_0 is the transmission instant of the tagged packet and T is the packet transmission time. This arrival probability is

$$Pr\{n\} = \frac{(2G)^n}{n!} \exp(-2G) \tag{4.1}$$

According to Borchardt et al. [Ref. 17], consider a receiver that captures a tagged packet in the presence of n interfering packets, if the tagged packet power sufficiently exceeds the joint interference power. These interferers form a stochastic proccess which consists of early interferers, whose transmission began in the interval $(t_0 - 1, t_0)$, and late interferers which enter the system in the interval $(t_0, t_0 + 1)$. With n interferers there are 2^n realizations of early and late interferers. C(n) is the number of realizations in which the maximum number of interferers does not exceed N (the maximum number of interferers that can be tolerated at any instant of time during the tagged packet transmission) and is given by [Ref. 18]

$$C(n) = \sum_{j=\lceil \frac{n}{2} \rceil}^{N} C_j(n) \qquad , [x] = \text{integer} \geq x \tag{4.2}$$

where

$$C_j(n) = \begin{cases} \binom{n}{j} \dfrac{(2j - n + 1)^2}{j + 1} & , j \geq n/2 \\ 0 & , \text{otherwise} \end{cases}$$

where $C_j(n)$ is the number of realizations in which the maximum number of interferers equals j.

The capture effect in a random access channel occurs naturally when fading reduces the joint power of interfering packets, as reported in [Ref. 19] for a slotted Aloha channel in a uniform Rayleigh fading environment. This thesis extends these results to unslotted Aloha in a Rician fading environment.

It is assumed that a tagged packet will capture the receiver if its signal-to-interference ratio exceeds a threshold γ_0.

The probability density function of a packet's power in a Rician fading channel is

$$f_P(p) = \frac{1}{\alpha} I_0\left(\frac{2A_0\sqrt{p}}{\alpha} \right) \exp\left(-\frac{p + A_0^2}{\alpha} \right) \tag{4.3}$$

The same expression for a normalized mean power $\alpha = 1$ is

$$f_P(p) = \exp(-A_0^2) I_0(2A_0\sqrt{p}) \exp(-p) \tag{4.4}$$

Thus given n interfering packets during the transmission of a tagged packet, the density function of the power of n interfering packets is [Ref. 17]

$$f_Y(y|n) = \frac{1}{2^n} \sum_{j=\lfloor \frac{n}{2} \rfloor}^{n} C_j(n) \{f_P(p)\}^{j\otimes} \tag{4.5}$$

Substituting equation (4.4) into equation (4.5) we get

$$f_Y(y|n) = \frac{1}{2^n} \sum_{j=\lfloor \frac{n}{2} \rfloor}^{n} C_j(n) \{ \exp(-A_0^2) I_0(2A_0\sqrt{y}) \exp(-y)\}^{j\otimes} \tag{4.6}$$

where $j\otimes$ denotes the j-fold convolution.

Appendix B illustrates the derivation of

$$\left[\exp(-A_0^2) I_0(2A_0\sqrt{y}) \exp(-y) \right]^{j\otimes} \quad \text{for} \quad j = 1,2,3,4,5 \text{ and } 6$$

The density function of the power of the signal-to-interference ratio $Z = \frac{X}{Y}$ is obtained by

$$f_Z(z|n) = \int_0^\infty y f_X(yz) f_Y(y|n) dy \tag{4.7}$$

Thus

$$f_Z(z|n) = \frac{1}{2^n} \int_0^\infty y \exp(-A_0^2) I_0(2A_0\sqrt{yz}) \exp(-yz) \left\{ \sum_{j=\lfloor n/2 \rfloor}^{n} C_j(n) [\exp - A_0^2 I_0(2A_0\sqrt{y}) \cdot \exp(-y)]^{j\otimes} \right\} \tag{4.8}$$

The capture probability is given by

$$Pr\{capture|n, n\geq 1\} = 1 - P_r\{0 \leq Z \leq \gamma_0 | n, n \geq 1\} \tag{4.9}$$

Therefore we have

$$Pr\{capture|n, n\geq 1\} = 1 - \int_0^{\gamma_0} f_Z(z|n) dz \tag{4.10}$$

Appendix B illustrates the derivation of the probabilities of capture for $n = 1,2,3,4,5$ and 6.

Channel throughput S is defined by

$$S = GPr\{capture\} = G\sum_{n=0}^{\infty} Pr\{capture|n\}Pr\{n\} \tag{4.11}$$

Replacing equations (4.1) and (4.9) in equation (4.11), the throughput of unslotted Aloha in a Rician fading channel is given by

$$S = G\sum_{n=0}^{\infty} \frac{(2G)^n}{n!} \exp(-2G) Pr\{capture|n\} \tag{4.12}$$

and given that $Pr\{capture|0\} = 1$ it reduces to

$$G\exp(-2G)\left[1 + \sum_{n=1}^{\infty} \frac{2G^n}{n!} Pr\{capture|n\}\right] \tag{4.13}$$

Figures 32, 33 and 34 illustrate the throughput for several capture thresholds γ_0 using $A_0 = 0.1$, $A_0 = 0.5$ and $A_0 = 1$ respectively. Finally, Figure 35 illustrates the throughput for the same capture thresholds γ_0, but letting parameter $A_0 = 0$ (Rayleigh fading). As expected the same throughput of unslotted Aloha in a Rayleigh fading environment [Ref. 17] were obtained.

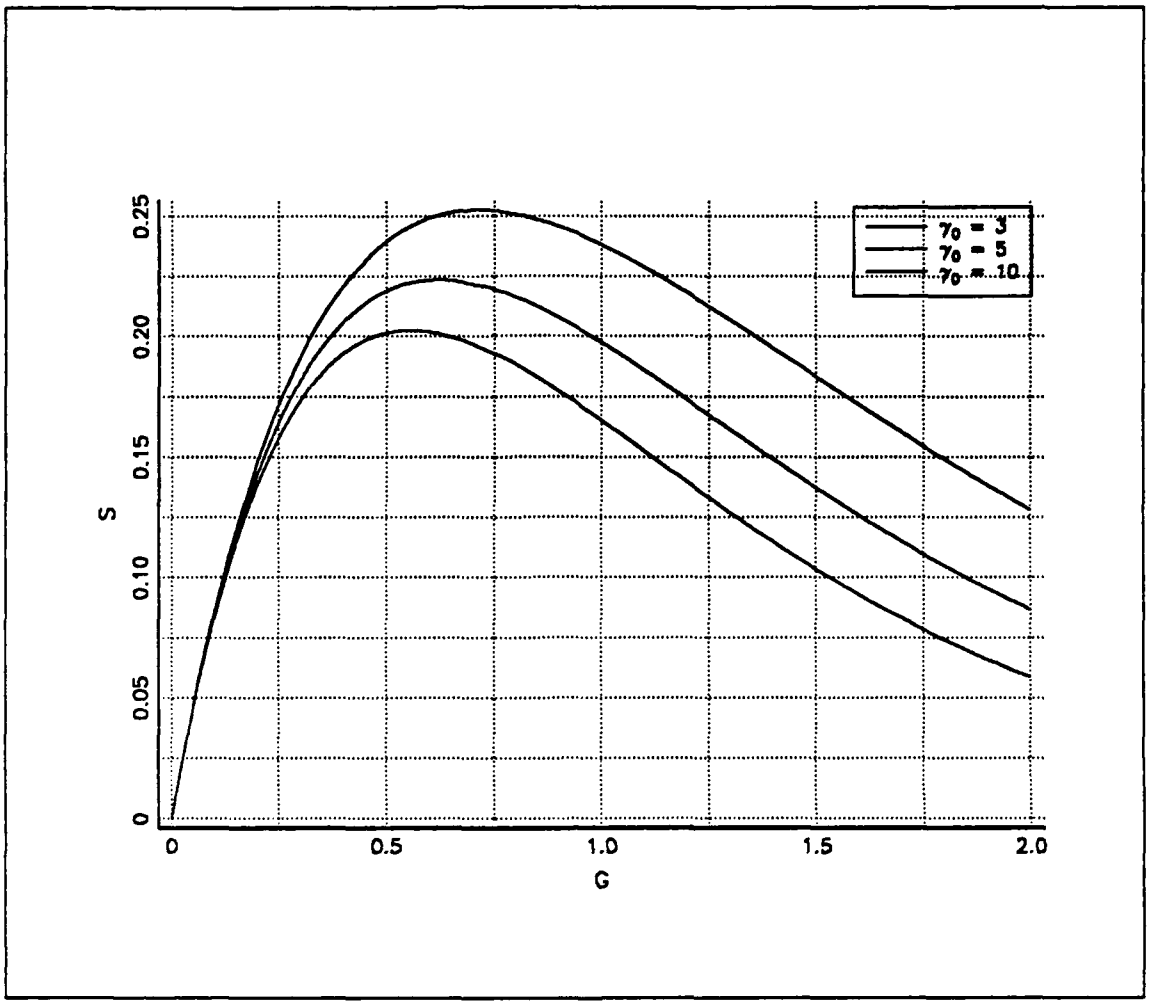

Figure 32. Unslotted Aloha throughput ($A_0 = 0.1$)

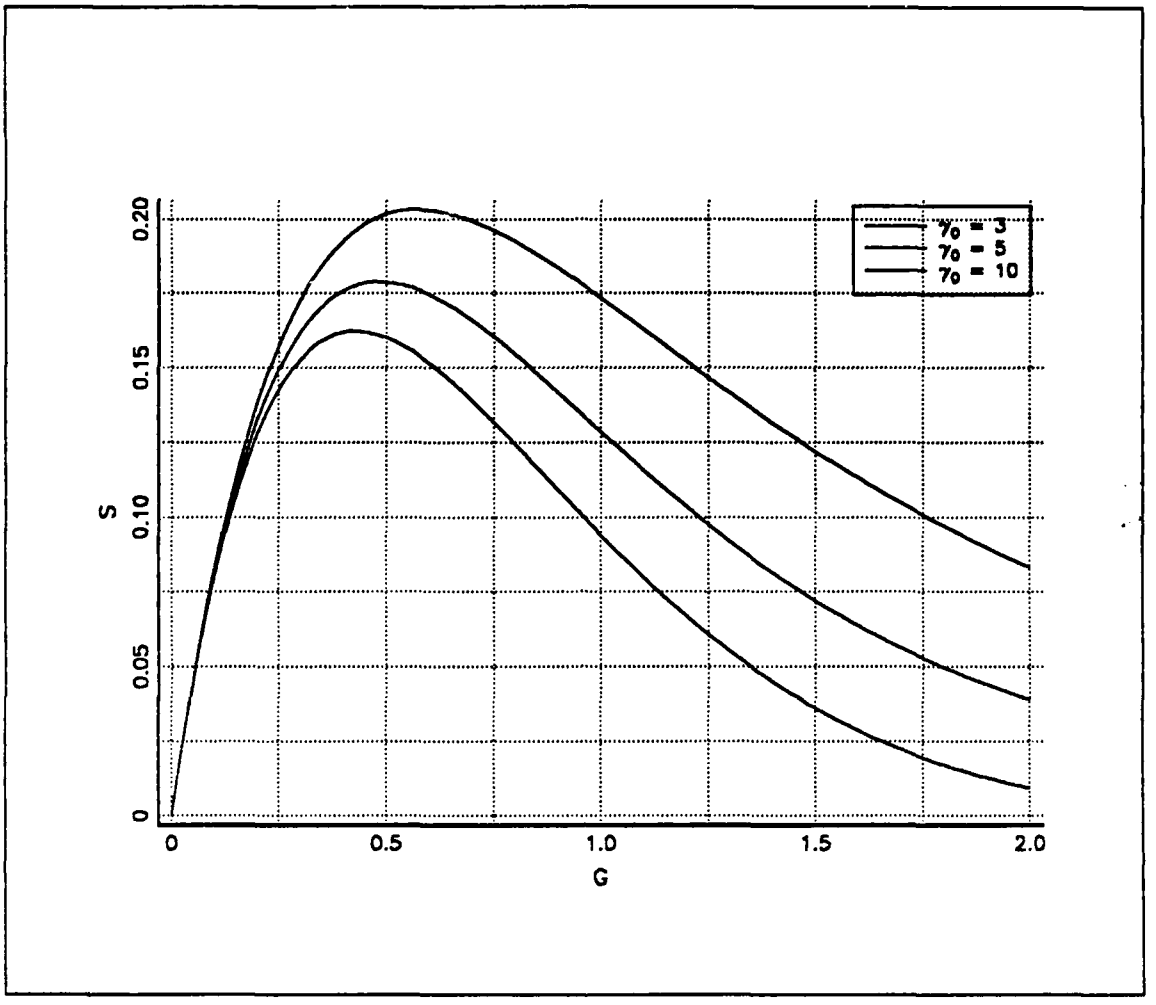

Figure 33. Unslotted Aloha throughput ($A_0 = 0.5$)

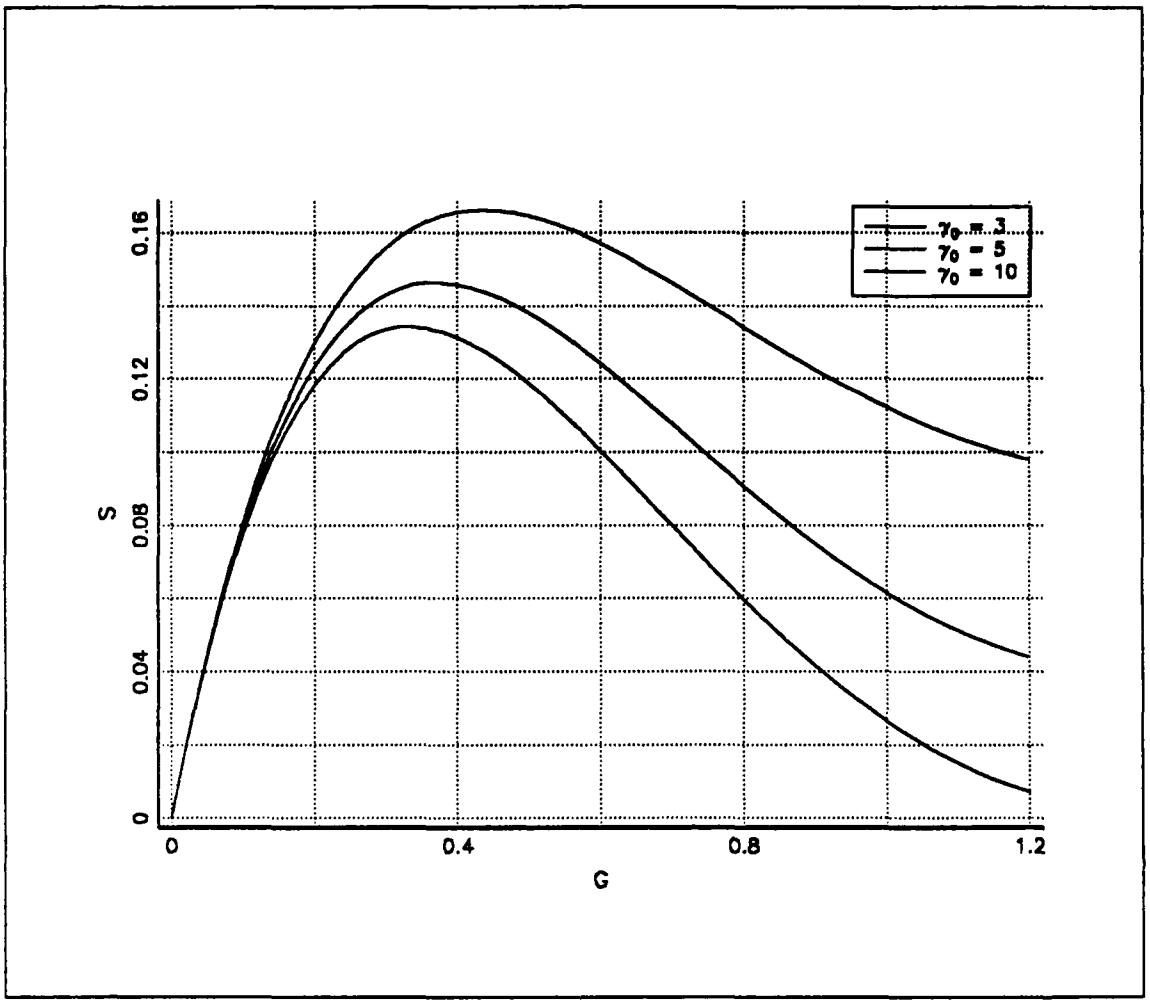

Figure 34. Unslotted Aloha throughput ($A_0 = 1$)

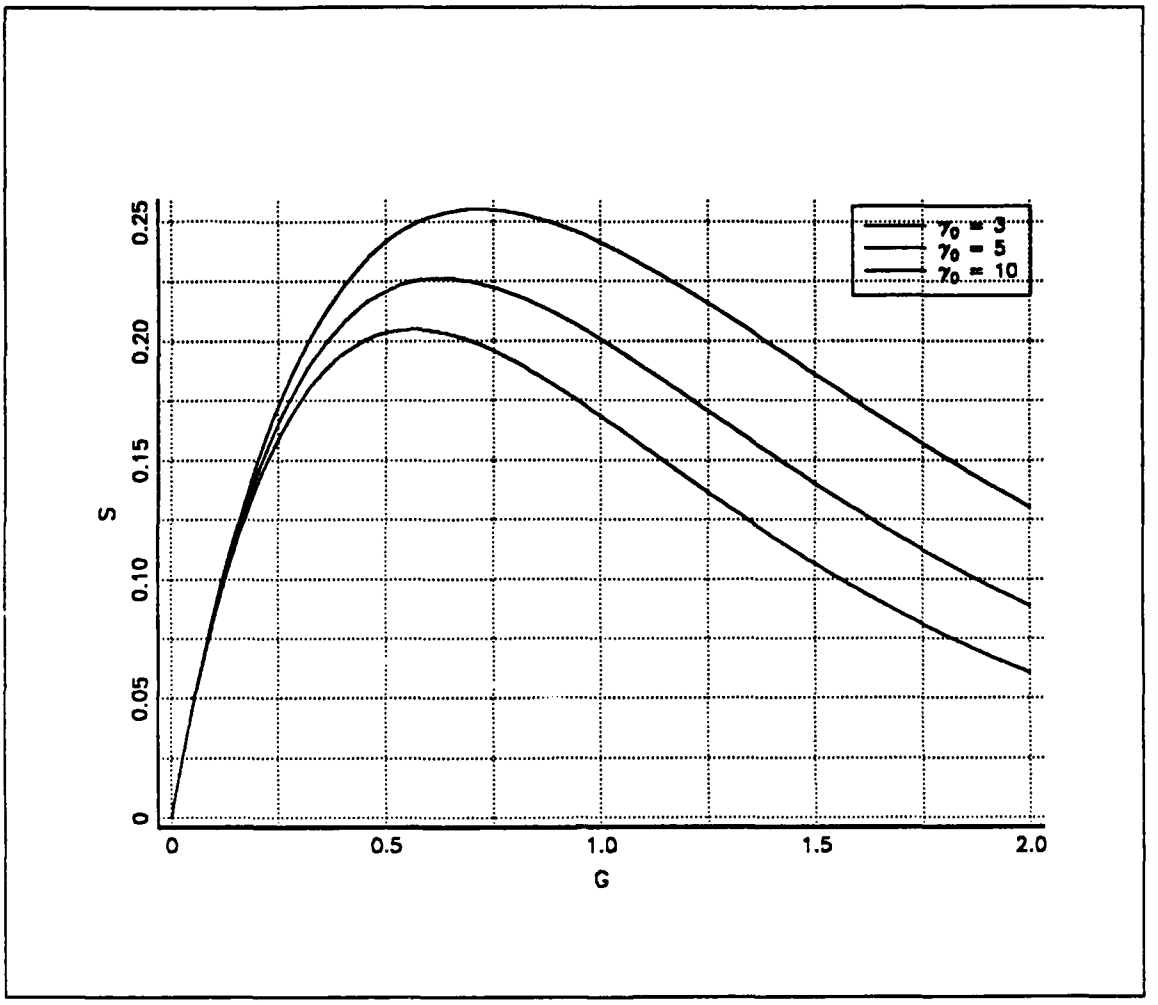

Figure 35. Unslotted Aloha throughput ($A_0 = 0$)

V. CONCLUSIONS

This thesis can be divided into two main parts. The first part describes the implementation of a software simulator for multipath fading in a maritime mobile satellite channel. The second part analyzes the throughput for an unslotted Aloha channel in a Rician fading environment.

The fading simulator generates Rician fading sequences for any value of frequency, velocity and Rice Factor (K). Fades can be simulated for communication links using a geostationary satellite or low altitude satellites.

Unfortunately, it was not possible to obtain data from experiments done in several institutions like JPL and CRC in order to compare results and make necessary adjustments to the simulator.

For the second part of the thesis, a set of equations are derived to compute the throughput of unslotted Aloha in a Rician fading channel. The obtained equations are tested for several values of the parameters A_0 and γ_0. Finally, a comparison is made with results obtained for a Rayleigh fading channel [Ref. 17] by setting the parameter A_0 equal to zero, and similar results are obtained. It is noted that the throughput of a Rician fading Aloha channel depends on the direct component power A_0^2. As A_0^2 increases, the joint interference power also increases and consequently the throughput is reduced.

APPENDIX A. SOFTWARE RICIAN SIMULATOR

This program generates a Rician fading sequence given variance, frequency and velocity.

```
C       *****  VARIABLE DEFINITIONS  *****
C       A    =   LOWER LIMIT
C       B    =   UPPER LIMIT
C       FCT  =   FUNCTION
C       S    =   PARTIAL SUM VALUE
C       H    =   INTERVAL LENGTH
C       AC   =   SIMPSON'S RULE VALUE
C       N    =   NUMBER OF EVEN SUBINTERVAL
C      NN2,NN,I,CC     = COUNTERS
C       X,H,D          = COMPONENTS OF THE RULES
C      VARIABLE DECLARATIONS
       COMPLEX RF(0:1024),R(0:1024),DSV(0:1024)
       REAL SI(0:1024),SQ(0:1024),V,ME,G(0:500),F(0:500),Y,W,CONST(0:1000
      &),WO,DS
       REAL*8 FR,WS,WL,A,B,FCT,S,X,H,D,AC(21),PI,Z,RGF(0:1000),AX(0:1000)
      &,IGF(0:1000),MAG(0:1024),TS
       INTEGER I,NN2,N,NN,NS
C      MAIN PROGRAM
C      N1:NUMBER OF SAMPLES OF THE GAUSSIAN RANDOM GENERATOR
       N1=500
C      N2:NUMBER OF COEFFICIENTS CALCULATED FOR THE SHAPING FILTER
       N2=21
       NP = N1 + N2
C
C      GAUSSIAN RANDOM GENERATOR 1 WITH VARIANCE 1, MEAN 0
       ISEED=23
       WRITE(*,*) 'ENTER VARIANCE'
       READ(*,*) V
       ME=0.0
       DO 10 I=0,N1
          CALL GAUSS (ISEED,V,ME,W)
          G(I)=W
 10    CONTINUE
C      GAUSSIAN RANDOM GENERATOR 2 WITH VARIANCE 1, MEAN 0
       DO 11 L=0,N1
          CALL GAUSS (ISEED,V,ME,Y)
          F(L)=Y
 11    CONTINUE
C      WRITE(8,*) (G(I),I=0,N1)
C      WRITE(4,*) (F(I),I=0,N1)
C
C      CALCULATION OF SHAPING FILTER COEFFICIENTS
C
C
C      TO CALCULATE A DEFINITE INTEGRAL FOR A FUNCTION USING SIMPSON'S
```

```
C      RULE.
C
       NS=21
       PI=DATAN(1D00)*4
       C=2.997925E+08
       WRITE(*,*) 'ENTER OPERATING FREQ'
       READ(*,*)FR
       WO = 2 * PI * FR
       WRITE(*,*) 'ENTER SPEED IN KNOTS'
       READ(*,*)WM
       IF (WM .EQ. 0) THEN
          DO 12 K=0,N1
             DS = COS(WO*K)
             RF(K) = CMPLX(G(K),F(K))
             DSV(K) = CMPLX(DS,0.0)
             R(K) = DSV(K) + RF(K)
             MAG(K) = CABS(R(K))
             WRITE(4,*) MAG(K)
12        CONTINUE
       ELSE
       WL=C/FR
       WRITE(*,*) 'WAVELENGTH = ',WL
       WM=2*PI*(WM*1852/3600)/WL
       WS=WM/2/PI
       WRITE(*,*) 'DOPPLER FREQ = ',WS
       B=0.97*WM
       WS=2*WM
       TS=2*PI/WS
       WRITE(*,*) 'ENTER (EVEN) N FOR SIMPSON INTEGRATION'
       READ(*,*)N
C
       A=0
       H=(B-A)/N
       D=H/3D00
       WRITE(*,*)'*******COMPUTING: PLEASE WAIT********'
       DO 13 K=0, (NS-1)/2
          S=FCT(WL,K,WS)
          DO 14 I=1,N-1, 2
             WL=A+I*H
             S=S+4.0*FCT(WL,K,WS)
14        CONTINUE
          DO 15 I=2, N-2, 2
             WL=A+I*H
             S=S+2.0*FCT(WL,K,WS)
15        CONTINUE
          S=S+FCT(B,K,WS)
          AC(K+1+(NS-1)/2)=S*D
13     CONTINUE
       DO 20 I=1,(NS-1)/2
20     AC(I)=AC(NS+1-I)
         DO 21 J=0,(NS-1)
            AX(J)=AC(J+1)
 21      CONTINUE

       DO 25 N=0,NS-1
```

```
         AX(N)=AX(N)*(0.54-0.46*DCOS(2*PI*N/(NS-1)))
25     CONTINUE
C
C      CONVOLUTION OF GAUSSIAN RANDOM VECTOR 1 AND SHAPING FILTER 1
       DO 26 N=N2,N1+N2
         AX(N)=0.0D+00
 26    CONTINUE
C
       CALL CONVOL (N1,N2,G,AX,RGF)
C
C      CONVOLUTION OF GAUSSIAN RANDOM VECTOR 2 AND SHAPING FILTER 2
       CALL CONVOL (N1,N2,F,AX,IGF)
C
C      APLYING DOPPLER EFFECT TO DIRECT SIGNAL
       DO 30 K = 0,NP
       DS = COS((WO + WS)*K*TS)
C
         RF(K) = CMPLX(RGF(K),IGF(K))
C      ADDING RAYLEIGH SIGNAL TO A CONSTANT TO OBTAIN RICEAN
         DSV(K) = CMPLX(DS,0.0)
         R(K) = DSV(K) + RF(K)
         WRITE(8,*) R(K)
         MAG(K) = CABS(R(K))
         WRITE(4,*) MAG(K)
 30    CONTINUE
       ENDIF
       STOP
       END
C
         REAL*8 FUNCTION FCT(WL,K,WS)
                 REAL*8 WL,WS,PI,D
                 INTEGER K
         PI=DATAN(1D00)*4D00
         D=2D00*PI*K*WL/WS
         FCT=2D00/WS*(1D00-(2D00*WL/WS)**2)**(-0.25)*DCOS(D)
         RETURN
         END
```

APPENDIX B. DERIVATION OF FORMULAS FOR UNSLOTTED ALOHA THROUGHPUT

A. J-FOLD CONVOLUTION

Given the expression

$$\left[e^{-A_0^2} I_0(2A_0\sqrt{y})e^{-y}\right] \tag{B.1}$$

in order to compute the j-fold convolution for j = 1, 2, 3, 4, 5 and 6, we evaluate the characteristic function and obtain

$$\Phi_Y(u) = \int_{-\infty}^{\infty} e^{-A_0^2} I_0(2A_0\sqrt{y})e^{-y}e^{juy}dy \tag{B.2}$$

Replacing the modified Bessel function of order 0 by its series approximation to the fourth power we have

$$\begin{aligned}\Phi_Y(u) = \int_{-\infty}^{\infty} e^{-A_0^2}\Big[& e^{-y}e^{juy} + e^{-y}A_0^2 y e^{juy} + e^{-y}\frac{A_0^4}{4}y^2 e^{juy} + e^{-y}\frac{A_0^6}{36}y^3 e^{juy} \\ & + e^{-y}\frac{A_0^8}{576}y^4 e^{jux}\Big]dy\end{aligned} \tag{B.3}$$

This is equivalent to

$$\begin{aligned}\Phi_Y(u) = e^{-A_0^2}\Bigg[& \int_{-\infty}^{\infty} e^{-(1-ju)y}dy + A_0^2\int_{-\infty}^{\infty} y e^{-(1-ju)y}dy + \frac{A_0^4}{4}\int_{-\infty}^{\infty} y^2 e^{-(1-ju)y}dy \\ & + \frac{A_0^6}{36}\int_{-\infty}^{\infty} y^3 e^{-(1-ju)y}dy + \frac{A_0^8}{576}\int_{-\infty}^{\infty} y^4 e^{-(1-ju)y}dy\Bigg]\end{aligned} \tag{B.4}$$

After evaluating the integrals we obtain

$$\Phi_Y(u) = e^{-A_0^2}\left[\frac{1}{(1-ju)} + A_0^2 \frac{1}{(1-ju)^2} + \frac{A_0^4}{4} \frac{2}{(1-ju)^3} + \frac{A_0^6}{36} \frac{6}{(1-ju)^4} + \frac{A_0^8}{576} \frac{24}{(1-ju)^5} \right] \tag{B.5}$$

Now, the j-fold convolution in time domain is equivalent to the jth power in the frequency domain, that is

$$(f_Y(y))^{j\otimes} \Leftrightarrow (\Phi_Y(u))^j$$

Evaluating the different jth powers and taking the inverse transform to each expression we obtain the desired j-fold convolutions.

For j = 1

$$(f_Y(y))^{1\otimes} = e^{-A_0^2}\left[e^{-y} + 2A_0^2 y e^{-y} + 0.5 \frac{A_0^4}{2!} y^2 e^{-y} + 0.1666 \frac{A_0^6}{3!} y^3 e^{-y} \right] \tag{B.6}$$

For j = 2

$$(f_Y(y))^{2\otimes} = e^{-2A_0^2}\left[y e^{-y} + 2 \frac{A_0^2}{2!} y^2 e^{-y} + 2 \frac{A_0^4}{3!} y^3 e^{-y} + 1.3333 \frac{A_0^6}{4!} y^4 e^{-y} + 0.5833 \frac{A_0^8}{5!} y^5 e^{-y} + 0.1666 \frac{A_0^{10}}{6!} y^6 e^{-y} + 0.0277 \frac{A_0^{12}}{7!} y^7 e^{-y} \right] \tag{B.7}$$

For j = 3

$$(f_Y(y))^{3\otimes} = e^{-3A_0^2}\left[\frac{1}{2!} y^2 e^{-y} + 3 \frac{A_0^2}{3!} y^3 e^{-y} + 4.5 \frac{A_0^4}{4!} y^4 e^{-y} + 4.5 \frac{A_0^6}{5!} y^5 e^{-y} + 3.25 \frac{A_0^8}{6!} y^6 e^{-y} + 1.75 \frac{A_0^{10})}{7!} y^7 e^{-y} + 0.7083 \frac{A_0^{12}}{8!} y^8 e^{-y} + 0.2083 \frac{A_0^{14}}{9!} y^9 e^{-y} + 0.0416 \frac{A_0^{16}}{10!} y^{10} e^{-y} + 0.0046 \frac{A_0^{18}}{11!} y^{11} e^{-y} \right] \tag{B.8}$$

For j = 4

$$(f_Y(y))^{4\otimes} = e^{-4A_0^2}\Bigg[\frac{1}{3!}y^3e^{-y} + 4\frac{A_0^2}{4!}y^4e^{-y} + 8\frac{A_0^4}{5!}y^5e^{-y} + 10.6666\frac{A_0^6}{6!}y^6e^{-y}$$
$$+ 9.6666\frac{A_0^8}{7!}y^7e^{-y} + 8\frac{A_0^{10})}{8!}y^8e^{-y} + 4\frac{A_0^{12}}{9!}y^9e^{-y} + 2.3333\frac{A_0^{14}}{10!}y^{10}e^{-y}$$
$$+ 0.8958\frac{A_0^{16}}{11!}y^{11}e^{-y} + 0.2685\frac{A_0^{18}}{12!}y^{12}e^{-y} + 0.6018\frac{A_0^{20}}{13!}y^{13}e^{-y} \qquad (B.9)$$
$$+ 0.0092\frac{A_0^{22}}{14!}y^{14}e^{-y} + 0.00077\frac{A_0^{24}}{15!}y^{15}e^{-y}\Bigg]$$

For j = 5

$$(f_Y(y))^{5\otimes} = e^{-5A_0^2}\Bigg[\frac{1}{4!}y^4e^{-y} + 5\frac{A_0^2}{5!}y^5e^{-y} + 12.5\frac{A_0^4}{6!}y^6e^{-y} + 20.8333\frac{A_0^6}{7!}y^7e^{-y}$$
$$+ 25.8333\frac{A_0^8}{8!}y^8e^{-y} + 25.1666\frac{A_0^{10})}{9!}y^9e^{-y} + 19.8611\frac{A_0^{12}}{10!}y^{10}e^{-y}$$
$$+ 12.9166\frac{A_0^{14}}{11!}y^{11}e^{-y} + 6.9791\frac{A_0^{16}}{12!}y^{12}e^{-y} + 2.6157\frac{A_0^{18}}{13!}y^{13}e^{-y} \qquad (B.10)$$
$$+ 1.1655\frac{A_0^{20}}{14!}y^{14}e^{-y} + 0.353\frac{A_0^{22}}{15!}y^{15}e^{-y} + 0.0848\frac{A_0^{24}}{16!}y^{16}e^{-y}$$
$$+ 0.0254\frac{A_0^{26}}{17!}y^{17}e^{-y} + 0.00096\frac{A_0^{28}}{18!}y^{18}e^{-y} + 0.000128\frac{A_0^{30}}{19!}y^{19}e^{-y}\Bigg]$$

For j = 6

$$(f_Y(y))^{6\otimes} = e^{-6A_0^2}\Bigg[\frac{1}{5!}y^5e^{-y} + 6\frac{A_0^2}{6!}y^6e^{-y} + 18\frac{A_0^4}{7!}y^7e^{-y} + 36\frac{A_0^6}{8!}y^8e^{-y}$$
$$+ 53.75\frac{A_0^8}{9!}y^9e^{-y} + 63.5\frac{A_0^{10})}{10!}y^{10}e^{-y} + 61.4166\frac{A_0^{12}}{11!}y^{11}e^{-y}$$
$$+ 49.6666\frac{A_0^{14}}{12!}y^{12}e^{-y} + 34.0208\frac{A_0^{16}}{13!}y^{13}e^{-y} + 19.8842\frac{A_0^{18}}{14!}y^{14}e^{-y} \qquad (B.11)$$
$$+ 9.0069\frac{A_0^{20}}{15!}y^{15}e^{-y} + 3\frac{A_0^{22}}{16!}y^{16}e^{-y} + 0.9184\frac{A_0^{24}}{17!}y^{17}e^{-y}$$
$$+ 0.3322\frac{A_0^{26}}{18!}y^{18}e^{-y} + 0.1013\frac{A_0^{28}}{19!}y^{19}e^{-y} + 0.0181\frac{A_0^{30}}{20!}y^{20}e^{-y}$$
$$+ 0.0036\frac{A_0^{32}}{21!}y^{21}e^{-y} + 0.000385\frac{A_0^{34}}{22!}y^{22}e^{-y}\Bigg]$$

B. PROBABILITY OF CAPTURE

First, evaluating equation (4.8), $f_Z(z \mid n)$ for n = 1 2, 3, 4, 5 and 6, the following expressions are obtained

For n = 1

$$f_Z(z \mid 1) = C_1(1)e^{-2A_0^2}\frac{1}{2^1}\Bigg[\sum_{g=1}^{4}K_g g\frac{1}{(1+z)^{g+1}} + A_0^2 z\sum_{g=2}^{5}K_{g-1}\frac{g(g-1)}{(1+z)^{g+1}} + A_0^4 \cdot$$
$$\cdot\frac{z^2}{4}\sum_{g=3}^{6}K_{g-2}\frac{g(g-1)(g-2)}{(1+z)^{g+1}} + A_0^6\frac{z^3}{36}\sum_{g=4}^{7}K_{g-3}\frac{g!}{(g-4)!(1+z)^{g+1}}\Bigg] \qquad (B.12)$$

For n = 2

$$f_Z(z \mid 2) = e^{-2A_0^2}\frac{1}{2^2}\left\{C_1(2)\left[\sum_{g=1}^{4}K_g g\frac{1}{(1+z)^{g+1}} + A_0^2 z\sum_{g=2}^{5}K_{g-1}\frac{g(g-1)}{(1+z)^{g+1}} + A_0^4\cdot\right.\right.$$
$$\left.\cdot\frac{z^2}{4}\sum_{g=3}^{6}K_{g-2}\frac{g(g-1)(g-2)}{(1+z)^{g+1}} + A_0^6\frac{z^3}{36}\sum_{g=4}^{7}K_{g-3}\frac{g!}{(g-4)!(1+z)^{g+1}}\right] \quad (B.13)$$
$$+ C_2(2)e^{-A_0^2}\left[\sum_{h=2}^{8}K_h h\frac{1}{(1+z)^{h+1}} + A_0^2 z\sum_{h=3}^{9}K_{h-1}\frac{h(h-1)}{(1+z)^{h+1}} + A_0^4\frac{z^2}{4}\cdot\right.$$
$$\left.\left.\cdot\sum_{h=4}^{10}K_{h-2}\frac{h(h-1)(h-2)}{(1+z)^{h+1}} + A_0^6\frac{z^3}{36}\sum_{h=5}^{11}K_{h-3}\frac{h!}{(h-4)!(1+z)^{h+1}}\right]\right\}$$

For n = 3

$$f_Z(z \mid 3) = e^{-3A_0^2}\frac{1}{2^3}\left\{C_2(3)\left[\sum_{h=2}^{8}K_h h\frac{1}{(1+z)^{h+1}} + A_0^2 z\sum_{h=3}^{9}K_{h-1}\frac{h(h-1)}{(1+z)^{h+1}} + A_0^4\cdot\right.\right.$$
$$\left.\cdot\frac{z^2}{4}\sum_{h=4}^{10}K_{h-2}\frac{h(h-1)(h-2)}{(1+z)^{h+1}} + A_0^6\frac{z^3}{36}\sum_{h=5}^{11}K_{h-3}\frac{h!}{(h-4)!(1+z)^{h+1}}\right] \quad (B.14)$$
$$+ C_3(3)e^{-A_0^2}\left[\sum_{l=3}^{12}K_l l\frac{1}{(1+z)^{l+1}} + A_0^2 z\sum_{l=4}^{13}K_{l-1}\frac{l(l-1)}{(1+z)^{h+1}} + A_0^4\frac{z^2}{4}\cdot\right.$$
$$\left.\left.\cdot\sum_{l=5}^{14}K_{l-2}\frac{l(l-1)(l-2)}{(1+z)^{l+1}} + A_0^6\frac{z^3}{36}\sum_{l=6}^{15}K_{l-3}\frac{l!}{(l-4)!(1+z)^{l+1}}\right]\right\}$$

For n = 4

$$f_Z(z \mid 4) = e^{-3A_0^2}\frac{1}{2^4}\left\{C_2(4)\left[\sum_{h=2}^{8}K_h h\frac{1}{(1+z)^{h+1}} + A_0^2 z\sum_{h=3}^{9}K_{h-1}\frac{h(h-1)}{(1+z)^{h+1}} + A_0^4\cdot\right.\right.$$
$$\left.\cdot\frac{z^2}{4}\sum_{h=4}^{10}K_{h-2}\frac{h(h-1)(h-2)}{(1+z)^{h+1}} + A_0^6\frac{z^3}{36}\sum_{h=5}^{11}K_{h-3}\frac{h!}{(h-4)!(1+z)^{h+1}}\right]$$
$$+ C_3(4)e^{-A_0^2}\left[\sum_{l=3}^{12}K_l l\frac{1}{(1+z)^{l+1}} + A_0^2 z\sum_{l=4}^{13}K_{l-1}\frac{l(l-1)}{(1+z)^{h+1}} + A_0^4\frac{z^2}{4}\cdot\right.$$
$$\left.\cdot\sum_{l=5}^{14}K_{l-2}\frac{l(l-1)(l-2)}{(1+z)^{l+1}} + A_0^6\frac{z^3}{36}\sum_{l=6}^{15}K_{l-3}\frac{l!}{(l-4)!(1+z)^{l+1}}\right] \qquad (B.15)$$
$$+ C_4(4)e^{-2A_0^2}\left[\sum_{j=4}^{16}K_j j\frac{1}{(1+z)^{j+1}} + A_0^2 z\sum_{j=5}^{17}K_{j-1}\frac{j(j-1)}{(1+z)^{j+1}} + A_0^4\frac{z^2}{4}\cdot\right.$$
$$\left.\left.\cdot\sum_{j=6}^{18}K_{j-2}\frac{j(j-1)(j-2)}{(1+z)^{j+1}} + A_0^6\frac{z^3}{36}\sum_{j=7}^{19}K_{j-3}\frac{j!}{(j-4)!(1+z)^{j+1}}\right]\right\}$$

For n = 5

$$f_Z(z \mid 5) = e^{-4A_0^2}\frac{1}{2^5}\left\{C_3(5)\left[\sum_{l=3}^{12}K_l l\frac{1}{(1+z)^{l+1}} + A_0^2 z\sum_{l=4}^{13}K_{l-1}\frac{l(l-1)}{(1+z)^{l+1}} + A_0^4\cdot\right.\right.$$
$$\left.\cdot\frac{z^2}{4}\sum_{l=5}^{14}K_{l-2}\frac{l(l-1)(l-2)}{(1+z)^{l+1}} + A_0^6\frac{z^3}{36}\sum_{l=6}^{15}K_{l-3}\frac{l!}{(l-4)!(1+z)^{l+1}}\right]$$
$$+ C_4(5)e^{-A_0^2}\left[\sum_{j=4}^{16}K_j j\frac{1}{(1+z)^{j+1}} + A_0^2 z\sum_{j=5}^{17}K_{j-1}\frac{j(j-1)}{(1+z)^{j+1}} + A_0^4\frac{z^2}{4}\cdot\right.$$
$$\left.\cdot\sum_{j=6}^{18}K_{j-2}\frac{j(j-1)(j-2)}{(1+z)^{j+1}} + A_0^6\frac{z^3}{36}\sum_{j=7}^{19}K_{j-3}\frac{j!}{(j-4)!(1+z)^{j+1}}\right] \qquad (B.16)$$
$$+ C_5(5)e^{-2A_0^2}\left[\sum_{m=5}^{20}K_m m\frac{1}{(1+z)^{m+1}} + A_0^2 z\sum_{m=6}^{21}K_{m-1}\frac{m(m-1)}{(1+z)^{m+1}} + A_0^4\frac{z^2}{4}\cdot\right.$$
$$\left.\left.\cdot\sum_{m=7}^{22}K_{m-2}\frac{m(m-1)(m-2)}{(1+z)^{m+1}} + A_0^6\frac{z^3}{36}\sum_{m=8}^{23}K_{m-3}\frac{m!}{(m-4)!(1+z)^{m+1}}\right]\right\}$$

For n = 6

$$
\begin{aligned}
f_Z(z \mid 6) = e^{-4A_0^2}\frac{1}{2^6}\Bigg\{ & C_3(6)\Bigg[\sum_{l=3}^{12} K_l l \frac{1}{(1+z)^{l+1}} + A_0^2 z \sum_{l=4}^{13} K_{l-1}\frac{l(l-1)}{(1+z)^{l+1}} + A_0^4 \cdot \\
& \cdot \frac{z^2}{4}\sum_{l=5}^{14} K_{l-2}\frac{l(l-1)(l-2)}{(1+z)^{l+1}} + A_0^6\frac{z^3}{36}\sum_{l=6}^{15} K_{l-3}\frac{l!}{(l-4)!(1+z)^{l+1}}\Bigg] \\
& + C_4(6)e^{-A_0^2}\Bigg[\sum_{j=4}^{16} K_j j \frac{1}{(1+z)^{j+1}} + A_0^2 z\sum_{j=5}^{17} K_{j-1}\frac{j(j-1)}{(1+z)^{j+1}} + A_0^4\frac{z^2}{4}\cdot \\
& \cdot \sum_{j=6}^{18} K_{j-2}\frac{j(j-1)(j-2)}{(1+z)^{j+1}} + A_0^6\frac{z^3}{36}\sum_{j=7}^{19} K_{j-3}\frac{j!}{(j-4)!(1+z)^{j+1}}\Bigg] \\
& + C_5(6)e^{-2A_0^2}\Bigg[\sum_{m=5}^{20} K_m m\frac{1}{(1+z)^{m+1}} + A_0^2 z\sum_{m=6}^{21} K_{m-1}\frac{m(m-1)}{(1+z)^{m+1}} + A_0^4\frac{z^2}{4}\cdot \\
& \cdot \sum_{m=7}^{22} K_{m-2}\frac{m(m-1)(m-2)}{(1+z)^{m+1}} + A_0^6\frac{z^3}{36}\sum_{m=8}^{23} K_{m-3}\frac{m!}{(m-4)!(1+z)^{m+1}}\Bigg] \\
& + C_6(6)e^{-3A_0^2}\Bigg[\sum_{u=6}^{23} K_u u\frac{1}{(1+z)^{u+1}} + A_0^2 z\sum_{u=7}^{24} K_{u-1}\frac{u(u-1)}{(1+z)^{u+1}} + A_0^4\frac{z^2}{4}\cdot \\
& \cdot \sum_{u=8}^{25} K_{u-2}\frac{u(u-1)(u-2)}{(1+z)^{u+1}} + A_0^6\frac{z^3}{36}\sum_{u=9}^{26} K_{u-3}\frac{u!}{(u-4)!(1+z)^{u+1}}\Bigg]\Bigg\}
\end{aligned}
\tag{B.17}
$$

where the $C_j(n)$ values are defined in equation (4.3), and K_g, K_h, K_l, K_j, K_m, and K_u are given in Table 3.

Table 3. CONSTANT VALUES USED IN EQUATIONS (B.12) THROUGH (B.23)

	K_g	K_h	K_i	K_j	K_m	K_u
1	1	1	1	1	1	1
2	$2A_0^2$	$2A_0^2$	$3A_0^2$	$4A_0^2$	$5A_0^2$	$6A_0^2$
3	$0.5A_0^4$	$2A_0^4$	$4.5A_0^4$	$8A_0^4$	$12.5A_0^4$	$18A_0^4$
4	$0.1666A_0^6$	$1.3333A_0^6$	$4.5A_0^6$	$10.1666A_0^6$	$20.8333A_0^6$	$36A_0^6$
5		$0.5833A_0^8$	$3.25A_0^8$	$9.6666A_0^8$	$25.8333A_0^8$	$53.75A_0^8$
6		$0.1666A_0^{10}$	$1.75A_0^{10}$	$8A_0^{10}$	$25.1666A_0^{10}$	$63.5A_0^{10}$
7		$0.0277A_0^{12}$	$0.7083A_0^{12}$	$4A_0^{12}$	$19.8611A_0^{12}$	$61.4166A_0^{12}$
8			$0.2083A_0^{14}$	$2.3333A_0^{14}$	$12.9166A_0^{14}$	$49.6666A_0^{14}$
9			$0.0416A_0^{16}$	$0.8958A_0^{16}$	$6.9791A_0^{16}$	$34.0208A_0^{16}$
10			$0.0046A_0^{18}$	$0.2685A_0^{18}$	$2.6157A_0^{18}$	$19.8842A_0^{18}$
11				$0.0602A_0^{20}$	$1.1655A_0^{20}$	$9.0069A_0^{20}$
12				$0.0092A_0^{22}$	$0.353A_0^{22}$	$0.3A_0^{22}$
13				$0.00077A_0^{24}$	$0.0848A_0^{24}$	$0.9284A_0^{24}$
14					$0.0254A_0^{26}$	$0.3322A_0^{26}$
15					$0.00096A_0^{28}$	$0.1013A_0^{28}$
16					$0.00013A_0^{30}$	$0.0181A_0^{30}$
17						$0.0036A_0^{32}$
18						$0.00038A_0^{34}$

Now, the probabilities of capture are evaluated by replacing equations (B.12) through (B.17) into equation (4.10), and we get

For n = 1

$$
\begin{aligned}
Pr\{capture|1\} = 1 - \Bigg\{ & \frac{1}{2^1} e^{-2A_0^2} C_1(1) \Bigg[\sum_{g=1}^{4} K_g g \Big(\frac{-1}{g} [\frac{1}{(1+\gamma_0)^g} - 1] \Big) + A_0^2 \sum_{g=2}^{5} K_{g-1} \cdot \\
& \cdot g(g-1) \Big(\frac{-1}{(g-1)} [\frac{1}{(1+\gamma_0)^{g-1}} - 1] + \frac{1}{g} [\frac{1}{(1+\gamma_0)^g} - 1] \Big) + \frac{A_0^4}{4} \sum_{g=3}^{6} K_{g-2} \cdot \\
& \cdot g(g-1)(g-2) \Big(\frac{-1}{(g-2)} [\frac{1}{(1+\gamma_0)^{g-2}} - 1] + \frac{2}{(g-1)} [\frac{1}{(1+\gamma_0)^{g-1}} - 1] \\
& - \frac{1}{g} [\frac{1}{(1+\gamma_0)^g} - 1] \Big) + \frac{A_0^6}{36} \sum_{g=4}^{7} K_{g-3} \frac{g!}{(g-4)!} \Big(\frac{1}{(3-g)} \frac{\gamma_0^3}{(1+\gamma_0)^g} + \frac{3}{(3-g)} \cdot \\
& \cdot \frac{1}{(g-2)} [\frac{1}{(1+\gamma_0)^{g-2}} - 1] - \frac{3}{(3-g)} \frac{2}{(g-1)} [\frac{1}{(1+\gamma_0)^{g-1}} - 1] + \frac{3}{(3-g)} \frac{1}{g} \cdot \\
& \cdot [\frac{1}{(1+\gamma_0)^g} - 1] \Big) \Bigg] \Bigg\}
\end{aligned}
\tag{B.18}
$$

For n = 2

$$Pr\{capture|2\} = 1 - \left\{ \frac{1}{2^2} e^{-2A_0^2} C_1(2) \left[\sum_{g=1}^{4} K_g g \left(\frac{-1}{g} \left[\frac{1}{(1+\gamma_0)^g} - 1 \right] \right) + A_0^2 \sum_{g=2}^{5} K_{g-1} \cdot \right.\right.$$

$$\cdot g(g-1) \left(\frac{-1}{(g-1)} \left[\frac{1}{(1+\gamma_0)^{g-1}} - 1 \right] + \frac{1}{g} \left[\frac{1}{(1+\gamma_0)^g} - 1 \right] \right) + \frac{A_0^4}{4} \sum_{g=3}^{6} K_{g-2} \cdot$$

$$\cdot g(g-1)(g-2) \left(\frac{-1}{(g-2)} \left[\frac{1}{(1+\gamma_0)^{g-2}} - 1 \right] + \frac{2}{(g-1)} \left[\frac{1}{(1+\gamma_0)^{g-1}} - 1 \right] \right.$$

$$\left. - \frac{1}{g} \left[\frac{1}{(1+\gamma_0)^g} - 1 \right] \right) + \frac{A_0^6}{36} \sum_{g=4}^{7} K_{g-3} \frac{g!}{(g-4)!} \left(\frac{1}{(3-g)} \frac{\gamma_0^3}{(1+\gamma_0)^g} + \frac{3}{(3-g)} \cdot \right.$$

$$\cdot \frac{1}{(g-2)} \left[\frac{1}{(1+\gamma_0)^{g-2}} - 1 \right] - \frac{3}{(3-g)} \frac{2}{(g-1)} \left[\frac{1}{(1+\gamma_0)^{g-1}} - 1 \right] + \frac{3}{(3-g)} \frac{1}{g} \cdot$$

$$\left.\left. \cdot \left[\frac{1}{(1+\gamma_0)^g} - 1 \right] \right) \right] + \frac{1}{2^2} e^{-3A_0^2} C_2(2) \left[\sum_{h=2}^{8} K_h h \left(\frac{-1}{h} \left[\frac{1}{(1+\gamma_0)^h} - 1 \right] \right) + A_0^2 \cdot \right. \qquad (B.19)$$

$$\cdot \sum_{h=3}^{9} K_{h-1} h(h-1) \left(\frac{-1}{(h-1)} \left[\frac{1}{(1+\gamma_0)^{h-1}} - 1 \right] + \frac{1}{h} \left[\frac{1}{(1+\gamma_0)^h} - 1 \right] \right) + \frac{A_0^4}{4} \cdot$$

$$\cdot \sum_{h=4}^{10} K_{h-2} h(h-1)(h-2) \left(\frac{-1}{(h-2)} \left[\frac{1}{(1+\gamma_0)^{h-2}} - 1 \right] + \frac{2}{(h-1)} \left[\frac{1}{(1+\gamma_0)^{h-1}} - 1 \right] \right.$$

$$- 1 \left] - \frac{1}{h} \left[\frac{1}{(1+\gamma_0)^h} - 1 \right] \right) + \frac{A_0^6}{36} \sum_{h=5}^{11} K_{h-3} \frac{h!}{(h-4)!} \left(\frac{1}{(3-h)} \frac{\gamma_0^3}{(1+\gamma_0)^h} \right.$$

$$+ \frac{3}{(3-h)} \frac{1}{(h-2)} \left[\frac{1}{(1+\gamma_0)^{h-2}} - 1 \right] - \frac{3}{(3-h)} \frac{2}{(h-1)} \left[\frac{1}{(1+\gamma_0)^{h-1}} - 1 \right]$$

$$\left.\left. + \frac{3}{(3-h)} \frac{1}{h} \left[\frac{1}{(1+\gamma_0)^h} - 1 \right] \right) \right] \right\}$$

For n = 3

$$Pr\{capture|3\} = 1 - \left\{ \frac{1}{2^3} e^{-3A_0^2} C_2(3) \left[\sum_{h=2}^{8} K_h h \left(\frac{-1}{h} \left[\frac{1}{(1+\gamma_0)^h} - 1 \right] \right) + A_0^2 \sum_{h=3}^{9} K_{h-1} \cdot \right.\right.$$

$$\cdot h(h-1) \left(\frac{-1}{(h-1)} \left[\frac{1}{(1+\gamma_0)^{h-1}} - 1 \right] + \frac{1}{h} \left[\frac{1}{(1+\gamma_0)^h} - 1 \right] \right) + \frac{A_0^4}{4} \sum_{h=4}^{10} K_{h-2} \cdot$$

$$\cdot h(h-1)(h-2) \left(\frac{-1}{(h-2)} \left[\frac{1}{(1+\gamma_0)^{h-2}} - 1 \right] + \frac{2}{(h-1)} \left[\frac{1}{(1+\gamma_0)^{h-1}} - 1 \right] \right.$$

$$\left. - \frac{1}{h} \left[\frac{1}{(1+\gamma_0)^h} - 1 \right] \right) + \frac{A_0^6}{36} \sum_{h=4}^{7} K_{h-3} \frac{h!}{(h-4)!} \left(\frac{1}{(3-h)} \frac{\gamma_0^3}{(1+\gamma_0)^h} + \frac{3}{(3-h)} \cdot \right.$$

$$\cdot \frac{1}{(h-2)} \left[\frac{1}{(1+\gamma_0)^{h-2}} - 1 \right] - \frac{3}{(3-h)} \frac{2}{(h-1)} \left[\frac{1}{(1+\gamma_0)^{h-1}} - 1 \right] + \frac{3}{(3-h)} \frac{1}{h} \cdot$$

$$\left.\left. \cdot \left[\frac{1}{(1+\gamma_0)^h} - 1 \right] \right) \right] + \frac{1}{2^3} e^{-4A_0^2} C_3(3) \left[\sum_{l=3}^{12} K_l l \left(\frac{-1}{l} \left[\frac{1}{(1+\gamma_0)^l} - 1 \right] \right) + A_0^2 \sum_{l=4}^{13} K_{l-1} \cdot \right. \quad (B.20)$$

$$\cdot l(l-1) \left(\frac{-1}{(l-1)} \left[\frac{1}{(1+\gamma_0)^{l-1}} - 1 \right] + \frac{1}{l} \left[\frac{1}{(1+\gamma_0)^l} - 1 \right] \right) + \frac{A_0^4}{4} \sum_{l=5}^{14} K_{l-2} \cdot$$

$$\cdot l(l-1)(l-2) \left(\frac{-1}{(l-2)} \left[\frac{1}{(1+\gamma_0)^{l-2}} - 1 \right] + \frac{2}{(l-1)} \left[\frac{1}{(1+\gamma_0)^{l-1}} - 1 \right] \right.$$

$$\left. - \frac{1}{l} \left[\frac{1}{(1+\gamma_0)^l} - 1 \right] \right) + \frac{A_0^6}{36} \sum_{l=6}^{15} K_{l-3} \frac{l!}{(l-4)!} \left(\frac{1}{(3-l)} \frac{\gamma_0^3}{(1+\gamma_0)^l} + \frac{3}{(3-l)} \cdot \right.$$

$$\cdot \frac{1}{(l-2)} \left[\frac{1}{(1+\gamma_0)^{l-2}} - 1 \right] - \frac{3}{(3-l)} \frac{2}{(l-1)} \left[\frac{1}{(1+\gamma_0)^{l-1}} - 1 \right] + \frac{3}{(3-l)} \frac{1}{l} \cdot$$

$$\left.\left.\left. \cdot \left[\frac{1}{(1+\gamma_0)^l} - 1 \right] \right) \right] \right\}$$

For n = 4

$$Pr\{capture|4\} = 1 - \Bigg\{ \frac{1}{2^4} e^{-3A_0^2} C_2(4) \Bigg[\sum_{h=2}^{8} K_h h \Bigg(\frac{-1}{h} \Big[\frac{1}{(1+\gamma_0)^h} - 1 \Big] \Bigg) + A_0^2 \sum_{h=3}^{9} K_{h-1} \cdot$$

$$\cdot h(h-1) \Bigg(\frac{-1}{(h-1)} \Big[\frac{1}{(1+\gamma_0)^{h-1}} - 1 \Big] + \frac{1}{h} \Big[\frac{1}{(1+\gamma_0)^h} - 1 \Big] \Bigg) + \frac{A_0^4}{4} \sum_{h=4}^{10} K_{h-2} \cdot$$

$$\cdot h(h-1)(h-2) \Bigg(\frac{-1}{(h-2)} \Big[\frac{1}{(1+\gamma_0)^{h-2}} - 1 \Big] + \frac{2}{(h-1)} \Big[\frac{1}{(1+\gamma_0)^{h-1}} - 1 \Big]$$

$$- \frac{1}{h} \Big[\frac{1}{(1+\gamma_0)^h} - 1 \Big] \Bigg) + \frac{A_0^6}{36} \sum_{h=4}^{10} K_{h-3} \frac{h!}{(h-4)!} \Bigg(\frac{1}{(3-h)} \frac{\gamma_0^3}{(1+\gamma_0)^h} + \frac{3}{(3-h)} \cdot$$

$$\cdot \frac{1}{(h-2)} \Big[\frac{1}{(1+\gamma_0)^{h-2}} - 1 \Big] - \frac{3}{(3-h)} \frac{2}{(h-1)} \Big[\frac{1}{(1+\gamma_0)^{h-1}} - 1 \Big] + \frac{3}{(3-h)} \frac{1}{h} \cdot$$

$$\cdot \Big[\frac{1}{(1+\gamma_0)^h} - 1 \Big] \Bigg) \Bigg] + \frac{1}{2^4} e^{-4A_0^2} C_3(4) \Bigg[\sum_{l=3}^{12} K_l l \Bigg(\frac{-1}{l} \Big[\frac{1}{(1+\gamma_0)^l} - 1 \Big] \Bigg) + A_0^2 \sum_{l=4}^{13} K_{l-1} \cdot$$

$$\cdot l(l-1) \Bigg(\frac{-1}{(l-1)} \Big[\frac{1}{(1+\gamma_0)^{l-1}} - 1 \Big] + \frac{1}{l} \Big[\frac{1}{(1+\gamma_0)^l} - 1 \Big] \Bigg) + \frac{A_0^4}{4} \sum_{l=5}^{14} K_{l-2} \cdot \qquad (B.21)$$

$$\cdot l(l-1)(l-2) \Bigg(\frac{-1}{(l-2)} \Big[\frac{1}{(1+\gamma_0)^{l-2}} - 1 \Big] + \frac{2}{(l-1)} \Big[\frac{1}{(1+\gamma_0)^{l-1}} - 1 \Big]$$

$$- \frac{1}{l} \Big[\frac{1}{(1+\gamma_0)^l} - 1 \Big] \Bigg) + \frac{A_0^6}{36} \sum_{l=6}^{15} K_{l-3} \frac{l!}{(l-4)!} \Bigg(\frac{1}{(3-l)} \frac{\gamma_0^3}{(1+\gamma_0)^l} + \frac{3}{(3-l)} \cdot$$

$$\cdot \frac{1}{(l-2)} \Big[\frac{1}{(1+\gamma_0)^{l-2}} - 1 \Big] - \frac{3}{(3-l)} \frac{2}{(l-1)} \Big[\frac{1}{(1+\gamma_0)^{l-1}} - 1 \Big] + \frac{3}{(3-l)} \frac{1}{l} \cdot$$

$$\cdot \Big[\frac{1}{(1+\gamma_0)^l} - 1 \Big] \Bigg) \Bigg] + \frac{1}{2^4} e^{-5A_0^2} C_4(4) \Bigg[\sum_{j=4}^{16} K_j j \Bigg(\frac{-1}{j} \Big[\frac{1}{(1+\gamma_0)^j} - 1 \Big] \Bigg) + A_0^2 \sum_{j=5}^{17} K_{j-1} \cdot$$

$$\cdot j(j-1) \Bigg(\frac{-1}{(j-1)} \Big[\frac{1}{(1+\gamma_0)^{j-1}} - 1 \Big] + \frac{1}{j} \Big[\frac{1}{(1+\gamma_0)^j} - 1 \Big] \Bigg) + \frac{A_0^4}{4} \sum_{j=6}^{18} K_{j-2} \cdot$$

$$\cdot j(j-1)(j-2) \Bigg(\frac{-1}{(j-2)} \Big[\frac{1}{(1+\gamma_0)^{j-2}} - 1 \Big] + \frac{2}{(j-1)} \Big[\frac{1}{(1+\gamma_0)^{j-1}} - 1 \Big]$$

$$- \frac{1}{j} \Big[\frac{1}{(1+\gamma_0)^j} - 1 \Big] \Bigg) + \frac{A_0^6}{36} \sum_{j=7}^{19} K_{j-3} \frac{g!}{(j-4)!} \Bigg(\frac{1}{(3-j)} \frac{\gamma_0^3}{(1+\gamma_0)^g} + \frac{3}{(3-j)} \cdot$$

$$\cdot\frac{1}{(j-2)}\left[\frac{1}{(1+\gamma_0)^{j-2}}-1\right]-\frac{3}{(3-j)}\frac{2}{(j-1)}\left[\frac{1}{(1+\gamma_0)^{j-1}}-1\right]+\frac{3}{(3-j)}\frac{1}{j}\cdot$$
$$\cdot\left[\frac{1}{(1+\gamma_0)^{j}}-1\right]\Bigg)\Bigg]\Bigg\}$$

For n = 5

$$Pr\{capture|5\}=1-\left\{\frac{1}{2^5}e^{-4A_0^2}C_3(5)\left[\sum_{l=3}^{12}K_l l\left(\frac{-1}{l}\left[\frac{1}{(1+\gamma_0)^{l}}-1\right]\right)+A_0^2\sum_{l=4}^{13}K_{l-1}\cdot\right.\right.$$
$$\cdot l(l-1)\left(\frac{-1}{(l-1)}\left[\frac{1}{(1+\gamma_0)^{l-1}}-1\right]+\frac{1}{l}\left[\frac{1}{(1+\gamma_0)^{l}}-1\right]\right)+\frac{A_0^4}{4}\sum_{l=5}^{14}K_{l-2}\cdot$$
$$\cdot l(l-1)(l-2)\left(\frac{-1}{(l-2)}\left[\frac{1}{(1+\gamma_0)^{l-2}}-1\right]+\frac{2}{(l-1)}\left[\frac{1}{(1+\gamma_0)^{l-1}}-1\right]\right.$$
$$\left.-\frac{1}{l}\left[\frac{1}{(1+\gamma_0)^{l}}-1\right]\right)+\frac{A_0^6}{36}\sum_{l=6}^{15}K_{l-3}\frac{l!}{(l-4)!}\left(\frac{1}{(3-l)}\frac{\gamma_0^3}{(1+\gamma_0)^{l}}+\frac{3}{(3-l)}\cdot\right.$$
$$\cdot\frac{1}{(l-2)}\left[\frac{1}{(1+\gamma_0)^{l-2}}-1\right]-\frac{3}{(3-l)}\frac{2}{(l-1)}\left[\frac{1}{(1+\gamma_0)^{l-1}}-1\right]+\frac{3}{(3-l)}\frac{1}{l}\cdot$$
$$\left.\left.\cdot\left[\frac{1}{(1+\gamma_0)^{l}}-1\right]\right)\right]+\frac{1}{2^5}e^{-5A_0^2}C_4(5)\left[\sum_{j=4}^{16}K_j j\left(\frac{-1}{j}\left[\frac{1}{(1+\gamma_0)^{j}}-1\right]\right)+A_0^2\sum_{j=5}^{17}K_{j-1}\cdot\right. \quad (B.22)$$
$$\cdot j(j-1)\left(\frac{-1}{(j-1)}\left[\frac{1}{(1+\gamma_0)^{j-1}}-1\right]+\frac{1}{j}\left[\frac{1}{(1+\gamma_0)^{j}}-1\right]\right)+\frac{A_0^4}{4}\sum_{j=6}^{18}K_{j-2}\cdot$$
$$\cdot j(j-1)(j-2)\left(\frac{-1}{(j-2)}\left[\frac{1}{(1+\gamma_0)^{j-2}}-1\right]+\frac{2}{(j-1)}\left[\frac{1}{(1+\gamma_0)^{j-1}}-1\right]\right.$$
$$\left.-\frac{1}{j}\left[\frac{1}{(1+\gamma_0)^{j}}-1\right]\right)+\frac{A_0^6}{36}\sum_{j=7}^{19}K_{j-3}\frac{j!}{(j-4)!}\left(\frac{1}{(3-j)}\frac{\gamma_0^3}{(1+\gamma_0)^{j}}+\frac{3}{(3-j)}\cdot\right.$$
$$\cdot\frac{1}{(j-2)}\left[\frac{1}{(1+\gamma_0)^{j-2}}-1\right]-\frac{3}{(3-j)}\frac{2}{(j-1)}\left[\frac{1}{(1+\gamma_0)^{j-1}}-1\right]+\frac{3}{(3-j)}\frac{1}{j}\cdot$$
$$\left.\left.\cdot\left[\frac{1}{(1+\gamma_0)^{j}}-1\right]\right)\right]+\frac{1}{2^5}e^{-6A_0^2}C_5(5)\left[\sum_{m=5}^{20}K_m m\left(\frac{-1}{m}\left[\frac{1}{(1+\gamma_0)^{m}}-1\right]\right)+A_0^2\sum_{m=6}^{21}K_{m-1}\cdot\right.$$

$$\cdot m(m-1)\left(\frac{-1}{(m-1)} \left[\frac{1}{(1+\gamma_0)^{m-1}} - 1 \right] + \frac{1}{m} \left[\frac{1}{(1+\gamma_0)^{m}} - 1 \right] \right) + \frac{A_0^4}{4} \sum_{m=7}^{22} K_{m-2} \cdot$$

$$\cdot m(m-1)(m-2)\left(\frac{-1}{(m-2)} \left[\frac{1}{(1+\gamma_0)^{m-2}} - 1 \right] + \frac{2}{(m-1)} \left[\frac{1}{(1+\gamma_0)^{m-1}} - 1 \right] \right.$$

$$\left. - \frac{1}{m} \left[\frac{1}{(1+\gamma_0)^{m}} - 1 \right] \right) + \frac{A_0^6}{36} \sum_{m=8}^{23} K_{m-3} \frac{m!}{(m-4)!} \left(\frac{1}{(3-m)} \frac{\gamma_0^3}{(1+\gamma_0)^m} + \frac{3}{(3-m)} \cdot \right.$$

$$\cdot \frac{1}{(m-2)} \left[\frac{1}{(1+\gamma_0)^{m-2}} - 1 \right] - \frac{3}{(3-m)} \frac{2}{(m-1)} \left[\frac{1}{(1+\gamma_0)^{m-1}} - 1 \right] + \frac{3}{(3-m)} \frac{1}{m} \cdot$$

$$\left. \cdot \left[\frac{1}{(1+\gamma_0)^{m}} - 1 \right] \right) \Bigg] \Bigg\}$$

And finally, for n = 6

$$Pr\{capture|6\} = 1 - \left\{ \frac{1}{2^6} e^{-4A_0^2} C_3(6) \left[\sum_{l=3}^{12} K_l l \left(\frac{-1}{l} \left[\frac{1}{(1+\gamma_0)^{l}} - 1 \right] \right) + A_0^2 \sum_{l=4}^{13} K_{l-1} \cdot \right.\right.$$

$$\cdot l(l-1)\left(\frac{-1}{(l-1)} \left[\frac{1}{(1+\gamma_0)^{l-1}} - 1 \right] + \frac{1}{l} \left[\frac{1}{(1+\gamma_0)^{l}} - 1 \right] \right) + \frac{A_0^4}{4} \sum_{l=5}^{14} K_{l-2} \cdot$$

$$\cdot l(l-1)(l-2)\left(\frac{-1}{(l-2)} \left[\frac{1}{(1+\gamma_0)^{l-2}} - 1 \right] + \frac{2}{(l-1)} \left[\frac{1}{(1+\gamma_0)^{l-1}} - 1 \right] \right.$$

$$\left. - \frac{1}{l} \left[\frac{1}{(1+\gamma_0)^{l}} - 1 \right] \right) + \frac{A_0^6}{36} \sum_{l=6}^{15} K_{l-3} \frac{l!}{(l-4)!} \left(\frac{1}{(3-l)} \frac{\gamma_0^3}{(1+\gamma_0)^l} + \frac{3}{(3-l)} \cdot \right. \qquad (B.23)$$

$$\cdot \frac{1}{(l-2)} \left[\frac{1}{(1+\gamma_0)^{l-2}} - 1 \right] - \frac{3}{(3-l)} \frac{2}{(l-1)} \left[\frac{1}{(1+\gamma_0)^{l-1}} - 1 \right] + \frac{3}{(3-l)} \frac{1}{l} \cdot$$

$$\left. \left. \cdot \left[\frac{1}{(1+\gamma_0)^{l}} - 1 \right] \right) \right] + \frac{1}{2^6} e^{-5A_0^2} C_4(6) \left[\sum_{j=4}^{16} K_j j \left(\frac{-1}{j} \left[\frac{1}{(1+\gamma_0)^{j}} - 1 \right] \right) + A_0^2 \sum_{j=5}^{17} K_{j-1} \cdot \right.$$

$$\cdot j(j-1)\left(\frac{-1}{(j-1)} \left[\frac{1}{(1+\gamma_0)^{j-1}} - 1 \right] + \frac{1}{j} \left[\frac{1}{(1+\gamma_0)^{j}} - 1 \right] \right) + \frac{A_0^4}{4} \sum_{j=6}^{18} K_{j-2} \cdot$$

$$\cdot j(j-1)(j-2)\left(\frac{-1}{(j-2)} \left[\frac{1}{(1+\gamma_0)^{j-2}} - 1 \right] + \frac{2}{(j-1)} \left[\frac{1}{(1+\gamma_0)^{j-1}} - 1 \right] \right.$$

$$-\frac{1}{j}\left[\frac{1}{(1+\gamma_0)^j}-1\right]\Bigg)+\frac{A_0^6}{36}\sum_{j=7}^{19}K_{j-3}\frac{j!}{(j-4)!}\Bigg(\frac{1}{(3-j)}\frac{\gamma_0^3}{(1+\gamma_0)^j}+\frac{3}{(3-j)}\cdot$$

$$\cdot\frac{1}{(j-2)}\left[\frac{1}{(1+\gamma_0)^{j-2}}-1\right]-\frac{3}{(3-j)}\frac{2}{(j-1)}\left[\frac{1}{(1+\gamma_0)^{j-1}}-1\right]+\frac{3}{(3-j)}\frac{1}{j}\cdot$$

$$\cdot\left[\frac{1}{(1+\gamma_0)^j}-1\right]\Bigg)\Bigg]+\frac{1}{2^6}e^{-6A_0^2}C_5(5)\Bigg[\sum_{m=5}^{20}K_m m\Bigg(\frac{-1}{n}\cdot\left[\frac{1}{(1+\gamma_0)^m}-1\right]\Bigg)+A_0^2\sum_{m=6}^{21}K_{m-1}\cdot$$

$$\cdot m(m-1)\Bigg(\frac{-1}{(m-1)}\left[\frac{1}{(1+\gamma_0)^{m-1}}-1\right]+\frac{1}{m}\left[\frac{1}{(1+\gamma_0)^m}-1\right]\Bigg)+\frac{A_0^4}{4}\sum_{m=7}^{22}K_{m-2}\cdot$$

$$\cdot m(m-1)(m-2)\Bigg(\frac{-1}{(m-2)}\left[\frac{1}{(1+\gamma_0)^{m-2}}-1\right]+\frac{2}{(m-1)}\left[\frac{1}{(1+\gamma_0)^{m-1}}-1\right]$$

$$-\frac{1}{m}\left[\frac{1}{(1+\gamma_0)^m}-1\right]\Bigg)+\frac{A_0^6}{36}\sum_{m=8}^{23}K_{m-3}\frac{m!}{(m-4)!}\Bigg(\frac{1}{(3-m)}\frac{\gamma_0^3}{(1+\gamma_0)^m}+\frac{3}{(3-m)}\cdot$$

$$\cdot\frac{1}{(m-2)}\left[\frac{1}{(1+\gamma_0)^{m-2}}-1\right]-\frac{3}{(3-m)}\frac{2}{(m-1)}\left[\frac{1}{(1+\gamma_0)^{m-1}}-1\right]+\frac{3}{(3-m)}\frac{1}{m}\cdot$$

$$\cdot\left[\frac{1}{(1+\gamma_0)^m}-1\right]\Bigg)\Bigg]+\frac{1}{2^6}e^{-7A_0^2}C_6(6)\Bigg[\sum_{u=6}^{23}K_u u\Bigg(\frac{-1}{u}\left[\frac{1}{(1+\gamma_0)^u}-1\right]\Bigg)+A_0^2\sum_{u=7}^{24}K_{u-1}\cdot$$

$$\cdot l(u-1)\Bigg(\frac{-1}{(u-1)}\left[\frac{1}{(1+\gamma_0)^{u-1}}-1\right]+\frac{1}{u}\left[\frac{1}{(1+\gamma_0)^u}-1\right]\Bigg)+\frac{A_0^4}{4}\sum_{u=8}^{25}K_{u-2}\cdot$$

$$\cdot u(u-1)(u-2)\Bigg(\frac{-1}{(u-2)}\left[\frac{1}{(1+\gamma_0)^{u-2}}-1\right]+\frac{2}{(u-1)}\left[\frac{1}{(1+\gamma_0)^{u-1}}-1\right]$$

$$-\frac{1}{u}\left[\frac{1}{(1+\gamma_0)^u}-1\right]\Bigg)+\frac{A_0^6}{36}\sum_{u=9}^{26}K_{u-3}\frac{u!}{(u-4)!}\Bigg(\frac{1}{(3-u)}\frac{\gamma_0^3}{(1+\gamma_0)^u}+\frac{3}{(3-u)}\cdot$$

$$\cdot\frac{1}{(u-2)}\left[\frac{1}{(1+\gamma_0)^{u-2}}-1\right]-\frac{3}{(3-u)}\frac{2}{(u-1)}\left[\frac{1}{(1+\gamma_0)^{u-1}}-1\right]+\frac{3}{(3-u)}\frac{1}{u}\cdot$$

$$\cdot\left[\frac{1}{(1+\gamma_0)^u}-1\right]\Bigg)\Bigg]\Bigg\}$$

where γ_0 is the preset threshold and the values of K_g, K_h, K_l, K_j, K_m, and K_u are given in table 3.

LIST OF REFERENCES

1. J.G. Walker, *Continuous Whole Earth Coverage By Circular Orbit Satellites*, International Conference on Satellite System for Mobile Communications and Surveillance, IEE, Conference publication n.95, 13-15 Mar. 1973.

2. Y. Karasawa and T. Shiokawa, *Characteristics of L-Band Multipath Fading due to Sea Surface Reflection*, IEEE Transactions on Antennas and Propagation, Vol. AP-32, No. 6, June 1984, pp. 618-623.

3. Y. Karasawa and T. Shiokawa, *Analysis of Multipath Fading due to Sea Surface Scattering in Maritime Satellite Communication*, Technical Group on Antennas and Propagation, IECE, Japan, October 1980.

4. R. H. Clarke, *A Statistical Theory of Mobile-Radio Reception* , Bell System Technical Journal, Vol. 47, pp. 957-1000, July-Aug. 1978.

5. P. Beckmann, *Probability in Communication Engineering*, Harcourt, Brace & World, New York, 1967.

6. P. Beckmann and A. Spizzichino, *The Scattering of Electromagnetic Waves from Rough Surfaces*, Pergamon Press, New York, 1963.

7. S. O. Rice, *Properties of Sine Wave Plus Random Noise*, Bell System Technical Journal 27, pp. 109-157, Jan. 1948.

8. E. K. Smith, J. F. Cavanagh, and W. L. Flock, *Propagation Effects for Land Mobile Satellite Systems*, Proceedings of the National Radio Science Meeting, Jan. 1983.

9. John S. Butterworth, *The Description and Evaluation of a Mobile Communications Channel Simulator*, Proceedings of the Propagation Workshop in support of MSAT-X, JPL, Pasadena, Ca., pp. 4.3-4.21, Jan. 1985.

10. CCIR Interim Working Party 5/2, *Propagation data for Land-Mobile Satellite Systems for Frequencies Above 100 MHz,* Document 5.12-E, Mar. 1983.

11. Gaston Arredondo, William Chriss and Edward H. Walker, *A Multipath Fading Simulator for Mobile Radio,* IEEE Trans. on Communications, Vol. COM-21, No.11, pp. 1325-1328, Nov. 1973

12. M. R. Karim, *Packet Communications in a Mobile Radio Channel,* AT & T Technical Journal, Vol. 65, Issue 3, pp. 12-20, June 1978.

13. Glen A. Myers, *Derivation of Equation for Doppler Shift of Satellite Signals,* Class notes EC4590, Naval Postgraduate School, 1987.

14. Faramaz Davarian, *Channel Simulation to Facilitate Mobile Satellite Communications Research,* IEEE Trans. on Communications, Vol. COM-35 , No.1, pp. 47-55, Jan. 1987.

15. T. Ha, *Digital Satellite Communications,* Macmillan, 1988, pp. 362-366.

16. J. C. Arnbak, and W. Van Blitterswijk, *Capacity of Slotted Aloha in Rayleigh Fading Channels.* Areas Comm., SAC-5, no. 2, 1987, pp. 261-260.

17. R. L. Borchardt and T. Ha, *Power Capture Aloha,* Milcom 88, San Diego, Ca., pp. 703-707, 23-26 Oct. 1988.

18. R. L. Borshardt, *Performance Analysis of Aloha Networks Utilizing Multiple Signal Power Levels,* Engineer's Degree thesis, Naval Postgraduate School, June 1988.

19. F. Kuperus, and J. C. Arnbak, *Packet Radio in a Rayleigh Channel* , Electron. Letters, vol. 18, June 1982, pp. 506-507.

INITIAL DISTRIBUTION LIST

		No. Copies
1.	Defense Technical Information Center Cameron Station Alexandria, VA 22304-6145	2
2.	Library, Code 0142 Naval Postgraduate School Monterey, CA 93943-5002	2
3.	Chairman, Code 62 Department of Electrical and Computer Engineering Naval Postgraduate School Monterey, CA 93943-5000	1
4.	Professor Tri T. Ha, Code 62Ha Department of Electrical and Computer Engineering Naval Postgraduate School Monterey, CA 93943-5000	5
5.	Professor Glen A. Myers, Code 62My Department of Electrical and Computer Engineering Naval Postgraduate School Monterey, CA 93943-5000	1
6.	Roger Casey, Code 805 Naval Ocean Systems Center San Diego, CA 92152-5000	1
7.	Sr. Almirante Comandante Armada Nacional Comando Armada Nacional C.A.N, Avenida El Dorado Bogota D.E / Colombia	1
8.	Sr. Contralmirante Director Escuela Naval Almirante Padilla Escuela Naval Cartagena / Colombia	1
9.	Sr. Contralmirante Agregado Naval Embassy of Colombia Office of Naval Attache 2118 Leroy Place, N.W Washington D.C. 20008	1

10. Sr. Capitan de Navio — 1
Director de Personal A.R.C
Comando Armada Nacional
C.A.N. Avenida El Dorado
Bogota D.E Colombia

11. Sr. Capitan de Corbeta — 1
Jorge Franco Lema
Escuela Naval
Barrio Manzanillo, casa fiscal No 2
Cartagena / Colombia

12. Teniente de Navio — 2
Augusto J. Zapata Diez
Escuela Naval
Cartagena / Colombia

13. Lt. Mohamed Hassan Khaidar — 1
NPGS SMC 2648
Monterey, CA 93943